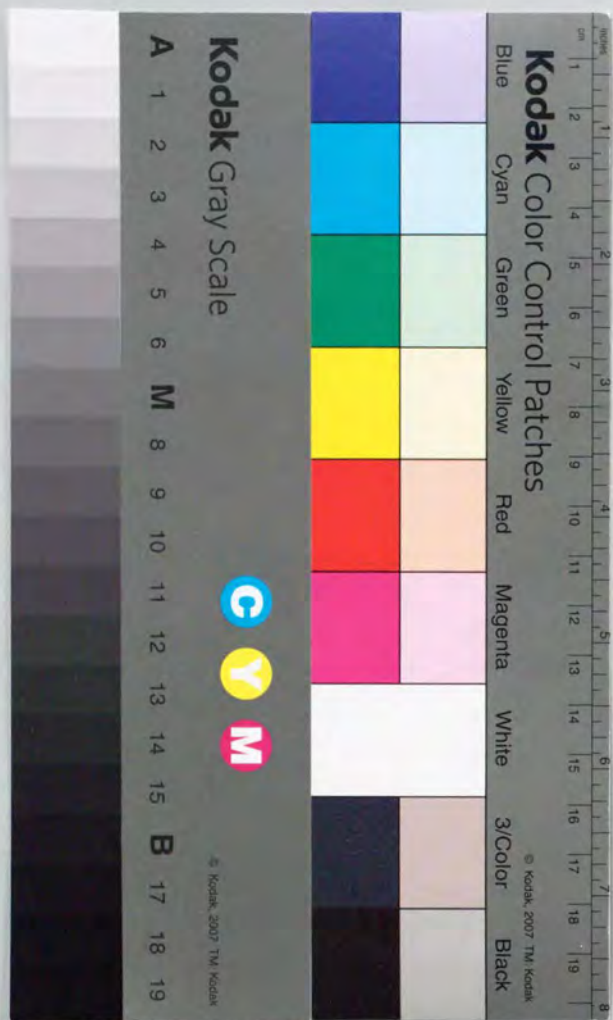


Study on Soliton Transmission
and its Control

(ソリトンの伝搬とその伝搬制御に関する研究)

Hirokazu Kubota



Study on Soliton Transmission
and its Control

(ソリトンの伝搬とその伝搬制御に関する研究)

Hirokazu Kubota

Acknowledgments

I have many people to thank for their help in the completion of this thesis. First of all I thank Professor Youichi Fujii of the Institute of Industrial Science, The University of Tokyo, for his guidance and encouragement throughout this work. I greatly appreciated his willingness to answer many of my questions. I also thank the following people for their invaluable advice to this work: Professor Yasuhiko Arakawa of the Institute of Industrial Science; Professor Kazuo Hotate of the Research Center for Advanced Science and Technology; Professor Takeshi Kamiya of the Faculty of Engineering; Professor Kazuo Kikuchi of the Faculty of Engineering; and Professor Tadashi Takano of the Institute of Space and Astronautical Science.

All of this work was performed at NTT Laboratories. I express my sincere thanks to Professor S. Kojima, Dr. N. Uchida, Dr. H. Sakamoto, Dr. H. Kimura, Dr. H. Ishio, Dr. M. Kawase, Dr. Y. Wakui, Dr. K. Ishihara, and Dr. Y. Koyamada. It was under their tenures as managers of NTT Laboratories that I had the opportunity to perform this research. I thank them all for their guidance and encouragement.

A very special thanks goes to my mentor Dr. Masataka Nakazawa, Group leader, NTT Laboratory. I am indebted to him for his continuous support and inspiration.

Many thanks are due to my colleagues Y. Kimura, K. Suzuki, K. Kurokawa, and E. Yamada at NTT who have performed many of the experiments that are recorded in this thesis. They have magic fingers for work in the laboratory. I thank Dr. K. Tamura for stimulating discussions. I also thank my many other colleagues at NTT. Finally, thanks to the engineers of NTT R&D management development for providing me a first rate computational environment that made this research possible.

Contents

acknowledgments	
index	
I. Introduction	1
I. 1 Background	1
I. 2 Brief history of soliton research	1
I. 3 Outline	6
references	6
II. Soliton Interaction Analysis	9
II. 1 Optical soliton propagation in fibers	9
II. 2 Nonlinear interaction	11
II.3 Optical loss and amplification of soliton	14
II. 4 High order nonlinearities	17
II. 5 ASE noise	17
II.5.1 SN ratio	18
II.5.2 Gordon-Haus jitter	19
references	20
III. Soliton Transmission with Lumped Amplifiers	22
III. 1 Physical image of new soliton transmission technique	23
III. 2 Long distance transmission system with lumped amplifiers	25
III.2.1 Automatic power control	25
III.2.2 Gain fluctuation	38
III.2.3 Dispersive waves	38
III. 3 Analytic solutions	43
III. 4 Conclusion	44
references	44

IV. Soliton Transmission Control in Time and Frequency Domain	46
IV. 1 Soliton transmission controls	46
IV.1.1 reduction of Jitter and interaction	46
IV.1.2 Noise reduction	54
IV. 2 Ultra-long distance soliton transmission	59
IV. 3 Soliton transmission with long amplifier spacings by soliton control	71
IV. 4 Ultrahigh speed transmission using soliton control under soliton self frequency shift	76
IV. 5 Conclusion	83
references	83
V. Dispersion management in soliton transmission	86
V. 1 Partial soliton communication	86
V. 2 Dispersion allocated soliton	96
V. 3 Conclusion	103
references	103
VI. General Conclusion	105
Appendices	108
A.1 Numerical procedure (split step Fourier method, BPM)	108
A.2 Soliton pulse generation methods	111
List of published papers	114

I. INTRODUCTION

I.1 Background

An optical soliton in an optical fiber is regarded as a dispersion-free carrier for optical communications. It is believed that Tbit/s communication will become possible through the use of optical solitons because they are supported by a balance between the group velocity dispersion and nonlinearity (optical Kerr effect) of the optical fiber. In the negative group velocity dispersion (GVD) region of optical fibers, solitons can be generated by balancing self phase modulation with negative GVD.

Since a small transmission fiber loss violates this balance, it is important to compensate for the loss with optical gain, otherwise the advantageous nature of the optical soliton disappears. Progress on the erbium-doped fiber amplifier (EDFA)^[1] and a new soliton transmission scheme which uses lumped amplifiers^[2-4] has enabled us to develop a simple and promising soliton transmission system.

We have succeeded in transmitting solitons over unlimited distances by using the dynamic soliton transmission technique and incorporating soliton control.^[5] Furthermore, the optical soliton can be propagated through a transmission line with dispersion fluctuations by using a dispersion allocation.

A soliton is a good information carrier because of its short duration and high stability. Furthermore a soliton is resistant to the polarization dispersion effect of optical fibers.^[6]

I.2 Brief history of optical soliton research

Solitons in optical fibers were first proposed by Hasegawa and Tappert in 1973, and they demonstrated the stability of solitons by numerical calculations.^[7] It was seven years after their prediction that an optical soliton was actually observed in an optical fiber because, until then, there had been no

high-power infra-red optical pulse sources. In 1980, Mollenauer et al. succeeded in observing solitons in optical fibers by using a high power color center laser.^[8] There have been many numerical and theoretical investigations of soliton propagation in connection with the transmission capacity of optical fiber communication systems.^[9-11] Those investigations were based on the soliton-soliton interaction force.

Many studies were also undertaken to extend transmission distances in parallel with high speed communication research. At that time, there were no good optical amplifiers operating in the 1.5 μm region. Hasegawa and Kodama proposed propagating an $A=1.5$ soliton in a fiber with loss.^[12] Blow and Doran also studied soliton propagation in fibers with loss, and concluded that it was necessary to generate higher order solitons for transmission over long distances.^[13] In addition, Shiojiri and Fujii pointed out that transmission capacity could be improved by increasing the peak power of the input soliton pulse in a fiber with loss.^[14]

For longer distance optical transmission systems, optical amplifiers must be used to compensate for fiber loss. Stimulated Raman scattering (SRS) in optical fiber is promising for soliton transmission since it operates as a distributed gain medium. This transmission method was first proposed by Hasegawa.^[15] The distributed amplifier is very suitable for soliton transmission because it provides a nearly loss-free transmission line. Mollenauer et al. demonstrated soliton transmission over 4000 km with Raman amplifiers by circulating a 50 ps soliton pulse in a 42 km long fiber loop.^[16]

Er^{3+} -doped fiber amplifiers operating in the 1.5 μm region are of great interest for optical communication because of their high gain and low insertion loss. It has been shown that solitons can be amplified and transmitted with Er^{3+} -doped fiber.^[17,18] A lumped amplifier system is very simple and easy to construct. However, the idea of using a lumped amplifier for soliton

transmission did not appear to be realistic because it would require a repeater spacing of as small as 10 km.^[19]

Table 1 Early work on lumped amplifier systems

Author/ Title	Published	Received
H. Kubota and M. Nakazawa: Long-distance Optical Soliton Transmission with Lumped Amplifiers [3]	Apr. 1990	June 22, 1989
M. Nakazawa, K. Suzuki, and Y. Kimura: 3.2-5 Gbit/s, 100 km error-free soliton transmission with erbium amplifiers and repeaters [2]	Mar. 1990	Nov. 28, 1989
K. Suzuki, M. Nakazawa, E. Yamada, and Y. Kimura: 5 Gbit/s, 250 km error-free soliton transmission with Er^{3+} -doped fibre amplifiers and repeaters [4]	Apr. 1990	Jan. 16, 1990
L. F. Mollenauer, S. G. Evangelides and H. A. Haus: Long distance soliton propagation using lumped amplifiers and dispersion-shifted fiber [21]	Feb. 1991	May 8, 1990
A. Hasegawa and Y. Kodama: Guiding-center solitons in optical fibers [20]	Dec. 1990	July 30, 1990
K. J. Blow, and N. J. Doran: Average soliton dynamics and operation of soliton systems with lumped amplifiers [22]	Apr. 1991	Nov. 21, 1990

We proposed a new soliton transmission system suitable for lumped gain media, which uses a slightly higher input power than the $A=1.0$ soliton. I showed in Ref. [3] that the repeater spacings can be extended to as much as 50

km with this technique for a fiber loss of 0.22 dB/km. This technique is very effective and various soliton transmission experiments were successfully completed by using EDFAs. Later the existence of a stable soliton in a lumped amplifier system was proved analytically by various groups. [20-22] Table 1 shows early work related to this technique. Today, experimental soliton transmissions exceed 100 Gbit/s in bit-rate, or 10,000 km in distance using EDFAs.

The combination of EDFAs and optical solitons seems a promising way to achieve ultra-long distance optical communication. However, the use of optical solitons implies two factors which limit transmission distances. One is the interaction between adjacent solitons. The other is the Gordon-Haus effect caused by coherent interaction between a soliton pulse and the amplified spontaneous emission noise (ASE noise) generated by the EDFA.[23] Furthermore, the accumulation of ASE noise is also unavoidable when signals are sent over long distances, and this has a detrimental effect on the SN ratio.

There is yet another problem for high-speed soliton communication. The self Raman effect causes a soliton pulse to experience a carrier frequency change, which is called the soliton self frequency shift (SSFS). [24] The amount of SSFS is inversely proportional to the 4th power of the pulse width which means that the effect becomes significant for an ultra-high speed soliton transmission system.

Soliton control, which was originally developed for long distance soliton transmission, is employed to resolve these difficulties. Prior to soliton control, there were some approaches for reducing soliton interaction, such as altering the amplitudes or phases of adjacent soliton pulses.[10] These techniques successfully reduced the soliton interaction and enabled transmission distances to be extended. However, these techniques were based on the physical properties of the soliton pulse, so the distance was still limited by physical effects such as perturbations and nonlinear interaction.

Soliton control involves applying additional external manipulation to the propagating soliton pulse to control it. There are two types of soliton transmission control scheme. One is time domain control, the other is frequency domain control.

Time domain control directly corrects any timing change caused by Gordon-Haus jitter or soliton interaction and frequency domain control stabilizes the soliton pulses. When used together, they eliminate dispersive noises such as ASE noise and non-soliton components from distorted soliton pulses. For soliton transmission control in the time domain, amplitude or phase modulation is applied to the soliton pulses. For frequency domain control a bandpass optical filter is installed in the transmission line [25,26] to stabilize the soliton pulses.

Mollenauer devised another soliton control scheme; sliding frequency-guiding filters. With this technique, a set of optical filters, each with a slightly different center frequency, is installed in the transmission system.[27] This technique uses only passive optical components and it succeeded in reducing the accumulation of ASE noise. A variation of this technique has also been demonstrated, which uses an A/O modulator and a fixed frequency optical filter instead of a sliding frequency filter.[28] It seems to be more practical than the original sliding frequency guiding filter technique.

The soliton controls eliminate noise accumulation and soliton interaction. It can be said that soliton control has paved the way for tera-bit soliton communication. [29]

There is yet another stream of research aimed at the practical introduction of soliton communication. The first problem is short repeater spacings. To lengthen the repeater spacings, we proposed a chirp compensation technique, in other words a dispersion compensation technique, combined with a lumped amplifier scheme. This method can extend the amplifier spacing to over 100 km even when using a fiber with a

high GVD of 2 ps/(km.nm). The other crucial problem is the dispersion fluctuation of commercially available dispersion shifted optical fiber. We developed a dispersion allocated soliton to deal with such perturbations. Through the use of this concept, currently installed non-soliton optical cable is being converted to soliton cable by adding a short section of optical fiber.^[30]

1.3 OUTLINE

The optical soliton has a history of only two decades. Furthermore, remarkable advances towards actual transmission systems have been achieved in the past five years.

This paper consists of six chapters (including the introduction), which describes the advances made in the last five years in soliton transmission research. The developments are described almost in chronological order, i.e. the order in which I engaged in the problems.

Chapter 2 relates to the era before the development of the EDFA. It describes the basics of soliton propagation in optical fiber. Chapter 3 describes soliton transmission with lumped gain amplifiers such as EDFAs. Chapter 4 describes soliton transmission control techniques in time and frequency domains which make ultra-long distance soliton transmission possible. Chapter 5 describes dispersion compensation and dispersion management techniques for soliton transmission which are very important in terms of realizing a soliton communication system. Chapter 6 is a general conclusion and describes the future of soliton transmission research.

- 1 M. Nakazawa, K. Suzuki, and Y. Kimura: Soliton amplification and transmission with Er³⁺-doped fiber repeater pumped by GaInAsP laser diode, *Electron. Lett.* Vol. 25, pp. 199-200 (1989).
- 2 M. Nakazawa, K. Suzuki, and Y. Kimura: 3.2-5 Gbit/s, 100 km error-free soliton transmission with erbium amplifiers and repeaters, *Photo. Tech. Lett.* Vol. 2, No.3, pp. 216-219 (1990).

- 3 H. Kubota and M. Nakazawa: Long-distance optical soliton transmission with lumped amplifiers, *IEEE J. Quantum Electron.* Vol. 26, No. 4, pp. 692-700 (1990).
- 4 K. Suzuki, M. Nakazawa, E. Yamada, and Y. Kimura: 5 Gbit/s, 250 km error-free soliton transmission with Er³⁺-doped fibre amplifiers and repeaters, *Electron. Lett.* vol. 26, p. 551 (1990)
- 5 M. Nakazawa, K. Suzuki, E. Yamada, H. Kubota, Y. Kimura, and M. Takaya: Experimental demonstration of soliton data transmission over unlimited distances with soliton control in time and frequency domains, Proc. OFC/IOOC '93, San Jose, PD-7, (Feb, 1993).
- 6 L. F. Mollenauer, K. Smith, and J. P. Gordon: Resistance of solitons to the effect of polarization dispersion in optical fibers, *Opt. Lett.* vol. 14, pp. 1219-1221 (1989).
- 7 A. Hasegawa and F. Tappert: Transmission of stationary nonlinear optical pulses in dispersive dielectric fibers. I: Anomalous dispersion, *Appl. Phys. Lett.* vol. 23, pp. 142-144 (1973).
- 8 L. F. Mollenauer, R. H. Stolen and J. P. Gordon: Experimental observation of picosecond pulse narrowing and solitons in optical fibers, *Phys. Rev. Lett.* vol. 45, p. 1095 (1980).
- 9 J. P. Gordon: Interaction forces among solitons in optical fibers, *Opt. Lett.* vol. 8, pp. 596-598 (1983).
- 10 P. L. Chu and C. Desem: Mutual interaction between solitons of unequal amplitudes in optical fibre, *Electron. Lett.* vol. 21, pp. 1133-1134 (1985).
- 11 B. Hemmerson and D. Yevik: Numerical investigation of soliton interaction, *Electron. Lett.* vol. 19, pp. 570-571 (1983)
- 12 A. Hasegawa and Y. Kodama: Signal transmission by optical solitons in monomode fiber, *Proc. IEEE* vol. 69, pp. 1145-1150, (1981).
- 13 K. J. Blow and N. J. Doran: Soliton in Optical Communications, *IEEE J. Quantum Electron.* vol. QE-19, pp. 1883-1888 (1983).
- 14 E. Shiojiri and Y. Fujii: Transmission capability of an optical fiber communication system using index nonlinearity, *Appl. Opt.* vol. 24, pp. 358-360, (1985).
- 15 A. Hasegawa: Numerical study of optical soliton transmission amplified periodically by the stimulated Raman process, *Appl. Opt.* vol. 23, pp. 3302-3309 (1984)
- 16 L. F. Mollenauer and K. Smith: Demonstration of soliton transmission over more than 4000 km in fiber with loss periodically compensated by Raman gain, *Opt. Lett.* Vol. 13, p. 675 (1988).
- 17 M. Nakazawa, Y. Kimura and K Suzuki: Soliton amplification and transmission with Er³⁺-doped fiber repeater pumped by GaInAsP laser diode, *Electron. Lett.* vol. 25, pp. 199-200 (1989).

- 18 G. P. Agrawal: Amplification of Ultrashort Solitons in Erbium-Doped Fiber Amplifiers, *IEEE Photo. Technol. Lett.* vol. 2, pp. 875-877 (1990).
- 19 Y. Kodama and A. Hasegawa: Amplification and reshaping of optical solitons in glass fiber-III. amplifiers with random gain, *Opt. Lett.* vol. 8, pp. 342-344 (1983).
- 20 A. Hasegawa and Y. Kodama: Guiding-center solitons in optical fibers, *Optics Lett.* vol. 15, pp. 1443-1445 (1990).
- 21 L. F. Mollenauer, S. G. Evangelides and H. A. Haus: Long distance soliton propagation using lumped amplifiers and dispersion-shifted fiber, *IEEE J. Lightwave Technol.* vol. 9, pp. 194-197 (1991).
- 22 K. J. Blow and N. J. Doran: Average soliton dynamics and the operation of soliton systems with lumped amplifiers, *IEEE Photo Tech. Lett.* vol. 4, p 639 (1991).
- 23 J. P. Gordon, and H. A. Haus: Random walk of coherently amplified solitons in optical fiber transmission, *Opt. Lett.* vol. 11, pp. 665-667 (1986).
- 24 J. P. Gordon: Theory of the soliton self-frequency shift, *Optics Lett.* vol. 11, pp. 662-664 (1986).
- 25 H. Kubota and M. Nakazawa: Soliton transmission control in time and frequency domains, *IEEE J. Quantum Electron.*, vol. 29, pp. 2189-2197 (1993).
- 26 M. Nakazawa, K. Suzuki, E. Yamada, H. Kubota, Y. Kimura and M. Takaya: Experimental demonstration of soliton data transmission over unlimited distance with soliton control in time and frequency domains, *Electron. Lett.* vol. 29, pp. 729-730 (1993).
- 27 L. F. Mollenauer, E. Lichtman, M. J. Newbelt and G. T. Harvey: Demonstration, using sliding-frequency guiding filters, of error-free soliton transmission over more than 20 Mm at 10 Gbit/s, single channel, and over more than 13 Mm at 20 Gbit/s in a two-channel WDM, *Elec. Lett.* vol. 29, pp. 910-911, (1993).
- 28 M. Suzuki, H. Taga, N. Edagawa, H. Tanaka, S. Yamamoto and S. Akiba: "Experimental investigation of Gordon-Haus limit on soliton transmission by using optical short pulses generated by an InGaAsP electroabsorption modulator", *Electron. Lett.* vol. 29, No. 18, pp. 1643-1644 (1993).
- 29 H. Kubota and M. Nakazawa: Soliton transmission control for ultra high speed system, *IEICE Trans. Electron.* vol. E78-C, pp. 5-11 (1995)
- 30 M. Nakazawa and H. Kubota: Construction of a dispersion-allocated soliton transmission line using conventional dispersion-shifted nonsoliton fibers, *Jpn. J. Appl. Phys.* vol. 34, pp. 681-683 (1995).

II SOLITON INTERACTION ANALYSIS

II.1 Optical Soliton Propagation in Fibers

In a nonlinear medium, the refractive index is given by

$$n(t) = n_0 + n_2 |E(t)|^2, \quad (2-1)$$

where n_0 and n_2 are the linear and nonlinear index of refraction, respectively, and $E(t)$ is an electric field.^[1] The second term represents the optical Kerr effect. When the intensity of the electric field changes, its phase $\phi(t)$ is modulated through the Kerr effect, namely self-phase modulation. The frequency change ($\Delta\omega$) of the pulse is given by

$$\Delta\omega = -\frac{\partial\phi(t)}{\partial t} = -\frac{2\pi n_2 l}{\lambda} \frac{\partial}{\partial t} |E(t)|^2, \quad (2-2)$$

so that the frequency of the leading edge of the pulse becomes lower than the carrier frequency ω_0 , and that of the trailing edge of the pulse becomes higher. This frequency swept pulse is called a chirped pulse.

When the chirped pulse propagates through a medium characterized by anomalous group velocity dispersion (GVD), the leading edge of the pulse propagates more slowly than its trailing edge, resulting in optical pulse compression. The temporal broadening due to the absolute value of GVD can be compensated for by the compression due to self phase modulation (SPM) with anomalous GVD, making a stable optical soliton. In a silica optical fiber, anomalous dispersion exists in the wavelength region longer than 1.3 μm . It is quite advantageous for optical solitons that the loss minimum wavelength of silica fiber is around 1.5 μm at which the optical soliton can be generated. This characteristic is beneficial for long distance, high bit rate communication systems.

The propagation of a nonlinear pulse in a fiber with loss is described by the nonlinear Schrödinger equation:

$$-i \frac{\partial u}{\partial \xi} = \frac{1}{2} \frac{\partial^2 u}{\partial \tau^2} + |u|^2 u + i\Gamma u. \quad (2-3)$$

When the loss is ignored ($\Gamma=0$), the equation has a steady state and periodic soliton solutions. The initial condition is $A \text{sech}(t)$, which is well known as the lowest order ($N=1$) soliton when $1/2 < A < 3/2$, and especially for $A=1.0$, steady state pulse propagates along the transmission line. When the A is a positive integer, waveform of the pulses changes periodically along the propagation distance. When the A is not a positive integer, some part of the pulse forms N soliton where N is a nearest integer of A , and rest of the pulse becomes dispersive wave. The periodic distance is called soliton period, Z_{sp} . It is given by

$$Z_{sp} = \frac{\pi^2 c \tau^2}{\lambda^2 |D|}, \quad (2-4)$$

where D is the GVD, λ is a vacuum wavelength, τ is the normalizing time ($\tau = \tau_{FWHM}/1.76$ for sech shape pulse), and c is the speed of light in a vacuum. The peak power of the pulse required for the generation of an exact $A=1$ soliton pulse (P_1) is given by

$$P_1 = \frac{2\lambda^3 |D|}{4\pi^2 n_2 \tau^2}, \quad (2-5)$$

where n_2 is the nonlinear index of refraction (which for silica is $3.2 \times 10^{-20} \text{ m}^2/\text{W}$). The $A=1$ soliton is preferable for high speed, long distance propagation because the it does not change its shape throughout propagation, and also requires the lowest generating power.

The optical power loss (γ) of the silica fiber is minimized at a wavelength of $1.55 \mu\text{m}$, but still has a small loss, for example 0.22 dB/km . Hence the steady state soliton solution cannot be maintained over long distances because pulse energy decreases gradually due to this small loss. The relation between γ (in dB/km), Z_{sp} and value Γ (in m^{-1}) is given by

$$\Gamma = \frac{2}{\pi} Z_{sp} \frac{\gamma}{20000} [\log_{10} e]^{-1}, \quad (2-6)$$

When Γ is small, the perturbation theory indicates that the soliton pulse width broadens in inverse proportion to its amplitude.[2] If the transmission line has a slight gain along its length, the pulse width is shortened and the amplitude is increased by maintaining this soliton condition. These process are adiabatic so that it is reversible and all transferred energy changes soliton energy and forms no additional dispersive waves.

The characteristics of the optical soliton in optical fiber is summarized as follows: dispersion free, robust for perturbations, and self formation. Because of these property, the $N=1$ soliton seems promising as carriers for long distance, high bit rate optical communication systems.

However this useful property can not be maintained when Γ (or gain) becomes large. Soliton transmission suitable for lossy condition is described later in section 3.

II.2 Nonlinear Interactions

For an ideal soliton, the origin of soliton interaction is the nonlinear coupling of soliton pulses. When pulse overlap, their carrier frequencies are affected. The nonlinear term in the nonlinear Schrödinger (NLS) equation, $|U|^2 U$, is important in terms of qualitative behavior. Let U be a pulse pair, $u+v$, expand the nonlinear term, and extract the term relating to u . This gives

$$u(|u|^2 + 2|v|^2 + uv^*) \quad (2-7)$$

The first and second terms are self and cross phase modulation (SPM and XPM), respectively. The last term is a phase-sensitive interference term. When we ignore the dispersive term, the nonlinear phase rotation on pulse u is proportional to $|u|^2 + 2|v|^2 + uv^*$. Here, the SPM term cancels out the GVD term of the NLS so the frequency shift is proportional to

$$\frac{\partial}{\partial t}(2|v|^2 + uv^*), \quad (2-8)$$

Let $u = \text{sech}(t)$ and $v = \text{sech}(t + \Delta t)e^{i\phi}$ which means that pulse v advances by Δt and has phase of ϕ relative to pulse u . When Δt is large, we disregard the term $|v|^2$ because its effect on the pulse u is small compared to the uv^* term. The frequency shift at the center of the pulse u is

$$\Delta\omega \propto \left. \frac{\partial}{\partial t}(uv^*) \right|_{t=0} \cong 2e^{-\Delta t} e^{-i\phi} \quad (2-9)$$

For an in-phase case, $\phi = 0$, $\Delta\omega$ is greater than 0, which means u becomes faster than its original speed because the carrier frequency is in the anomalous dispersion region. This results in the generation of the attraction force. While $\phi = \pi$, $\Delta\omega$ becomes less than 0.

Quantitative results are obtained by a two-soliton solution of the NLS equation by the inverse scattering method. Various analyses have been performed by using this method to analyze the soliton transmission capacity.[3-5] From these analyses and numerical simulations, a criterion was found for avoiding soliton interaction: the soliton pulses should be separated by a distance of at least 6 times the pulse width.[6] Although soliton interaction can be ignored under this condition, the bit rate of the system is fairly limited.

Phase control or amplitude control was employed between input soliton pulses to avoid or reduce the interaction force [5,7] This approach reduced the interaction force, although precise control of the amplitude or phase of each pulse is required. Furthermore it might not be possible to maintain these conditions because of the existence of perturbations such as loss, noise during transmission, and optical filters. This means that it may not be easy to realize ultra-long distance transmission with these methods.

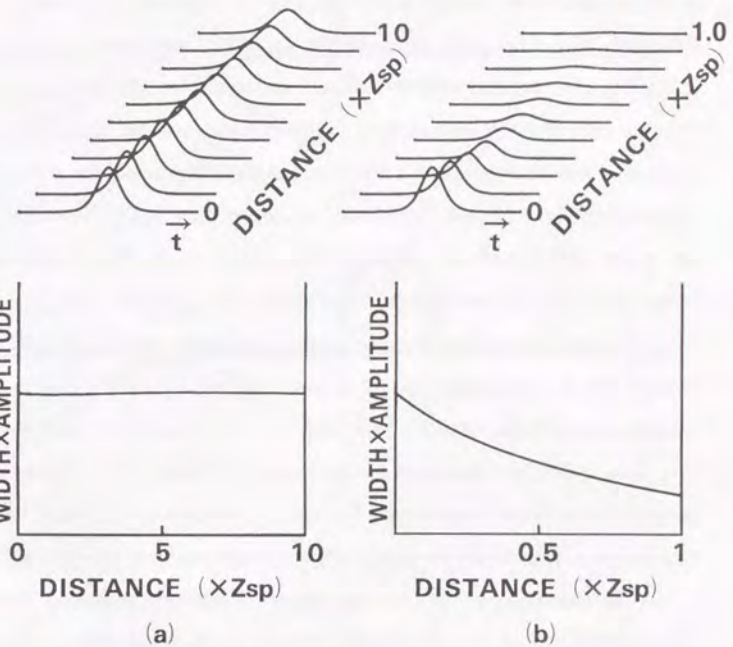


Figure 2.1 Relation between the soliton pulse width and its peak amplitude during propagation. The upper half of the figure shows pulse shape (amplitude) change along the propagation distance and the lower half of the figure shows the product of amplitude and pulse width. (a) $G=0.01$, (b) $G=1.0$.

II.3 Optical Loss and Amplification of Soliton

Figure 2.1 shows the relation between soliton pulse width and its peak amplitude throughout propagation. The data for $\Gamma = 0.01$ and 1.0 are illustrated in Fig. 2.1(a) and (b), respectively. The upper half of the figure shows pulse shape (amplitude) change along the propagation distance, assuming $\text{sech}(t)$ as an input pulse (i.e., exact $N=1$ soliton). The lower half of the figure shows the product of amplitude and pulse width. For Fig. 2.1(a) ($\Gamma = 0.01$), this product remains almost constant throughout propagation, which means that the perturbation theory is valid and the pulse propagates as an $N=1$ soliton over a long distance. On the other hand, for a large Γ of 1.0 given in Fig. 2.1(b), the amplitude decreases very rapidly, and therefore the pulse width can not preserve the soliton state. This pulse cannot propagate as an $N=1$ soliton because of its small amplitude.

In long distance optical transmission systems, periodic amplification is required to compensate for fiber loss. Figure 2.2 shows two types of amplification scheme used for this purpose. One uses distributed amplifier (Fig. 2.2a) and the other uses lumped amplifier (Fig. 2.2b). The former is suitable for soliton transmission because it provides an artificial loss-free transmission line, while the latter is very simple and easy to construct.

The Raman amplifier (A1) is a typical distributed amplifier. That is, a conventional optical fiber itself becomes an amplifying medium through the Raman process. An Er-doped fiber with a low Er ion concentration can also be used as a distributed amplifier (A2). In the Raman amplifier, the pump intensity decreases due to intrinsic fiber loss and pump depletion. In an Er-doped fiber amplifier, the pump intensity decreases due to fiber loss and absorption by Er ions. These amplifiers act as a pure distributed gain medium only when the gain distributes uniformly. Hasegawa pointed out that the decreases in pump intensity produce a periodic perturbation to the solitons, and either gain or loss dominates at certain positions. The

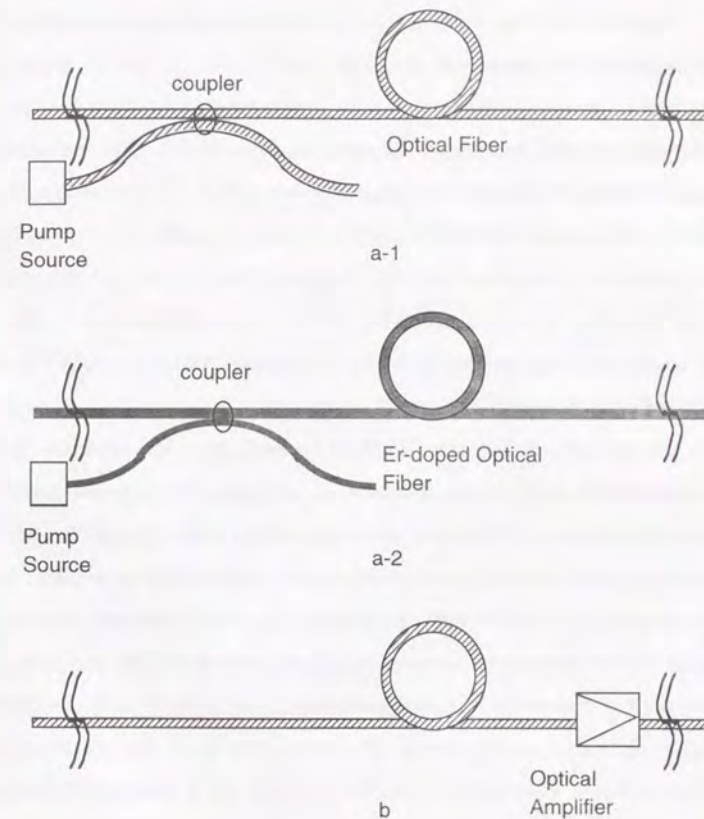


Figure 2.2 Two types of amplification scheme used for long distance optical transmission systems. (a) distributed amplifier, (b) lumped amplifier.

transmission loss of the soliton can only be compensated for by the overall periodic Raman gain.^[8] When Γ is small, the soliton pulse behaves as described in Fig. 2.1(a), and the pulse can propagate as an $N=1$ soliton over many multiples of Z_{sp} .

Based on this idea, long distance soliton transmission using periodic amplification by Raman amplifier is proposed.^[9] Smith and Mollenauer have demonstrated pulse transmission over more than 6000 km in a recirculating 42-km fiber loop with a Raman amplifier.^[10] The conditions of their system are $L=41.7$ km, $Z_{sp}=66$ km, $\gamma=0.22$ dB/km (fiber loss coefficient for signal), and $\alpha=0.29$ dB/km (fiber loss coefficient for pump). The loop length L (amplifier spacing) is of the order of Z_{sp} . In that case, even though they use a Raman amplifier, it cannot be described as an ideal distributed amplifier system. Γ at the input of the fiber becomes +0.58, at which the perturbation theory cannot be applied.

On the other hand, laser diode (LD) amplifiers and erbium-doped fiber amplifiers (EDFA) can be used as lumped amplifiers for soliton communication (Fig. 2.2b). An advantage of the lumped amplifier is its simple configuration, i.e., the amplifier region is clearly separated from the transmission line. The LD amplifier is very compact and reliable, but it has polarization dependent gain and a slight fluctuation in the transmitting signal pattern (pattern effect) due to the first gain recovery time which is comparable to transmitting speed. In contrast, the EDFA has the excellent characteristics of polarization insensitivity, high gain, low insertion loss, and no pattern effect because of its very slow gain recovery time. Since the EDFA needs a pumping laser, it was very important to discover a compact and efficient pumping source. Nakazawa et al. showed that 12.5 dB gain could be obtained by an EDFA pumped by a 1.48 μm distributed feedback laser diode (DFB LD),^[11] and the current gain thus achieved exceeds 45 dB.^[12] It was also demonstrated that picosecond and femtosecond solitons

can be amplified by the EDFA.^[13,14] Recently, the EDFA has been widely used for the optical amplification in the 1.5 μm region in addition to its optical soliton application.

II. 4 High order nonlinearities

Besides the optical loss, high order dispersion and high order nonlinearity strongly affect the soliton propagation characteristics. These effects are considered as a perturbation to the NLS equation consists of SPM and GVD.^[15,16] The leading terms are third order dispersion, self steepening effect, and self Raman effect. With these terms NLS becomes

$$i \frac{\partial u}{\partial \xi} + \frac{1}{2} \frac{\partial^2 u}{\partial \tau^2} + |u|^2 u = i \frac{k'''}{6k''\tau_0} \frac{\partial^3 u}{\partial \tau^3} - i \frac{2}{\omega_0 \tau_0} \frac{\partial}{\partial \tau} (|u|^2 u) + \frac{\tau_n}{\tau_0} u \frac{\partial}{\partial \tau} |u|^2 \quad (2-10)$$

The third order dispersion, named after third derivative of the wave vector k , is originated from wavelength dependence of the GVD.^[17] The self-steepening of the light pulse results from the intensity dependence of the group velocity,^[18] and soliton self frequency shift from the response time of the nonlinear index change or self Raman effect.^[19]

The coefficient of these terms are $1.1 \times 10^{-14} / \tau_0$, $1.7 \times 10^{-15} / \tau_0$, $5.3 \times 10^{-15} / \tau_0$, respectively, for $D=1$ ps/km-nm, $D_\lambda = 0.52$ ps/km-nm², and $\lambda=1.55$ μm , so that these terms should be taken into account when the pulse width becomes shorter than few pico-seconds.

II. 5 ASE noise

Although the optical amplifier successfully removed the limitation due to optical loss, it induced other limitations. One is degradation of signal to noise ratio (SNR) due to accumulation of ASE noise. The other is Gordon-Haus effect^[20] which gives rise to a random frequency change in the carrier frequency of the soliton pulse.

II.5.1 SN Ratio

Average ASE photon number added by one optical amplifier is given by

$$\mu m_i (G-1) \Delta\nu, \quad (2-11)$$

where G is a amplifier gain, $\Delta\nu$ is a bandwidth of the amplifier, and μ is a inversion parameter of the gain medium. m_i is a number of the polarization modes, for example, which is unity for LD amplifier and 2 for EDFA. Incorporating this ASE noise, the output from the optical amplifier $\langle n_{out} \rangle$ is given as

$$\langle n_{out} \rangle = G \langle n_{in} \rangle + \mu m_i (G-1) \Delta\nu. \quad (2-12)$$

Using the square law detector, the variance of the photon number is written as^[21]

$$\begin{aligned} \langle \sigma_{out}^2 \rangle &= \langle n_{out}^2 \rangle - \langle n_{out} \rangle^2 \\ &= G \langle n_{in} \rangle + (G-1) \mu m_i \Delta\nu + 2G(G-1) \mu \langle n_{in} \rangle \\ &\quad + (G-1)^2 \mu^2 m_i \Delta\nu + G^2 \beta \langle n_{in} \rangle \end{aligned} \quad (2-13)$$

The first and second terms are shot noise of the signal pulse and ASE, third is a signal-spontaneous beat noise, fourth is a spontaneous-spontaneous beat noise and last is a excess noise due to incoherency. For coherent pulse, β becomes zero. When G becomes large, shot terms can be neglected.

Long distance transmission system which consists of k amplifiers with gain G , and each section has a transmission loss $L (= 1/G)$, is given as

$$\langle n_k \rangle = \langle n_{in} \rangle GL + k(G-1)L \mu m_i \Delta\nu, \quad (2-14)$$

and variance of the photon number σ_k^2 is calculates by the same manner.

The SNR for this k -stage amplifier system is given as

$$S/N = \frac{\langle n_k \rangle^2 T}{\sigma_k^2}, \quad (2-15)$$

where T is a time slot width of the detector.

Minimum required SNR is determined by the error rate allowed to the system. Assuming that the distribution of the noise is a gaussian, the required SNR for error rate of 10^{-11} is about 22.5 dB.^[22] More precise

analyses for the bit-error probability with optical amplifier is also reported.^[23]

II.5.2 Gordon-Haus jitter

The mean square frequency fluctuation due to an amplifier with gain G is given as

$$\langle \delta\Omega^2 \rangle = (G-1) A / 3N_0, \quad (2-11)$$

where $A = 1.76/t_0$, t_0 is the pulse width, and N_0 is the number of photons per unit energy ($= p_0 t_0 / h\omega$, ω is carrier frequency, p_0 is the peak power of the soliton). The random frequency change results in timing jitter through the group velocity dispersion of the fiber and the accumulation of jitter finally causes a bit error.

The variance of jitter is given as

$$\langle \delta t^2 \rangle = (G1)AL^3 / 9N_0 Z_a, \quad (2-12)$$

where Z_a is the amplifier spacing and L is the overall length of the transmission line. To ensure a bit error rate of 10^{-9} , the detector window acceptance width must be 6.1 times wider than the standard deviation of the timing jitter for a Gaussian distribution.

The limit of the bandwidth and distance product is

$$\begin{aligned} (RL)^3 &\leq 0.1372 t_0^2 R^3 N_0 / \Gamma \\ &= \frac{0.1372 t_0^2 R^3 A_{eff}}{h\Gamma n_2 |D|} \end{aligned} \quad (2-12)$$

where R is the bit rate of the system, and t_0 and $2t_w$ are the full width at half maximum pulse width and the detector window width, respectively. For example, when $R = 10$ Gbit/s, $t_0 = 30$ ps, $2t_w = 67$ ps, fiber loss $\gamma = 0.24$ dB/km, $D = -2$ ps/(km-nm), the amplifier spacing is 50 km and $A_{eff} = 50 \mu\text{m}^2$, the maximum distance L is only 4600 km. To ensure a smaller bit error rate, the total transmission distance should be shortened.

Another derivation of the Gordon-Haus effect which directly compute the timing jitter have also reported.^[24]

- 1 R. H. Stolen and Chin Lon Lin: Self-phase-modulation in silica optical fibers, *Phys. Rev.* vol. **A17**, pp. 1448-1453 (1978).
- 2 J. Satsuma and N. Yajima: Initial Value Problems of One-Dimensional Self-Modulation of Nonlinear Waves in Dispersive Media, *Suppl. Prog. Theor. Phys.* vol. **55**, pp. 284-307 (1974).
- 3 B. Hemmerson and D. Yevik: Numerical investigation of soliton interaction, *Electron. Lett.* vol. **19**, pp. 570-571 (1983).
- 4 J.P. Gordon: Interaction forces among solitons in optical fibers, *Opt. Lett.* vol. **8**, pp. 596-598 (1983).
- 5 P. L. Chu and C. Desem: Mutual interaction between solitons of unequal amplitudes in optical fibre, *Electron. Lett.* vol. **21**, pp. 1133-1134 (1985).
- 6 A. Hasegawa: Numerical study of optical soliton transmission amplified periodically by the stimulated Raman process, *Appl. Opt.* vol. **23**, pp. 3302-3309, (1984).
- 7 J. P. Gordon: Interaction forces among solitons in optical fibers, *Opt. Lett.* vol. **8**, p. 596 (1983)
- 8 A. Hasegawa: Numerical Study of soliton transmission amplified periodically by the stimulated Raman process, *Appl. Opt.* vol. **23**, pp. 3302-3309 (1984).
- 9 L. F. Mollenauer, J. P. Gordon, and M. N. Islam: Soliton propagation in long fibers with periodically compensated loss, *IEEE J. Quantum Electron.* vol. **QE-22**, pp. 157-173 (1986).
- 10 R. G. Smith and L. F. Mollenauer: Experimental observation of adiabatic compression and expansion of soliton pulses over long fiber paths, *Opt. Lett.* vol. **14**, pp. 751-753 (1989).
- 11 M. Nakazawa, K. Suzuki, and Y. Kimura: Efficient Er^{3+} -doped optical fiber amplifier pumped by 1.48 μm InGaAsP laser diode, *Appl. Phys. Lett.* vol. **54**, pp. 295-297 (1989).
- 12 Y. Kimura, K. Suzuki, and M. Nakazawa: 46.5 dB gain in Er^{3+} -doped fibre amplifier pumped by 1.48 μm GaInAsP laser diodes, *Electron. Lett.* vol. **25**, pp. 1656-1657 (1989).
- 13 M. Nakazawa, K. Suzuki, and Y. Kimura: Soliton amplification and transmission with Er^{3+} -doped fibre repeater pumped by GaInAsP laser diode, *Electron. Lett.* vol. **25**, pp. 199-200 (1989).
- 14 B. J. Ainslie, K. J. Blow, A. S. Gouveia-Neto, P. G. J. Wigley, A. S. B. Sombra, and J. R. Taylor: Femtosecond soliton amplification in erbium doped silica fibre, *Electron. Lett.* vol. **26**, pp. 186-187 (1990).
- 15 V. I. Karpman and E. M. Maslov: Perturbation theory for solitons, *Sov. Phys. JETP* vol. **46**, pp. 281-291 (1977).
- 16 M. J. Potasek and M. Tabor: Exact solutions for an extended nonlinear Schrödinger equation, *Phys. Lett. A* **154**, pp. 449-452 (1991).
- 17 D. Marcuse: Pulse distortion in single-mode fibers, *Appl. Opt.* vol. **19**, pp. 1653-1660 (1980).
- 18 F. De Martini, C. H. Townes, T. K. Gustafson and P. L. Kelley: Self-steepening of light pulses, *Phys. Rev. vol.* **164**, pp. 312-323 (1967).
- 19 J. P. Gordon: Theory of the soliton self-frequency shift, *Opt. Lett.* vol. **11**, pp. 662-554 (1986).
- 20 J. P. Gordon and H. A. Haus: Random walk of coherently amplified solitons in optical fiber transmission, *Opt. Lett.* vol. **11**, pp. 665-667 (1986).
- 21 H. Ishio et al.: Optical amplifiers and its applications, Ohm press, Tokyo (1992). (in Japanese)
- 22 Y. Shigei: High-Speed PCM, Corona publishing, Tokyo (1975). (in Japanese)
- 23 D. Marcuse: Derivation of analytical expression for the bit-error probability in lightwave systems with optical amplifiers, *IEEE J. Lightwave Technol.* vol. **8**, No. 12, pp. 1816-1823 (1990).
- 24 D. Marcuse: An alternative derivation of the Gordon-Haus effect, *J. Lightwave Technol.* vol. **10**, No. 2, pp. 273-278 (1992).

III. SOLITON TRANSMISSION WITH LUMPED AMPLIFIERS

It was long believed that soliton pulses could not be propagated over long distances with lumped amplifiers because the pulse loses its soliton property if the gain or loss is large. In 1982, a simple and interesting soliton transmission method using a lumped amplifier was reported with a 10 km repeater spacing and an $A=1$ soliton.^[1] However, the repeater spacing was too short to apply it to actual systems and there were no practically applicable lumped amplifiers. This meant that distributed amplifier methods such as Raman amplification remained the main area of soliton transmission research at that time.

In the late 1980's, great progress was made on the erbium-doped fiber amplifier (EDFA), which is a lumped amplifier in the 1.5 μm region. The success of laser diode pumped EDFAs^[2,3] has provided optical amplifiers that are easy to operate. The EDFA has advantageous characteristics for a transmission system such as high gain, high output power, wide bandwidth, and polarization independence. Its capacity for soliton amplification has also been demonstrated.

While undertaking research on soliton transmission technology using this new amplifier we developed the idea of using the dynamic waveform change which occurs during non-integer order soliton pulse propagation in an optical fiber with optical loss. Here I describe this new soliton communication method which is suitable for a lumped amplifier system, and which we call the dynamic soliton communication method.^[4] This technique requires no additional elements but uses a slightly higher input than ordinary soliton transmission. The advantages of this technology and EDFA were proved by various experiments which were performed directly after the development of this technology.^[5-9]

III.1 Physical image of new soliton transmission technique

Because of fiber loss (Γ), for example -0.22 dB/km at a wavelength of 1.55 μm , the steady state soliton solution cannot be maintained. We solve eq. (2.3) numerically by using split-step Fourier method. [see Appendix 1] When the fiber loss is small, the perturbation theory indicates that the soliton pulse width broadens in inverse proportion to its amplitude. This no longer holds true when the loss becomes large as already shown in Fig. 2.1(b). This pulse cannot propagate as an $A=1$ soliton because of its small amplitude.

First we study the propagation of $A \neq 1$ soliton pulses. It is well known that lowest order ($N=1$) solitons are asymptotically produced in the lossless optical fiber when the pulse amplitude is $1/2 < A \leq 3/2$. While $\Gamma \neq 0$, input amplitude must somewhat increase to create $N=1$ soliton. Figure 3.1 shows the evolution of the soliton waveform along fibers. The conditions for Fig. 3.1(a) and (b) refer to a $\Gamma=-0.01$ with 1.4 sech(t) input, and $\Gamma=-1$ with 1.4sech(t) input, respectively. The loss is the same as described in section 2.3 but the amplitude is 1.4 times larger than that of described in the section. For small Γ corresponding to Fig. 3.1(a), the pulse width first narrows and then varies around a certain value. For $\Gamma=-1$ shown in Fig. 3.1(b), the rate of intensity decrease is fast, and pulses soon lose nonlinearity due to their small intensity.

Figure 3.2 shows the pulse width, the peak amplitude and the chirp at the center of the pulse as a function of distance for various A values with $\Gamma=-1$. The pulse width and the peak amplitude are shown by a solid line and a broken line, respectively, in the upper half of the figure. The chirp is shown in the lower half. Distances in km are also given in the abscissa of the upper halves of the figures. Here, fiber parameters of $D=3$ ps/km/nm and $\Gamma=-0.22$ dB/km are used. The corresponding pulse width is 21.6 ps and the corresponding soliton period is 62 km. The curves of $A=1.4$ in Fig. 3.2

show the same condition as Fig. 3.1(b). For $A=1.4$ through 2.5 in Fig. 3.2, the pulse first narrows and then broadens. When Γ is small the pulse width narrows again, but for a large Γ the pulse broadens monotonously. It has been suggested that increasing the peak power of the soliton pulse can improve transmission capacity.^[10] Unnecessarily high input power produces more non-soliton parts, therefore, we must be careful not to use extremely high input power as input pulse. Furthermore, it is not always true that the higher input power enables longer transmission distances. High input power cause pulse broadening due to GVD because SPM produces wider frequency broadening than low input power, as in Fig. 3.2. Here, it can be said that there is an optimum condition for maximizing transmission capacity.

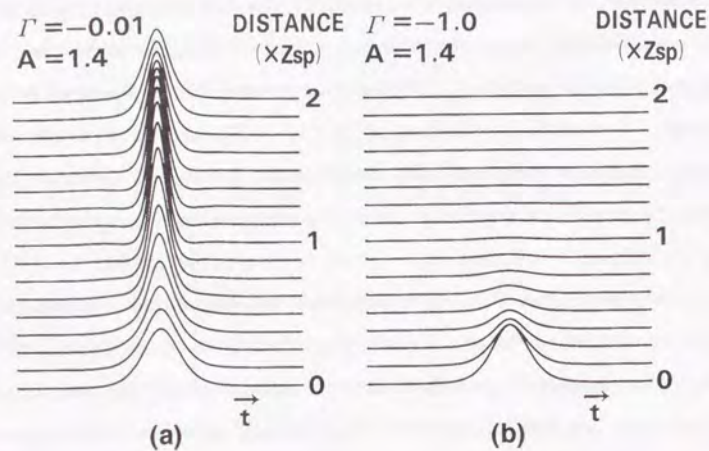


Figure 3.1 The evolution of the soliton waveform along fibers. (a) $G=-0.01$ with 1.4 sech (t) input, (b) $G=-1$ with 1.4sech (t) input.

As seen in Fig. 3.2, the pulse width recovers its input value at a certain distance when $A>1$. While amplitude of the pulse at that distance is quite low to support a soliton. If the pulse is amplified to a certain power, the pulse will recover the soliton property as far as the pulse distortion at that distance is small. Repeating this process will enable soliton to propagate for long distance with lumped amplifiers.

III.2 Long distance transmission system with lumped amplifiers

Here we discuss the long distance transmission with lumped amplifiers. For simplicity, we assume an ideal amplifier, which amplifies pulses with no distortion and add no noise such as ASE. Coupling loss is omitted from the calculation because coupling loss suddenly reduces the amplitude without increasing the pulse width and does not affect the nonlinear phase, this loss can be compensated for by the ideal amplifier. In the calculation, pulse width around 20 ps is assumed so as not to induce higher order nonlinearity such as optical shock^[11] and Raman self frequency shift.^[12]

III.2.1 Automatic Power Control

The actual amplifier installed in a transmission system has automatic gain controlling circuit (AGC) to stabilize the transmission system. A feedback circuit in an amplifier stabilizes output power of the amplifier, so that it is referred to as automatic power control (APC) circuit. Here I study a long distance pulse propagation under lumped amplifier with APC.

Figure 3.3 shows the evolution of a soliton pulse in the optical fibers with loss and lumped amplifiers with amplifier spacing of 31 km. Here, the parameters of $\gamma=-0.22$ dB/km, and $D = 3$ ps/km/nm are used ($\Gamma = -1.0$). Because of large D value and wide pulse width, dispersion slope and soliton self frequency shift are neglected. For simplicity, ASE noise is also ignored

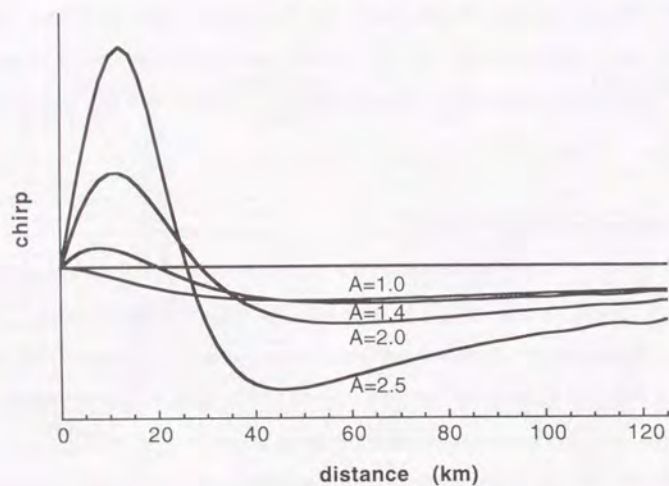
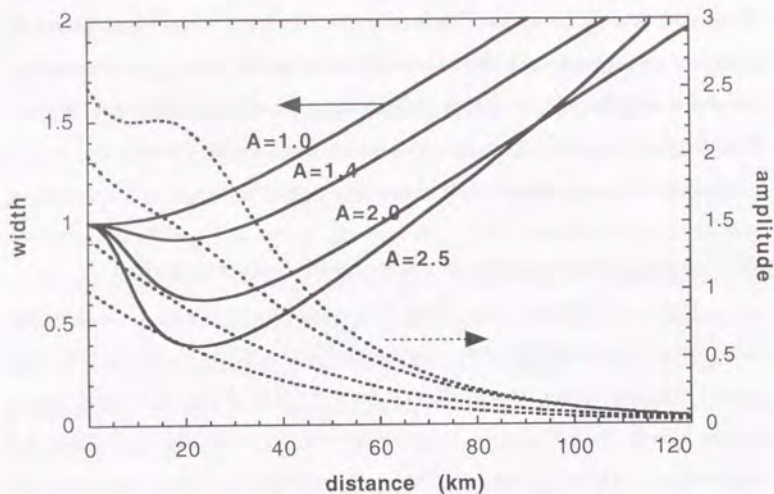
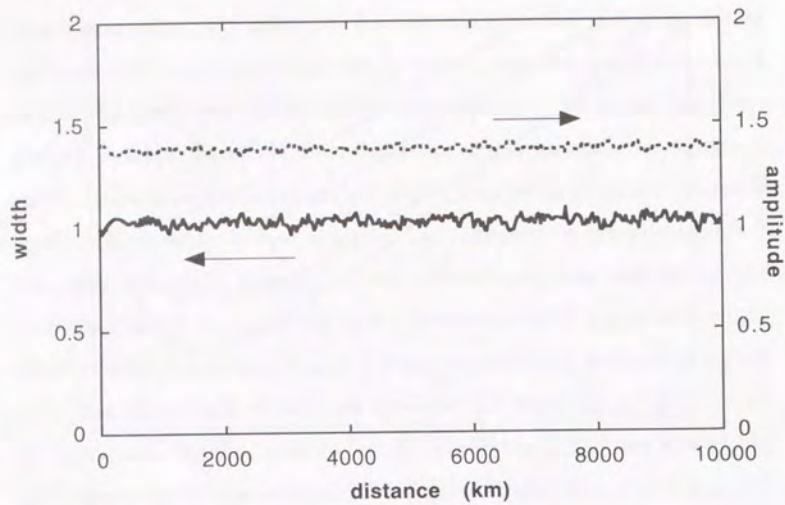


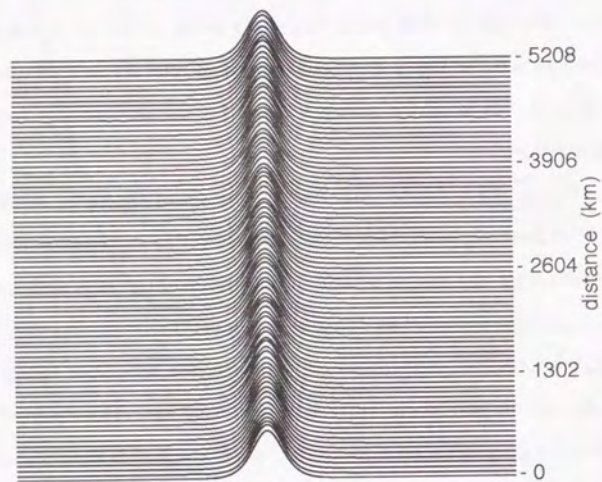
Figure 3.2 The pulse width, the peak amplitude and the chirp at the center of the pulse as a function of distance for $A = 1.0, 1.4,$ and 2.0 .

in the simulation. Figure 3.3(a) is the pulse width and the peak amplitude of the pulse just before it reaches each amplifier (output of each fiber). Figure 3.3(b) is a panoramic view of the pulse envelope. The amplifier spacing is determined so that the pulse width at the output end of the fiber is almost the same as that at the input end. The pulse width is slightly different at each input because of residual nonlinear phase change. When the pulse changes periodically, i.e., the pulse regains its amplitude, shape and phase after each amplification, the propagation distance is extended. The critical length L_c is characterized here that a certain distance at which the pulse recovers its width, making the pulse shape close to that at input. From Fig.3.2(b), L_c is $0.55 Z_{sp}$ for $A=1.4$ and $\Gamma=-1.0$. For $\lambda = 1.55 \mu\text{m}$, $D = 3 \text{ ps/km/nm}$ and $t_{FWHM} = 21.6 \text{ ps}$ ($\tau = 12.3 \text{ ps}$), $0.55Z_{sp}$ correspond to 34 km. In the present case, it should be noted that the pulse energy at each input of the fiber is kept constant even though the amplitude and pulse width of the output of the fibers are not equal. This occurs due to the fact that the periodically steady state pulse has slight chirp while the initial pulse is not chirped as seen in Fig. 3.2. Take this effect into account, amplifier spacing L_a should set slightly shorter than L_c to accomplish long distance transmission.

Figure 3.3 indicates that the fluctuation of the pulse width is within 25 % at 250 amplifications. When the pulse separation is 100 ps, the fluctuation of the pulse width does not produce any serious problems. Figure. 3.3(b) shows that the pulse distortion is small even after many amplifications (140 amplifications). Here, the amplifier spacing is 31 km and the 140 amplifications corresponds to 4200 km. This means that a single soliton can propagate over more than 4000 km in this simple system. It has been shown that this amount of gain is easily obtained with an Er^{3+} -doped fiber amplifier pumped at $1.48\text{--}1.49 \mu\text{m}$,^[13, 2] even when a laser diode is used as a pump source.

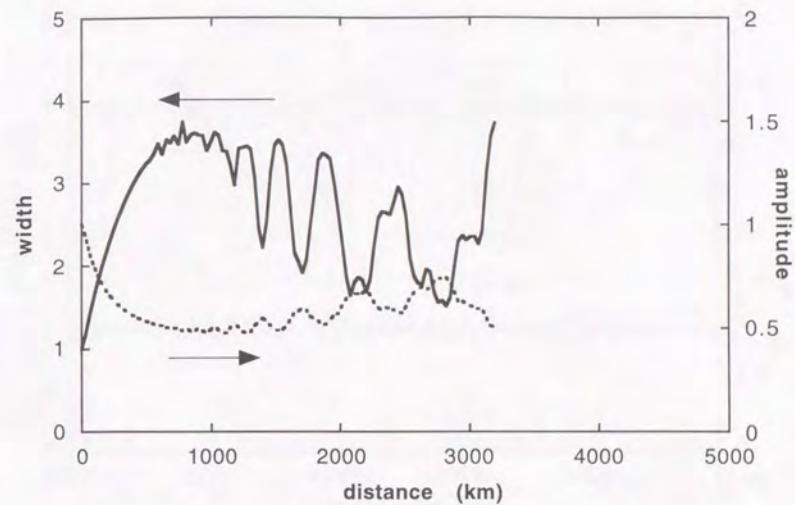


(a)

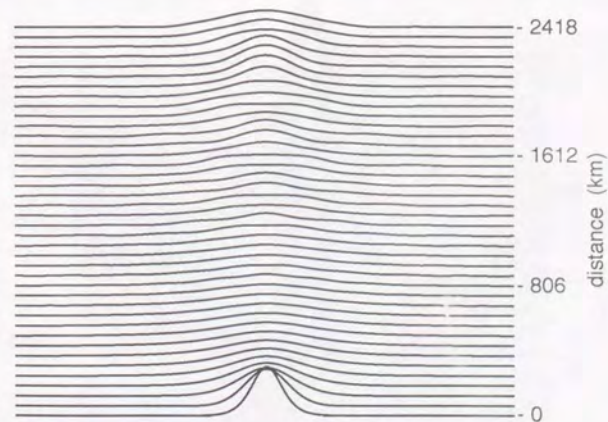


(b)

Figure 3.3 The evolution of a soliton pulse in the optical fibers with loss and lumped amplifiers. $A=1.4$ and $L_a=31$ km.



(a)



(b)

Figure 3.4 Same as Fig. 3.3 except that $A=1.0$.

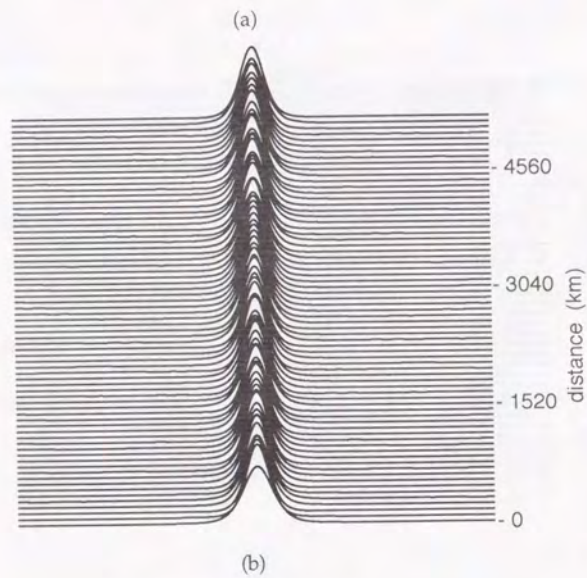
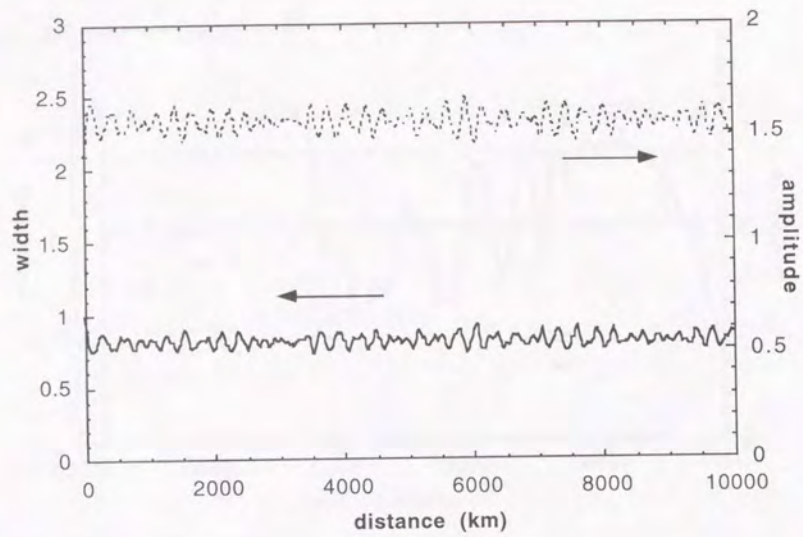


Figure 3.5 Same as Fig. 3.3 except that amplifier spacing is $0.3 Z_{sp}$ (19 km).

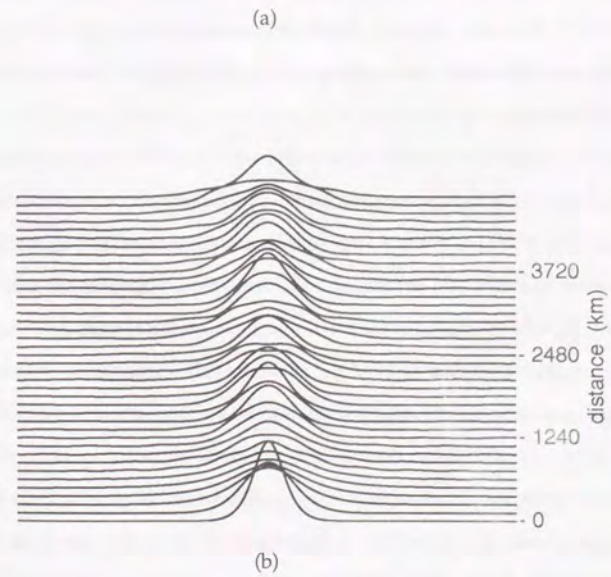
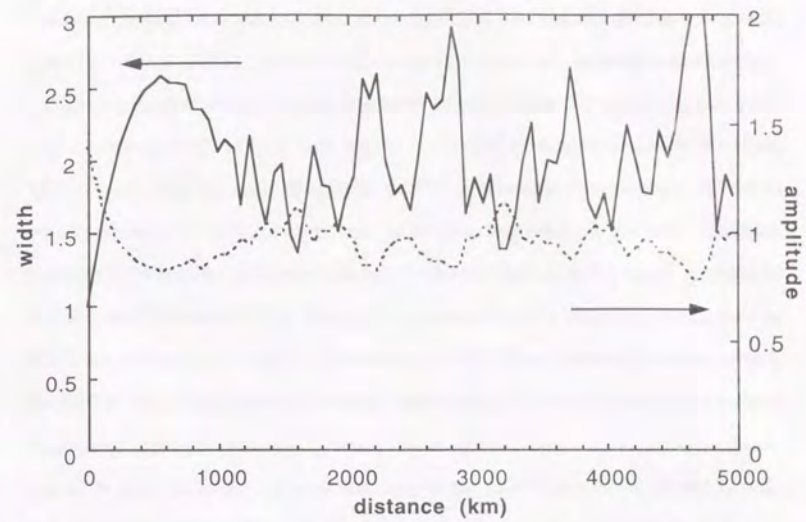


Figure 3.6 Same as Fig. 3.3 except that amplifier spacing is $1.0 Z_{sp}$ (62 km).

For comparison, the same calculation for $A=1.0$ is shown in Fig. 3.4. The pulse width shown in Fig. 3.4(a) broadens quickly and pulse could not holds its shape even 1000 km as seen in Fig. 3.4(b). This clearly indicates that simply increasing the input power is very advantageous for long distance soliton transmission.

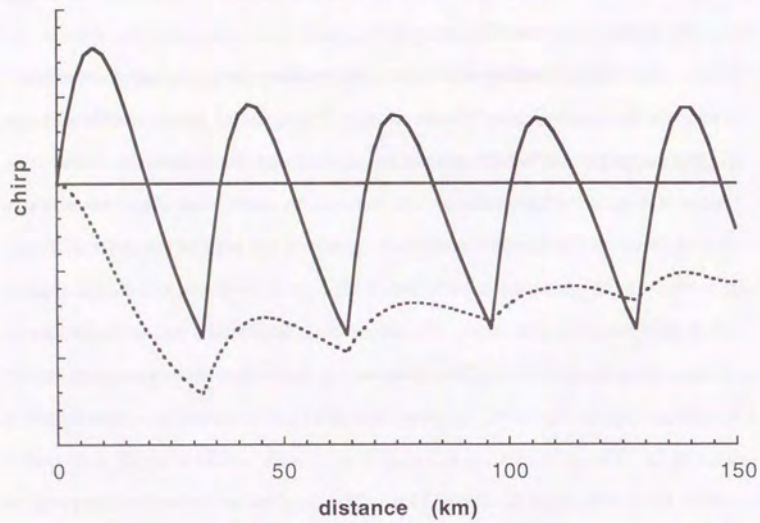
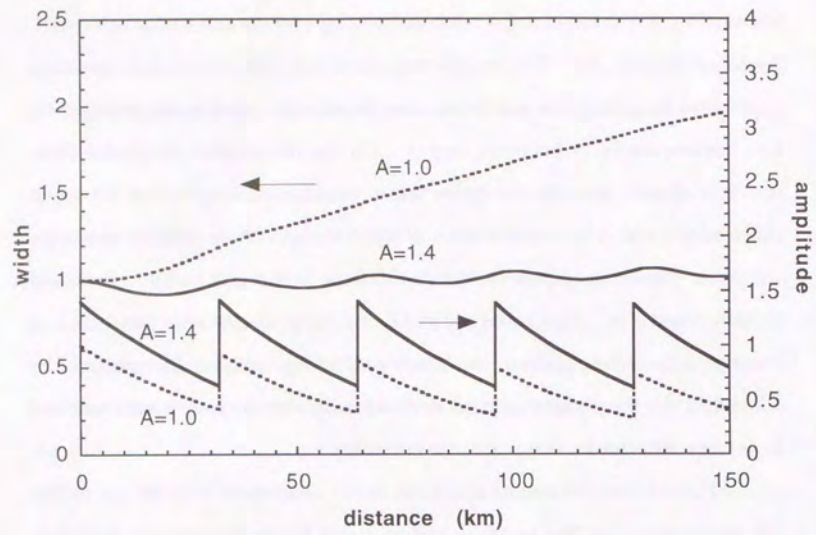
To investigate the effect of the amplifier spacing change in this method, shorter and longer amplifier spacings z than L_c for $A=1.4$ are shown in Figs. 3.5 and 3.6, respectively. An example of shorter amplifier spacing, $z=19$ km ($0.3 Z_{sp}$), is shown in Fig. 3.5. It does not adversely affect propagation characteristics. The pulse width suddenly decreases to 80 % and the fluctuation of the pulse width is ± 10 % throughout the 10,000 km transmission. The disadvantage of employing shorter amplifier spacing is that it needs more amplifiers for the same distance. An example of longer amplifier spacing, $z = 62$ km (Z_{sp}), is shown in Fig. 3.6. In contrast with Fig. 3.5, longer amplifier spacing drastically shortens the propagation distance. Furthermore the pulse shape shown in Fig. 3.6(b) is not maintained after 40 amplifications.

Peak amplitude, width, and chirp for Figs. 3.3~3.6 are given in Fig. 3.7 as a function of propagation distance. The conditions of the broken lines in Fig. 3.7(a) are $A=1.4$, $\Gamma=-1.0$ and $z=31$ km (0.52 times Z_{sp}), and those of the solid lines are $A=1.0$, $\Gamma=-1.0$ and $z=31$ km. Note here that 31 km is a little shorter than L_c for $A=1.4$ with $\Gamma=-1.0$ because of the reason described before. When an $A=1.4$ soliton is used as an input pulse, the pulse width recovers its input value at the first amplifier (i.e., at the output end of the fiber). At that point, the amplifier returns the pulse to its initial power, so that the pulse remains an $A=1.4$ soliton. However when an $A=1$ soliton is used as an input pulse, the pulse width becomes 1.2 times broader than the input pulse width at the first amplifier. The amplifier returns the broadened pulse to its initial power, so that the pulse becomes an $A=1.2$ soliton. This

acts as a increased input of the broader soliton in the next fiber. The broken lines in Fig. 3.7(b) are $A=1.4$, $\Gamma=-1.0$ and $z=Z_{sp}$, and the solid lines are $A=1.4$, $\Gamma=-1.0$ and $z=0.3 Z_{sp}$. For the repeater spacing $z=Z_{sp}$, which is longer than L_c , we see that the pulse width becomes broader than the input pulse width and consequently A becomes higher. On the other hand, for $z=0.3 Z_{sp}$, which is shorter than L_c , the pulse width becomes narrower than the input pulse width and A becomes lower. If the distortion of the pulse is not large, the pulse gains steady states which is different from input pulse. It should be also noted that when z is equal to L_c , the chirp oscillates around zero as shown by the broken line in the lower part of Fig. 3.7(a). Comparing Fig. 3.7(a) and (b), the present method in which amplifier spacing is set at around L_c is very efficient for long distance transmission.

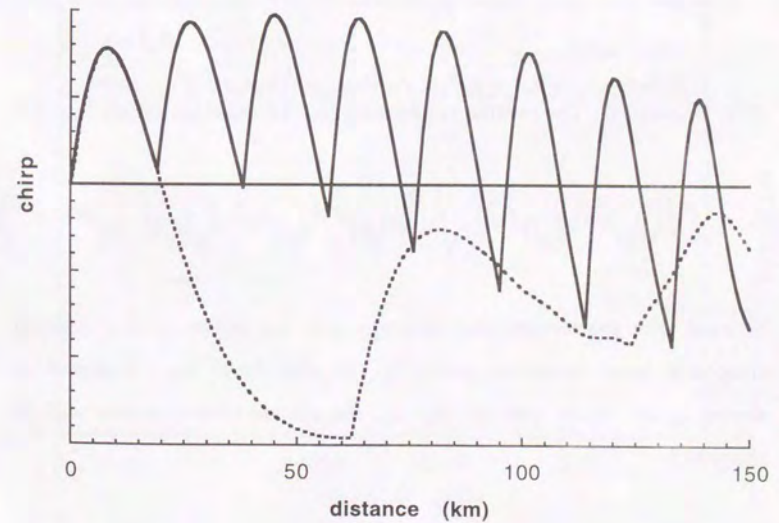
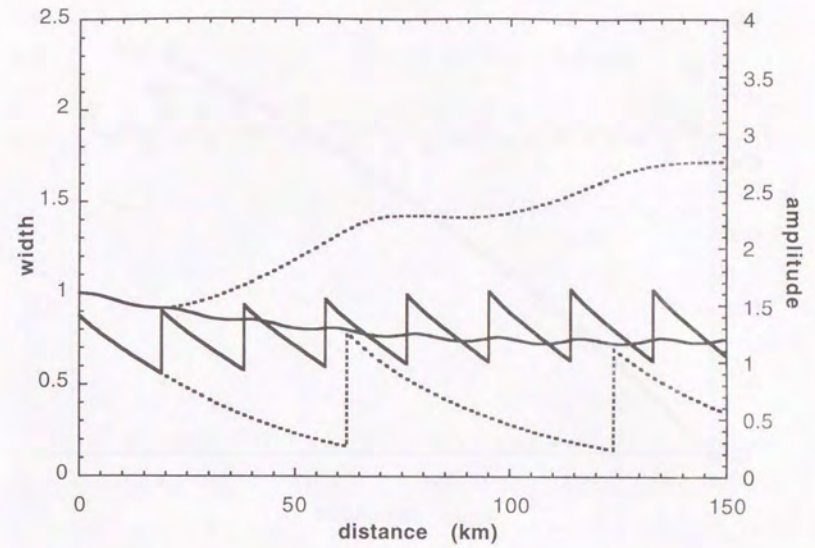
The relation between L_c and the input amplitude A is shown in Fig. 3.8 where Γ is -1.0 . The actual values of A and L_c are determined from Eqs. (3) and (4) when λ , τ and $|D|$ are given.

One factor limiting the pulse propagation in the lumped amplifier system is the nonrestoring phase change. It originates in amplitude change during propagation, which results in pulse shape distortion. One reason is that $A \neq 1$ solitons have dispersive nonsoliton parts, and these nonsoliton parts become background noise. In general, the higher the A for a fiber with loss the greater the occurrence of dispersive parts and additional nonlinear phase change. Therefore the transmitted pulse shape is considerably distorted. Calculations are carried out to investigate the amplitude dependence of the present method. The amplitude spacings are set at L_c . The conditions are $A=1.2$, $\Gamma=-1.0$ with $z=0.33 Z_{sp}$ (20 km) and $A=1.6$, $\Gamma=-1.0$ with $z=0.7 Z_{sp}$ (43 km). The results are shown in two parts of Fig. 3.9, which are drawn in the same manner as Fig. 3.3(b). The upper part of Fig. 3.9 indicates that transmission distance will be extended if more amplifiers can be used in the same transmission distance. A smaller A can



(a)

Figure 3.7 Evolution of pulse characteristics along the fiber.



(b)

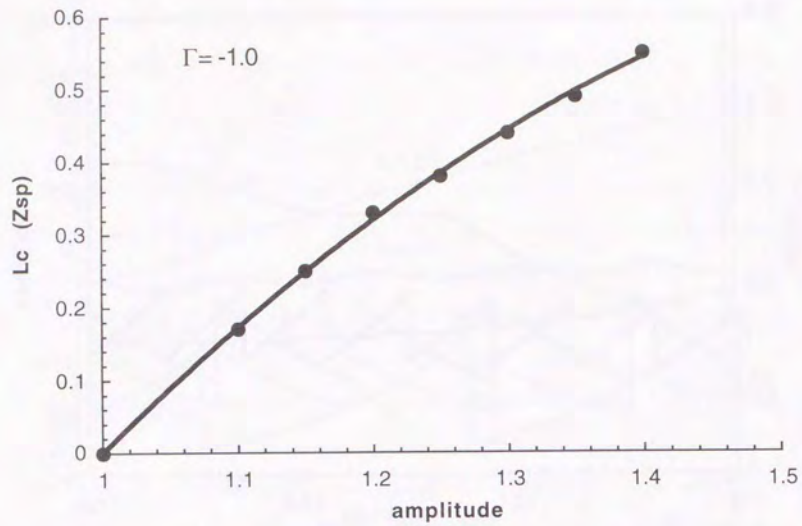


Figure 3.8 The relation between L_c and the input amplitude A .

be used with shorter amplifier spacings, and that causes smaller residual chirp and fewer nonsoliton parts. On the other hand, for a higher A as shown in the lower part of Fig. 3.9, the transmission distance will be shortened.

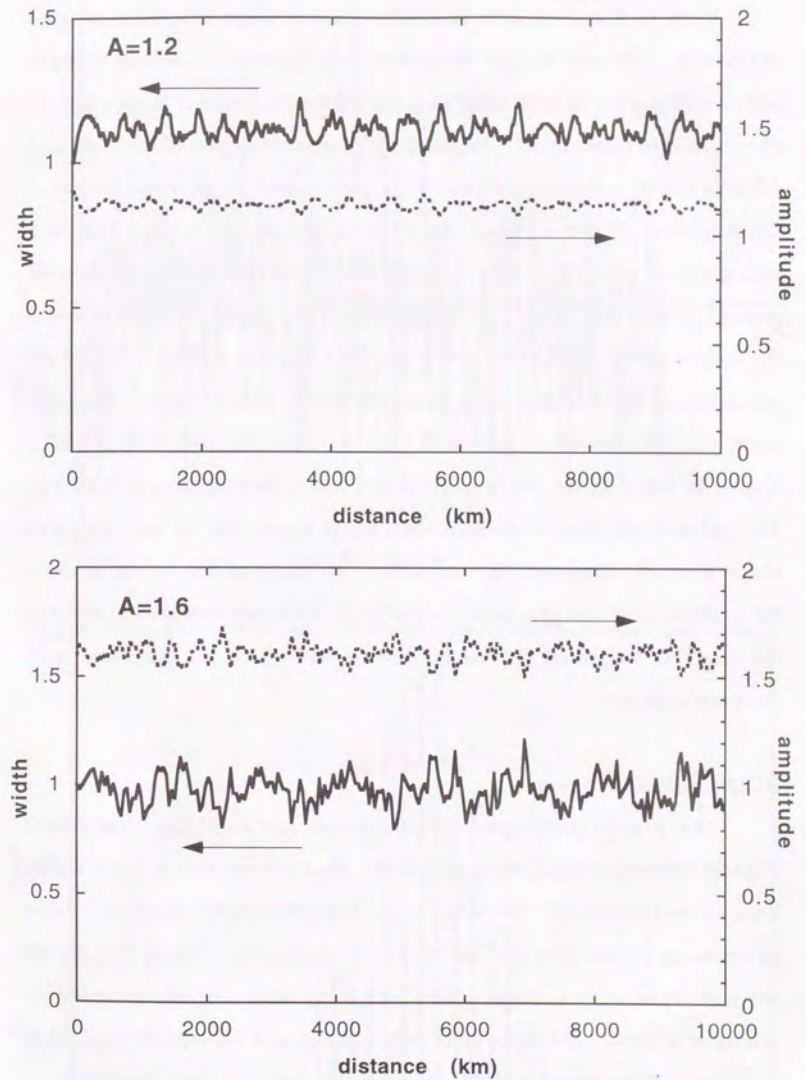


Figure 3.9 Effect of amplifier change on preemphasis method. (a) $A=1.2$ and $z=0.33 Z_{sp}$, (b) $A=1.6$ and $z=0.7 Z_{sp}$.

III.2.2 Gain Fluctuation

Even in a system with feedback, there is a small amount of gain fluctuation. To take the gain fluctuation into account, a random value is added to the gain of each amplifier, in which a fluctuation is assumed to obey Gaussian distribution. Standard deviations of the gain of $\sigma=0.1$ dB and 0.3 dB are used in the calculations. First, we checked the gain distribution of the amplifiers. Figure 3.10(a) is the error of each gain and Fig. 3.10(b) is a histogram of the gain error for $\sigma=0.3$ dB. This distribution is random enough to represent actual gain fluctuations. The random gain is added to the soliton pulse. Results for $A=1.4$ and $z=31$ km with $\sigma=0.1$ dB and 0.3 dB are shown in Fig. 3.11 and Fig. 3.12, respectively. In both figures, the pulse width variation increases compared with Fig. 3.3. However, for $\sigma=0.1$ dB shown in Fig. 3.11 the pulse is good enough to propagate over 9000 km. The pulse width fluctuation over 9000 km is within $\pm 10\%$, and the pulse shape is clearly distinguished from noises. In this condition, 0.1 dB is about 1.5% of the amplifier gain ($0.22 \times 31=6.82$ dB), and therefore we can say that the lumped amplifier system is stable even when the amplifier gain fluctuate a little.

III.2.3 Dispersive Waves

The present technique, which uses an $A>1.0$ soliton, produces a slightly dispersive wave compared to an ideal soliton transmission which uses an $A=1.0$ soliton. Here, we check the effect of the dispersive wave components by calculating a soliton pair transmission. Figure 3.13 shows the waveforms of an in-phase soliton pair of the same intensity separated by ten pulse widths. The input amplitude is $A=1.4$ and the repeater spacing is $z=31$ km. There seems to be no serious problems under these conditions.

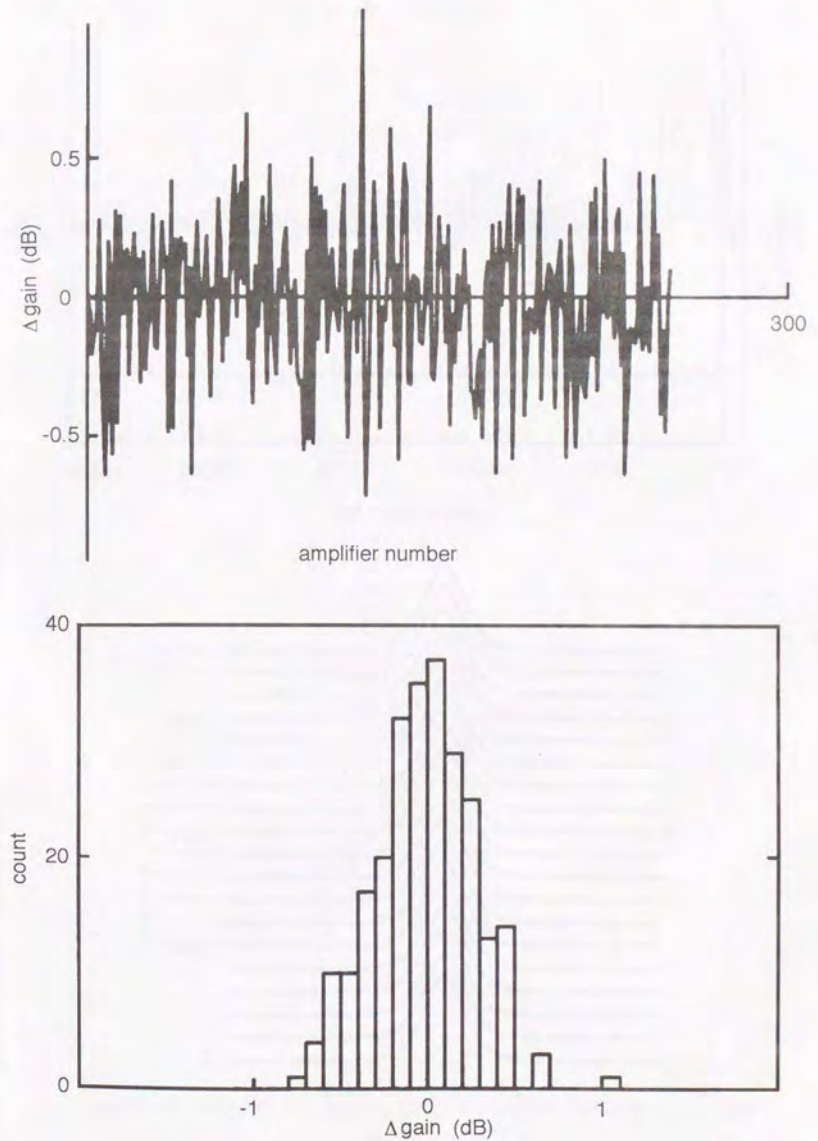


Figure 3.10 Distribution of gain fluctuation. Standard deviation is 0.3dB.

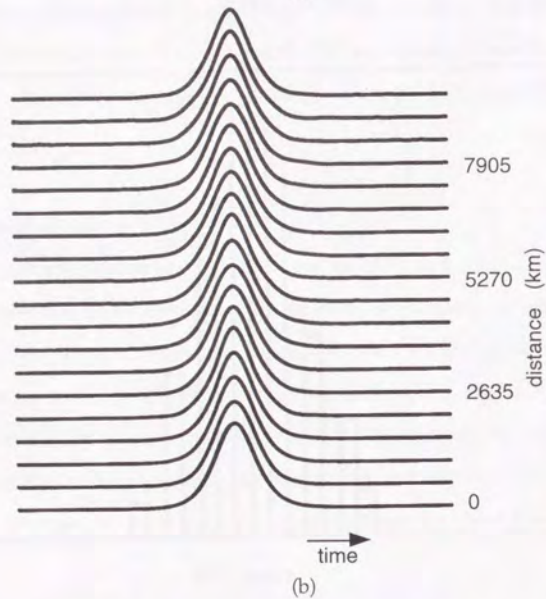
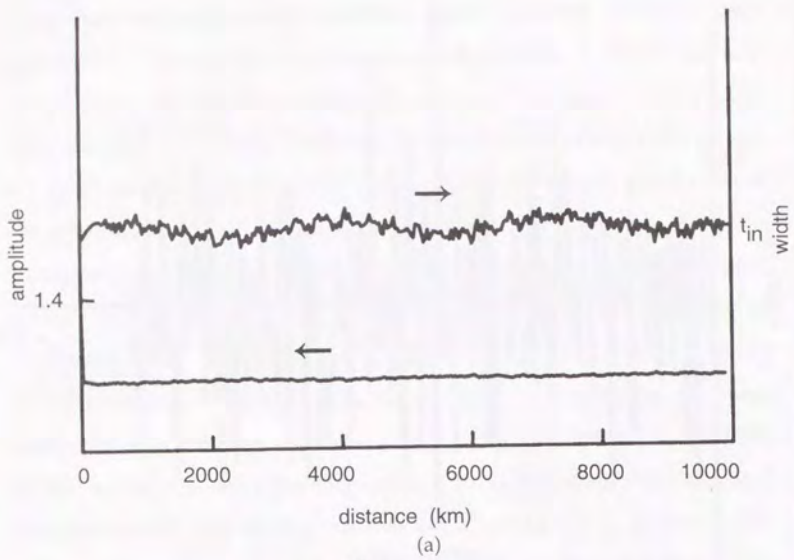


Fig. 3.11 Evolutoin of the pulse width and peak amplitude with gain fluctuation (standard deviation is 0.1 dB). Conditions are the same as Fig. 3.3.

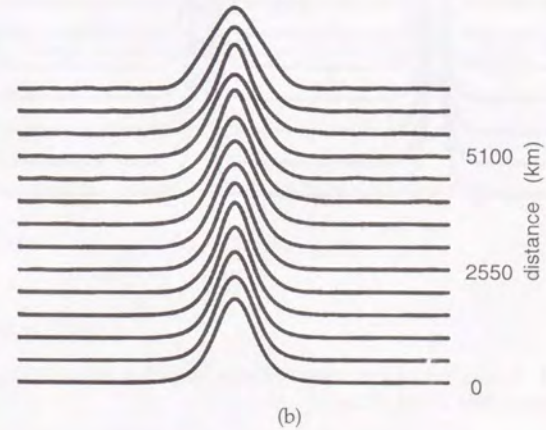
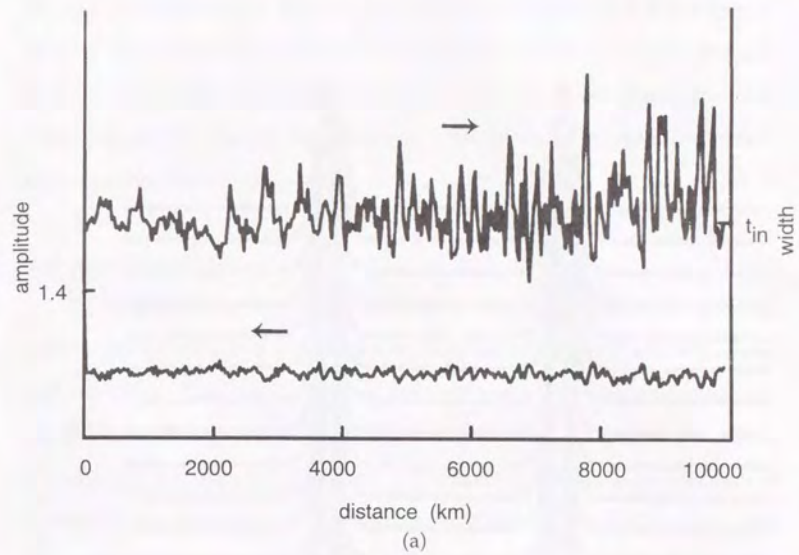


Figure 3.12 Same as Fig. 3.11 except that standard deviation is 0.3 dB.

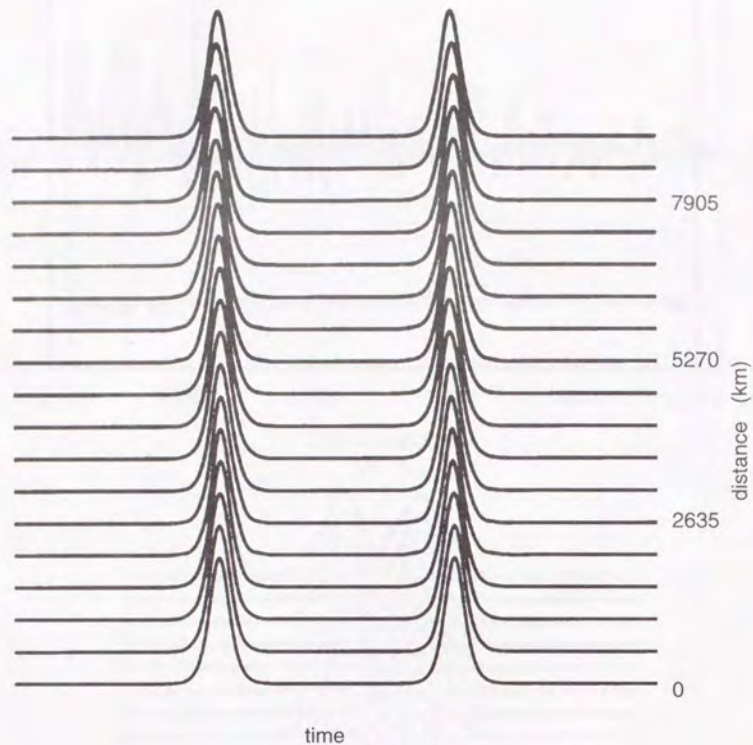


Figure 3.13 Evolution of the same intense, in-phase soliton pair separated by ten pulse widths along a fiber.

In actual transmission systems, there are perturbative effects which are not incorporated in the present calculation. Some of them originate from the amplifier itself, such as spontaneous emission, some of them originate from third order dispersion, optical shock, and the soliton self frequency shift in fibers. The effects of these perturbation are incorporated in the simulations in section V.

III.3 Analytic Solutions

The existence of a stable soliton in a lumped gain system has been analytically proved and named the average soliton^[14,15] or guiding center soliton.^[16] The main issue is that soliton exists under large gain perturbations if the amplifier spacing (L_a) is short compared to the soliton period (Z_{sp}) (i.e., $Z_a = L_a/Z_{sp} \ll 1$). The nonlinear Shrödinger equation is linearized by ignoring the non-commuting nature of nonlinearity and dispersion. In terms of physical image, it is assume that there is no significant change in pulse width. Under this condition, the soliton waveform u is written as

$$u(\xi, \tau) = \frac{\exp(-\Gamma\xi)}{K} v(\xi, \tau). \quad (3-1)$$

Incorporating this solution in NLS eq. (2-3), one obtains a loss-less NLS eq. of the form

$$-i \frac{\partial v}{\partial \xi} = \frac{1}{2} \frac{\partial^2 v}{\partial \tau^2} + |v|^2 v. \quad (3-2)$$

The factor K is given as

$$K = \sqrt{\frac{1 - \exp(-2\Gamma Z_a)}{2\Gamma Z_a}}, \quad (3-3)$$

and eq (3-2) is accurate to $O(Z_a^2)$.

Recently, a more precise analysis, which is accurate to $O(Z_a^3)$ has been reported.^[17]

III.4 Conclusion

A new soliton transmission technique was described which is suitable for lumped gain media. The lumped amplifier system is very promising for use in realizing a soliton transmission system because of its simplicity. All that is required is to locate optical amplifiers every 30-50 km in the transmission line. This technique requires no additional elements but uses a slightly higher input than an ordinary soliton transmission. Various experiments and analytical research have proved the appropriateness of this technique. This is a very beneficial alternative to linear optical communication systems.

- [1] Y. Kodama and A. Hasegawa: Amplification and reshaping of optical solitons in glass fiber - II, *Opt. Lett.* vol. 7, pp. 339-341 (1982).
- [2] M. Nakazawa, Y. Kimura and K. Suzuki: Soliton amplification and transmission with Er^{3+} -doped fiber repeater pumped by InGaAsP laser diode, *Electron. Lett.* vol. 25, pp. 199-200 (1989).
- [3] Nakazawa, Y. Kimura, and K. Suzuki: Efficient Er^{3+} -doped optical fiber amplifier pumped by a 1.48 μm InGaAsP laser diode, *Appl. Phys. Lett.* vol. 54, pp. 295-297(1989).
- [4] H. Kubota, and M. Nakazawa: Long-Distance Optical Soliton Transmission with Lumped Amplifiers, *IEEE J. Quantum Electron.* vol. 26, pp. 692-700 (1990).
- [5] M. Nakazawa, K. Suzuki, and Y. Kimura: 3.2-5 Gbit/s, 100 km error-free soliton transmission with erbium amplifiers and repeaters, *Photo. Technol. Lett.* vol. 2, p. 216 (1990).
- [6] E. Yamada, K. Suzuki and M. Nakazawa: 10 Gbit/s single-pass soliton transmission over 1000 km, *Electron. Lett.* vol. 27, No. 14, pp. 1289-1290 (1991).
- [7] M. Nakazawa, K. Suzuki, E. Yamada, and Y. Kimura: 20 Gbit/s soliton transmission over 200 km using erbium-doped fibre repeaters, *Electron. Lett.* vol. 26, pp. 1592-1593, (1990).
- [8] K. Suzuki, M. Nakazawa, E. Yamada, and Y. Kimura: 5 Gbit/s, 250 km error-free soliton transmission with Er^{3+} -doped fibre amplifiers and repeaters, *Electron. Lett.* vol. 26, p. 551 (1990).
- [9] E. Yamada, K. Suzuki and M. Nakazawa: 10 Gbit/s single-pass soliton transmission over 1000 km, *Electron. Lett.* Vol. 27, No. 14, pp. 1289-1290, (1991).
- [10] E. Shiojiri and Y. Fujii: Transmission capability of an optical fiber communication system using index nonlinearity, *Appl. Opt.* vol. 24, p. 358 (1985).

- [11] F. De Martini, C. H. Townes, T. K. Gustafson and P. L. Kelley: Self-steepening of light pulses, *Phys. Rev.* vol. 164, pp. 312-323 (1967).
- [12] J. P. Gordon: Theory of the soliton self-frequency shift, *Opt. Lett.* vol. 11, pp. 662-554 (1986).
- [13] E. Desurvire, J. R. Simpson, and P. C. Becker: High-gain erbium-doped traveling wave fiber amplifier, *Opt. Lett.* vol. 12, pp. 888-890 (1987).
- [14] L. F. Mollenauer, S. G. Evangelides and H. A. Haus: Long distance soliton propagation using lumped amplifiers and dispersion-shifted fiber, *IEEE J. Lightwave Technol.* vol. 9, pp. 194-197 (1991)
- [15] K. J. Blow, and N. J. Doran: Average soliton dynamics and operation of soliton systems with lumped amplifiers, *IEEE Photo. Technol. Lett.* vol. 3, pp. 369-371 (1991)
- [16] A. Hasegawa and Y. Kodama: Guiding-center soliton, *Phys. Rev. Lett.* vol. 66, pp. 161-164 (1991).
- [17] W. Forysiak, N. J. Doran, F. M. Knox and K. J. Blow: Average soliton dynamics in strongly perturbed systems, *Optics Commun.* vol. 117 pp. 65-70 (1995).

IV SOLITON TRANSMISSION CONTROL IN TIME AND FREQUENCY DOMAINS

IV.1 Soliton Transmission Controls

Previous approaches to reducing soliton interaction were based on the physical property of the soliton pulse itself, so that the distance was still limited by physical effects such as perturbations and nonlinear interaction. Furthermore, once the pulses were sent into the transmission line, the previous approaches had no effect on the pulses.

The novel approach we present here is to apply additional external manipulation to the propagating soliton pulses to control the soliton pulses. The principle of this approach lies in different behavior of soliton pulse and linear waves. So that soliton transmission control is applicable only for optical soliton but not for linear IM/DD system, in which pulse and noise behaves same manner.

There are two types of the soliton transmission control scheme. One is control in the time domain, the other is control in the frequency domain. Time domain control directly corrects any position change due to Gordon-Haus jitter and soliton interaction. For soliton transmission control in the time domain, a sinusoidal shaping function is applied to the soliton pulses. For frequency domain control, a band pass optical filter is installed into the transmission line^[1,2] to stabilize the soliton pulses. It can also reduce the frequency deviation of the soliton pulse, consequently, it can reduce the Gordon-Haus jitter.

IV.1.1 Reduction of Jitter and Interaction

Figure 4.1 shows the reduction in the Gordon-Haus effect achieved with soliton transmission controls. The input pulse width is 40 ps and the input amplitude is 1.72. The fiber conditions of loss, dispersion D , and

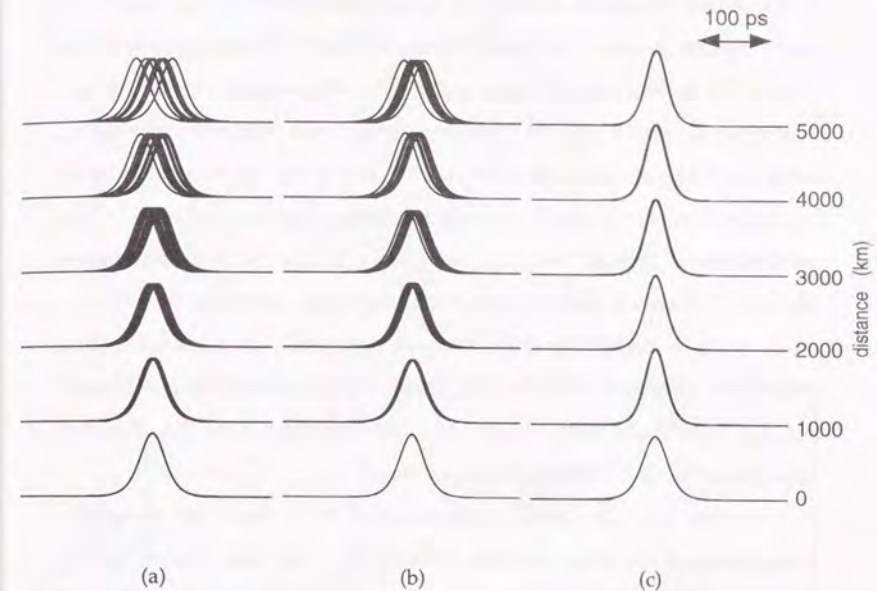


Figure 4.1 Reduction of Gordon-Haus jitter with soliton transmission controls. (a) soliton pulses without soliton transmission control, (b) with a band pass filter, (c) with a synchronous modulation.

length Z_a are 0.24 dB/km, -2 ps/(km·nm), and 50 km, respectively. The amplifier spacing is 50 km and the amplifier gain is 12 dB which corresponds to the gain required to compensate for the optical loss in a 50-km optical fiber. To simulate the Gordon-Haus jitter, random frequency shifts are introduced at each amplifier position to evaluate Gordon-Haus jitter without waveform distortion. Each figure is composed of 10 independent computer runs. The waveforms in an ordinary soliton transmission system without soliton transmission controls is shown in Fig.

4.1(a). The pulse position changes more than the pulse width at 5000 km. In Fig. 4-1(b), the soliton pulse is controlled by band pass filters installed at each amplifier position (frequency domain control). The bandwidth of the filter is 10.3 times that of the input pulse. The jitter was reduced to one half that seen in Fig. 4.1(a) at 5000 km because the frequency change is suppressed by the band pass filters. In Fig. 4.1(c), the soliton pulse is controlled by synchronous modulation (time domain control). The modulation is applied at every amplifier position and the modulation depth of the each shaping is only 2 dB. Although extinction ratio is only 0.37, most of the timing jitter has been removed. In addition to this successful reduction in the Gordon-Haus jitter, synchronous modulation can also reduce ASE which is a source of Gordon-Haus jitter. Detail of the noise reduction is described in the next section.

In Fig. 4.2, the standard deviations of the timing jitter versus the transmission distance are rewritten from Fig. 4.1. The thick broken line is a result without soliton transmission controls, which agrees well with a theoretical Gordon-Haus curve shown with a thin broken line. The synchronous modulation successfully reduces the timing jitter to an almost negligible level as shown by the solid line. When band pass filters are installed in the transmission line, the frequency deviation of the soliton pulse is reduced to within a certain amount as shown by the dot-dashed line. Here we assume that the frequency deviation obeys Gaussian distribution. The distribution of the timing jitter, which occurs in each transmission fiber (between two amplifiers), is also Gaussian distribution and these distributions are mutually independent. When the variance in the jitter is written as σ^2 and the mean timing jitter is zero, the moment generating function can be written as $M_x(t) = \exp(\sigma^2 t^2 / 2)$. After the k -th transmission fiber, i.e., the pulse experiences jitter k times, the moment generating function becomes $[M_x(t)]^k = \exp(k\sigma^2 t^2 / 2)$. This shows that the

variance in the timing jitter is $k\sigma^2$, i.e., the standard deviation of the jitter ($k^{1/2}\sigma$) accumulates by the square root of the transmission distance ($L^{1/2}$, $L=kZ_a$) in contrast to $L^{3/2}$ for the Gordon-Haus jitter.

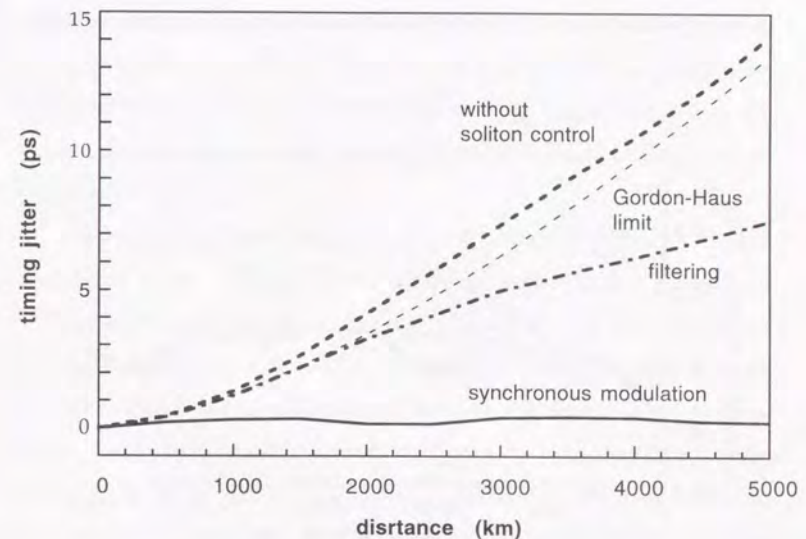


Figure 4.2 Standard deviation of the timing jitter versus transmission distance. solid line: with synchronous modulation, dot-dashed line: with band pass filter, dashed line: without soliton transmission control. The soliton transmission control is applied every 50 km. Theoretical value of the Gordon-Haus jitter is shown by the thin broken line.

Figure 4.3 shows the frequency deviations as a function of the propagation distance. The frequency deviation increases monotonously with the square root of the propagation distance. It is important to note that the frequency deviation can also be suppressed by a synchronous modulation scheme. The suppression of the frequency deviation is due to the fact that the propagation speed of the soliton pulse is determined solely by the GVD of the soliton carrier wavelength. The synchronous modulation enhances the same spectral components as the original soliton pulse. Since other frequency components arrive at the modulator at different times, frequency control is also possible. This technique is the same as the dispersion tuned fiber Raman laser proposed by Stolen et al.^[3]

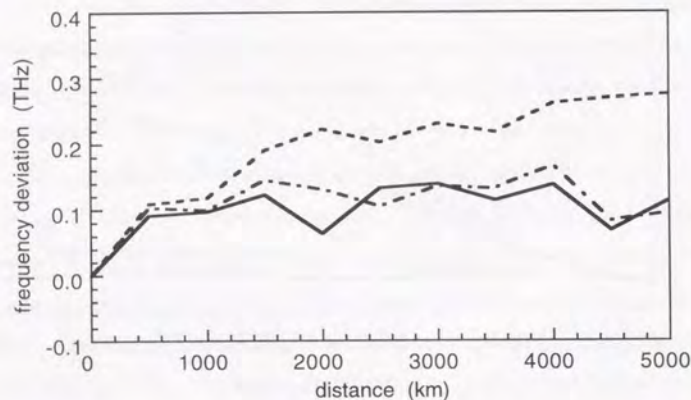


Figure 4.3 Accumulation of frequency deviation versus propagation distance. Solid line: with synchronous modulation, dot-dashed line: with band pass filter, dashed line: without soliton transmission control.

It should be noted that these soliton transmission controls work well even when they are spaced further apart. Figure 4.4 shows the standard deviations of timing jitter along the propagation distance with soliton transmission controls applied every 10 amplifiers. Instead of frequent control, strong controls were applied. The solid line shows time domain control in which the modulation depth is 20 dB ($2 \text{ dB} \times 10$), and the dot-dashed line shows frequency domain control in which the bandwidth of the filter is 3.3 ($10.3 / \sqrt{10}$). The effects are almost equivalent to those of the controls applied every 50 km. The main difference is the waveform distortion due to strong perturbations. Figure 4.4 also shows waveforms at 5000 km with time domain control applied every 500 km. One of the effects of waveform distortions is the appearance of fluctuation in the timing jitter. The solid curve in Fig. 4.4 exhibit greater variation than that in Fig. 4.2. However, less frequent control is very useful for the construction of an economical system.

Synchronous modulation is also effective for reducing soliton interaction forces. Figure 4.5 shows the propagation of a soliton pair without and with synchronous shaping. 20-dB shaping is applied every 500 km. The pulse width t_0 is 40 ps, and the initial pulse separation is 160 ps. For an ordinary soliton transmission system, the separation of $4t_0$ is so small that strong soliton interaction prevents long distance soliton propagation as shown in Fig. 4.5(a). However, when synchronous modulation is incorporated, the two pulses are clearly separated as shown in Fig. 4.5(b), which indicates that bit rates can be increased with this scheme. The soliton pulses tend to pull each other, but the modulation pulls them back to their original position.

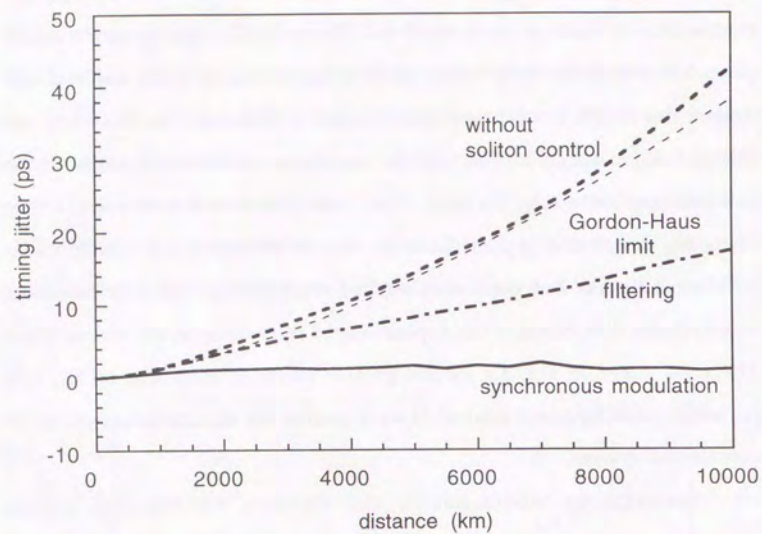


Figure 4.4 Same as Fig. 2 except soliton transmission control is applied every 500 km. The inset shows pulse shape with synchronous modulation at 5000 km.

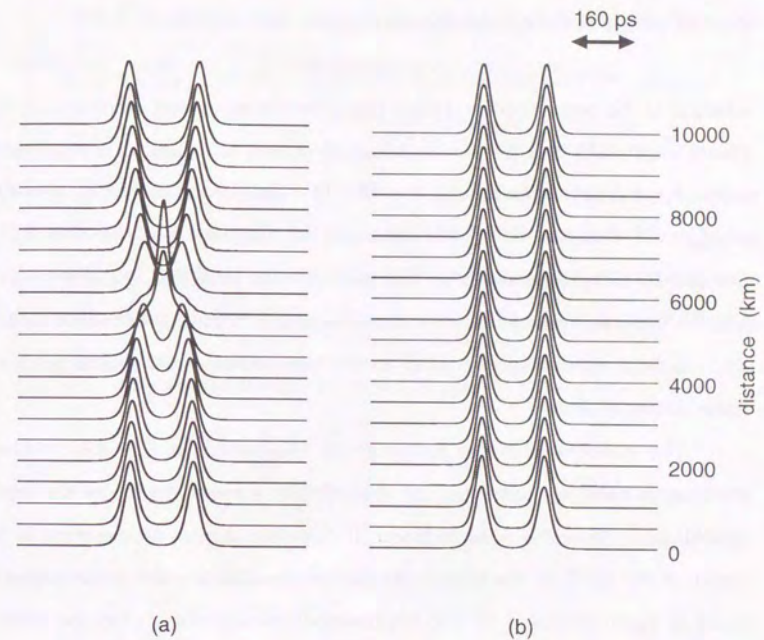


Figure 4.5 Reduction of soliton interaction by synchronous modulation. (a) without synchronous modulation, (b) with synchronous modulation

IV.1.2 Noise Reduction

The use of an optical amplifier such as an EDFA is accompanied by ASE noise and this limits the propagation distance in terms of S/N ratio. The peak power required for an $N=1$ soliton pulse is given by Eq. (2-5), and the ASE power of the optical amplifier is given as

$$P_{ASE} = \mu(G1)h\nu B, \quad (4-1)$$

where μ is the population inversion parameter of an optical amplifier, h is Planck's constant, B is the bandwidth of an optical filter, and G is amplifier gain. For example, when $\mu = 2$, $B = 5.5 \times 10^{10}$ Hz, $G = 15.85$ (12 dB), $t_0 = 40$ ps, $A_{eff} = 39 \mu\text{m}^2$, and $D = 2$ dB/(km-nm), the P_{ASE} and $P_{N=1}$ become 0.21 μW and 1.5 mW, respectively, so that the S/N ratio is 38 dB. 100 amplifiers add the same amount of noise 100 times, so that S/N ratio is decreased to 18 dB. Soliton transmission control in the time domain can reduce such a noise accumulation.

The concept of noise reduction is illustrated in Fig. 4.6. The continuous noise is modulated (or shaped) like a pulse stream by the first modulator. Since the noise is linear, it disperses during propagation as a result of the GVD of the fiber. At the next modulator, the re-broadened noise is again removed by the synchronous modulation. On the other hand, soliton pulses propagate without broadening when excess gain is provided. Repeating this process reduces the noise considerably.

We assume the sinusoidal modulation for the shaping function $f(t)$ and that its extinction ratio is $1/x$ ($x < 1$). For example, $x=0.01$ means an extinction ratio of 20 dB. The signal pulse shape $g(t)$ is assumed to be a hyperbolic secant squared.

$$f(t) = x + (1-x)\cos^2(\pi t/T) = x + (1-x)\frac{\cos(2\pi t/T) + 1}{2}, \quad (4-2)$$

$$g(t) = \text{sech}^2(1.76t/\Delta t),$$

where T is the period of the shaping function ($= 1/\text{bit-rate}$).

The transfer function for the noise, or noise reduction ratio, due to $f(t)$ is $T_R = (1+x)/2$ per shaping if the sinusoidally modulated noise disperses during propagation and becomes cw noise again before it reaches the next modulator.

While the transmitting signal power through the modulator T_m is

$$T_m = \int_{-T/2}^{T/2} f(t)g(t)dt / \int_{-T/2}^{T/2} g(t)dt \equiv \int_{-\infty}^{\infty} f(t)g(t)dt / \int_{-\infty}^{\infty} g(t)dt$$

$$= x + \frac{(1-x)}{2} \left[1 + \frac{\pi^2/1.76\alpha}{\sinh(\pi^2/1.76\alpha)} \right], \quad (4-3)$$

where $\alpha = T/\Delta t$ and is assumed to be > 1 . It is necessary to compensate for the attenuation to maintain the soliton pulse. The required excess gain is $G_m = 1/T_m$ per shaping. The next amplifier also adds noise but the noise is also reduced by succeeding modulators. Thus the total amount of noise from k amplifiers is written as

$$\begin{aligned} \langle N_T \rangle &= (\langle N \rangle T_R G + \langle N \rangle) T_R G + \langle N \rangle T_R G + \langle N \rangle \dots \\ &= \langle N \rangle \sum_{n=0}^{k-1} (T_R G)^n \\ &= \langle N \rangle \frac{1 - (T_R G)^k}{1 - T_R G}, \end{aligned} \quad (4-4)$$

where $\langle N \rangle$ is the ASE power from each amplifier.

Here,

$$T_R G_m = \frac{\frac{1+x}{2}}{x + \frac{(1-x)}{2} \left[1 + \frac{\pi^2/1.76\alpha}{\sinh(\pi^2/1.76\alpha)} \right]} < \frac{\frac{1+x}{2}}{x + \frac{(1-x)}{2}} = 1, \quad (4-5)$$

therefore, $T_R G_m$ is always less than unity so that $\langle N_T \rangle$ converges for any x value. For example, $x=0$ (100 % modulation) and $\alpha \gg 1$ gives $\langle N_T \rangle = 2.0 \langle N \rangle$, $x=0.1$ (10 dB modulation) and $\alpha = 2.5$ gives $\langle N_T \rangle = 3.5 \langle N \rangle$. The Mach-Zehnder intensity modulator has a sinusoidal transmission as a function of the applied voltage, and the driving voltage is sinusoidal. Therefore, the transmission function has a steeper edge than sinusoidal modulation which is simply assumed here. In an actual

situation, this asymmetric modulation function can remove the noise more efficiently.

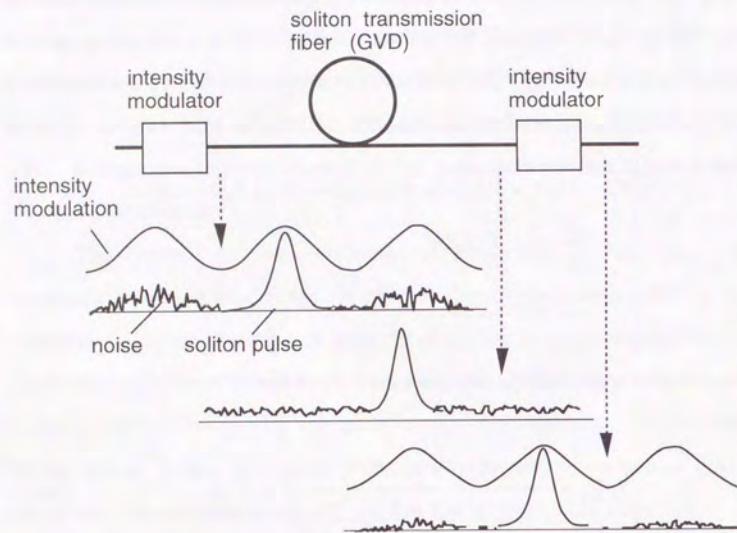


Figure 4.6 Concept of noise reduction by synchronous modulation.

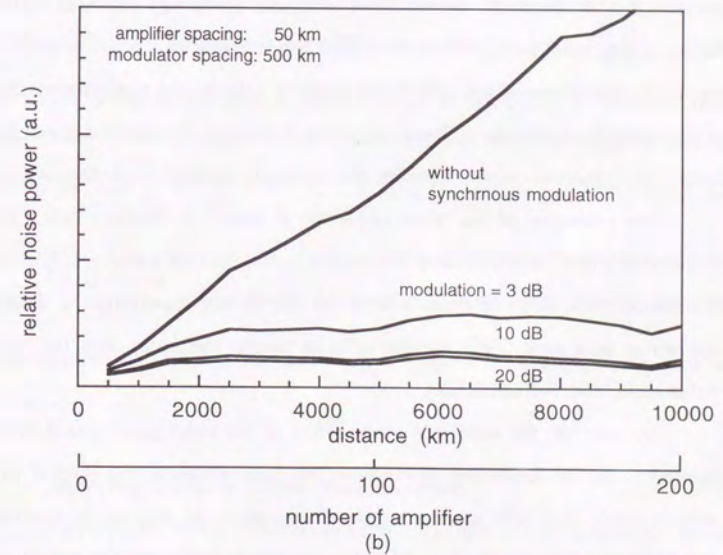
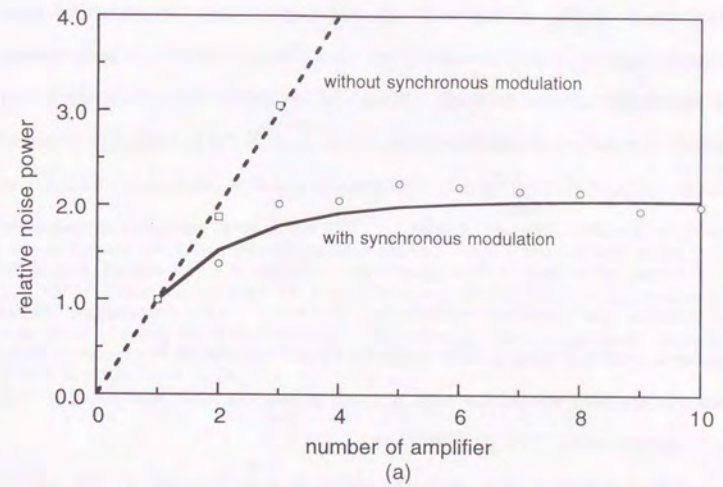


Figure 4.7 Noise accumulation with and without synchronous modulation. (a) solid and dashed lines are analytical values, the circles and squares represent numerical simulations where a is infinite and $\chi=0.01$ (20 dB modulation). (b) noise accumulation for various extinction ratios.

Figure 4.7 shows the noise reduction effect through synchronous modulation. In Fig. 4.7 (a), the solid and dashed lines are analytic values, the circles and squares represent numerical simulations where α is infinite and $x=0.01$ (20 dB modulation). When the synchronous modulation is not applied, the noise accumulates linearly as shown by the dashed line and squares. Synchronous modulation greatly reduces noise accumulation as shown by the solid line and circles. The noise level saturates at twice the input value after only a few shapings. Figure 4.7 (b) shows the same calculations for various modulation depths. The converged value calculated with Eq. (4-4) is also indicated by the squares in the figure. Even when an intensity modulator with a small extinction ratio was used, it still converges the noise to a very low level.

When coherent ASE noise is added to a soliton pulse, the soliton waveform and spectrum are modified, and this eventually prevents a stable soliton pulse from being transmitted over long distances. If the noise is not too large, the perturbation still yields a stable soliton and a dispersive wave with a small amplitude. Therefore, it is important to install a modulator before the coherent noise builds up and interacts strongly with the soliton.

The principle of the noise reduction is based on the fact that a non-dispersive pulse (soliton) and dispersive noise (linear) behave differently. Therefore, this scheme does not work for linear transmission systems operating at a zero-GVD wavelength, in which the noise and the signal pulse behave in the same way.

In contrast, the noise reduction effect of the band pass optical filter is limited. In the following discussion, the bandwidth of the optical filter, soliton pulse, and ASE noise are assumed to be B , Δf and white spectrum, respectively, and $B/\Delta f > 1$. We also assume a hyperbolic secant-shaped pulse spectrum and a Lorentzian filter transmission function. In the transmission system many optical filters are cascaded. Let us consider the

ASE noise generated by the first amplifier. At the first filter, the profile of the ASE noise becomes the same as that of the optical filter. The transmission function of the succeeding $M(\geq 1)$ stage filter is $\{1/(1+(2f/B)^2)\}^M$. After the M stage filter the noise energy is reduced to

$$\int_{-\infty}^{\infty} \{1/(1+(2f/B)^2)\}^{M+1} df / \int_{-\infty}^{\infty} \{1/(1+(2f/B)^2)\} df = \frac{(2M-1)!!}{(2M)!!} \quad (M \geq 0). \quad (4-6)$$

$M=0$ means there are no succeeding filters. While the soliton pulse passes the same filter bandwidth M times, because the soliton pulse recovers its spectrum during the propagation. The energy transmission of the soliton pulse at each filter T_f is

$$T_f = \frac{\int_{-\infty}^{\infty} \text{sech}^2(1.76f/\Delta f) \{1/(1+(2f/B)^2)\} df}{\int_{-\infty}^{\infty} \text{sech}^2(1.76f/\Delta f) df} = \frac{1.76B}{2\Delta f\pi} \psi^{(1)}\left(\frac{1.76B}{2\Delta f\pi} + \frac{1}{2}\right), \quad (4-7)$$

where $\psi^{(n)}(z) (= \frac{\partial^n}{\partial z^n} \psi(z))$ is a polyGamma function ($\psi(z) = \frac{\Gamma'(z)}{\Gamma(z)}$). It is important to add excess gain G_f at each filter to maintain a constant soliton pulse energy. Thus, $G_f T_f$ should equal unity. The total noise power is written as $\lim_{N \rightarrow \infty} \sum_{M=0}^{N-1} \frac{(2M-1)!!}{(2M)!!} G_f^M$ ($G_f > 1$). If the excess gain is ignored for simplicity, the amount of total noise becomes a simple series $\lim_{N \rightarrow \infty} \sum_{M=0}^{N-1} \frac{(2M-1)!!}{(2M)!!}$. This series does not converge when $N \rightarrow \infty$, i.e., the noise level in the filtering technique is never stable even if the excess gain is ignored.

IV. 2 Ultra-Long Distance Soliton Transmission

A schematic of the calculated model for ultra-long distance soliton transmission is shown in Fig. 4.8. Each amplifier spacing is 50 km, and modulators and band pass optical filters are installed every 10 amplifiers, i.e., every 500 km. Sinusoidal modulation with a modulation depth of 20

dB and a 10 GHz modulation frequency, corresponding to the pulse separation, is utilized in the calculation. Every 10 amplifiers an excess gain Δg is provided, which is slightly larger than that of the other amplifiers, to compensate for the power loss due to the band pass filter and synchronous modulation. The bandwidth of the optical filter is twice that of the input pulse spectrum. A broader bandwidth filter could be used if installed more frequently.

The soliton control in the frequency domain operates successfully as a stabilizer.^[4,5] Soliton stability when the filter and modulator are used is analyzed by the transmission function. Precise transmission functions are calculated with eqs. (4-3) and (4-7), but here for simplicity we assume that the pulse shape, filter profile, and modulation function are Gaussian. On this assumption, the pulse shape and its spectrum remains Gaussian after the modulation and/or the filter is applied. Let the full width at half maximum (FWHM) of the pulse shape, the filter bandwidth, and the modulation shape be w_t , W_f and W_m , respectively, and the spectral width of the pulse w_v be $0.44/w_t$. Since the transmitted pulse remains Gaussian with the same peak amplitude, the transmitted energy is the same as the ratio of the width. The spectral width after passing the filter is $w'_v = w_v \sqrt{W_f^2 / (w_v^2 + W_f^2)}$ so that the transmitted energy for a filter of bandwidth W_f is

$$T_{gf} = \sqrt{W_f^2 / (w_v^2 + W_f^2)}. \quad (4-8)$$

When the pulse passes the filter, the pulse width broadens to $w'_t = w_t \sqrt{(w_v^2 + W_f^2) / W_f^2}$. In the same manner the transmitted energy for a pulse width of w_t and a modulation of W_m is

$$T_{gm} = \sqrt{W_m^2 / (W_m^2 + w_t^2)}. \quad (4-9)$$

When the modulation is applied to the broaden pulse of w'_t , the transmitted energy ratio is $\sqrt{W_m^2 / (W_m^2 + w_t'^2)}$. The overall transmission for succeeding filter and modulation operation is

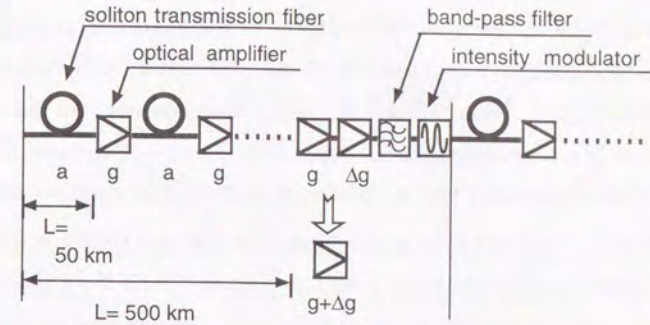


Figure 4.8 Schematic of the long distance soliton transmission system.

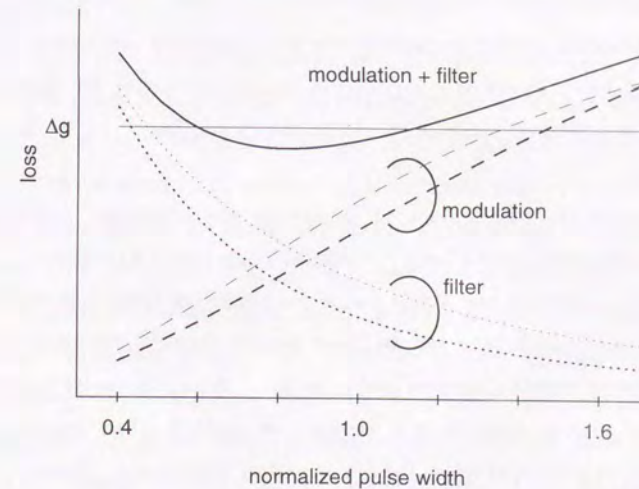


Figure 4.9 Insertion loss of filter and modulator versus pulse width.

$$T_g = \sqrt{W_m^2/(W_m^2 + w_t^2)} \sqrt{W_f^2/(w_v^2 + W_f^2)}. \quad (4-10)$$

Figure 4.9 is a schematic of the loss (= 1 - transmittance) for the filter and modulator system versus pulse width w_t . The dotted line is the loss by the optical filter, the broken line is the loss by the modulator, and the solid line is that of the combined system. They are calculated with eqs. (4-8), (4-9), and (4-10), respectively, and $W_f = 2.0 \times 0.44$ and $W_m = 1.25$ are used in the calculation. For stable pulse propagation, loss and gain should be equal. Synchronous shaping successfully reduces jitter and noise but the system becomes unstable after long distance transmission. That is, once the soliton pulse energy becomes smaller than the required energy, the pulse broadens due to dispersion. A broadened pulse experiences larger loss than an unbroadened pulse at the modulator (broken line), so the energy becomes small. It has been shown that a band-pass filter stabilizes not only the frequency but also the amplitude of the soliton pulse. A pulse with less energy broadens during propagation and has a narrower bandwidth than a normal pulse. Therefore it experiences less attenuation at the band-pass filter than a normal pulse as shown by the dotted line, i.e., the energy recovers.

There are two balancing points in the combined filter and modulation system (solid line). A narrow pulse (point A) behaves in the same way as with a filter. While a wide pulse (point B) behaves in the same way as with a modulator and the pulse escapes from the balancing point, i.e., point B couldn't support stable pulse. When the pulse width is narrower than at point B, it is captured at point A. Thus the pulse is stabilized at point A at which the filtering effect is dominant. Points A and B can be obtained by setting Eq. (4-10) equal to $1/\Delta g$,

$$\sqrt{W_m^2/(W_m^2 + w_t^2)} \sqrt{W_f^2/(w_v^2 + W_f^2)} = 1/\Delta g \quad (4-11)$$

By noting $w_t' = w_t \sqrt{(w_v^2 + W_f^2)/W_f^2}$ and $w_v = 0.44/w_t'$, w_t' , which gives points A and B, are expressed as

$$w_t' = \sqrt{\frac{-2(0.44/W_f)^2 - W_m^2(1 - \Delta g^2) \pm \sqrt{\kappa}}{2}} \quad (4-12)$$

where $\kappa = [2(0.44/W_f)^2 + W_m^2(1 - \Delta g^2)]^2 - 4(0.44/W_f)^2((0.44/W_f)^2 + W_m^2)$.

The \pm signs in eq. (4-12) correspond to points B and A, respectively. Since the Gaussian pulse, modulation, and filter shape are assumed in eq. (4-10), this result gives a rough estimation of the stability condition.

A similar approach to the stability analysis is reported in ref. 6. This stabilizer is passive, so that no external feedback controls are required. In addition, when EDFAs operating in a saturating region are cascaded, this stabilizes the soliton energy,^[7] and achieves more stable soliton propagation.

Here we estimate the excess gain Δg . Equations (4-3) and (4-7) represent estimations of Δg for synchronous modulation alone and a band pass filter alone. The excess gains for modulation of $\alpha = 2.5$ and filter of $B/\Delta f = 2.0$ are about 1.3 dB and 0.72 dB, respectively, with a sum of about 2.0 dB. However, simultaneous operation of the filter and the modulation results in larger attenuation. This is because the soliton input into the synchronous modulator has a slightly broader pulse width since it has passed the optical filter. We made an assumption that the pulse broadening due to the band pass filter is inversely proportional to the energy loss due to the filter. In other words, the output pulse from the filter can be approximately described by a sech shape. When the energy loss (i.e. the pulse broadening) calculated from Eq. (4-6) is incorporated into Eq. (4-3), we obtain an attenuation of 1.63 dB rather than 1.3 dB, because the broadened pulse experiences a larger attenuation than the original pulse with the same modulation. The estimated overall loss, or excess gain, for

the filter-modulator system is 2.35 dB (1.63 + 0.72). As we previously mentioned, the actual shaping function has a more complex shape. In such a case, numerical integration will be helpful in estimating the precise excess gain.

Figure 4.10 shows a numerical simulation of one million kilometer soliton transmission. Δg of 2.5 dB, which is obtained by the above estimation, is used for the calculation of Fig. 4-10 (a). Figure 4.10 (b) incorporates amplifier saturation in addition, and Δg was set at 3.0 dB to make use of the gain saturation induced stabilization. In both calculations, the initial pulse separation is 100 ps, the input pulse width is 40 ps and the propagating pulse width is about 30 ps. In spite of the noise and the soliton interaction, the soliton pulses are very stable due to the synchronous modulation and stabilization by the band pass filter. The noise appearing at the base line is less than -20 dB to the pulse peak intensity even after a one million kilometer propagation incorporating 20,000 amplifiers. This means that the noise accumulation is negligible. In addition, saturated amplifiers realize more stable soliton propagation.

The amplitude fluctuation of the soliton pulse in the one million kilometer transmission with saturated amplifiers, corresponding to Fig. 4.10 (b), is shown in Fig. 4.11. A histogram of the amplitude distribution is also shown in the figure, in which the amplitudes are calculated every 1000 km. The estimated standard deviation of the amplitude is 0.022, which means that the bit error caused by amplitude fluctuation is negligible.

The validity of the soliton transmission control is proved by various experiments. [8-10] Figure 4.12 through 4.15 is a significant result of one million km transmission from reference [8]. The experimental setup for the ultra-long distance soliton transmission scheme is shown in Fig. 4.12. The soliton is generated by a gain switched DFB LD and the spectral windowing

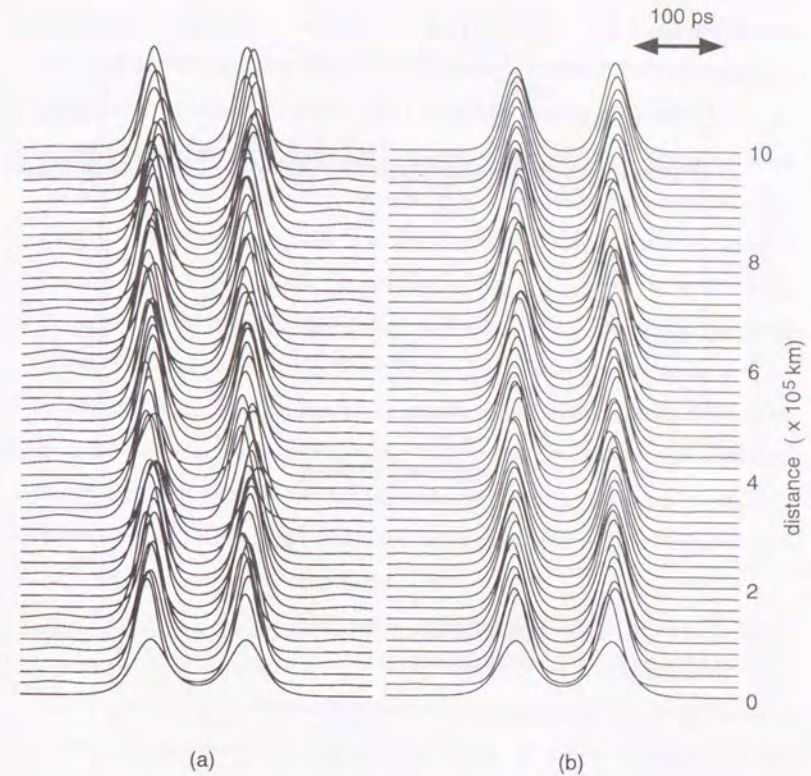


Fig. 4.10 Numerical results of a one million km soliton transmission. (a) without saturated amplifiers, (b) with saturated amplifiers.

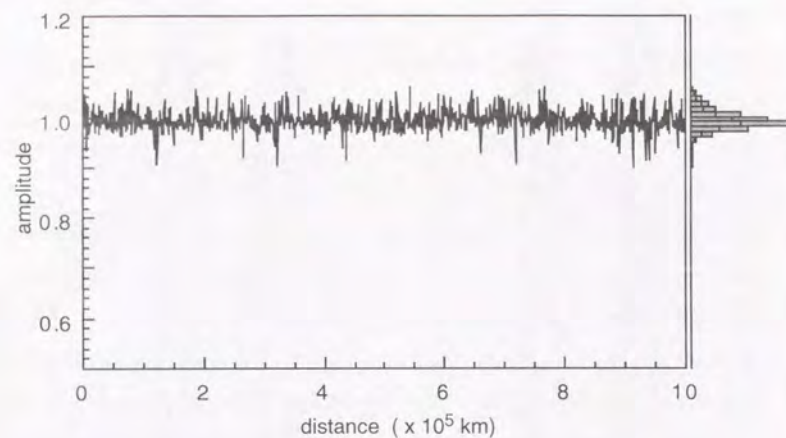


Figure 4.11 The amplitude fluctuation of the soliton pulse in a one million km transmission with saturated amplifiers.

technique.^[11] The soliton data was coded using a Mach-Zehnder light modulator and data speeds were between 5 and 10 Gbit/s. Since a loop with a short length of about 100 km does not reflect the conditions in an actual fibre system, we have been continuously investigating a single-pass long distance soliton transmission. In the paper, 510 km fiber loop with 50 km amplifier spacing was used. The soliton transmission fibers (STF) were ten

fibers approximately 50 km long with anomalous group velocity dispersions at $-0.7 \sim -2.2$ ps/km/nm (average -1.5 ps/km/nm). The coded soliton was coupled into the 510 km loop through a 3 dB coupler and the dynamic soliton communication method was used to circulate the solitons in the loop. The soliton was reshaped and retimed by a LiNbO₃ light modulator and optical delay, which means that this soliton circulation loop is a kind of synchronously mode-locked laser. Therefore, in a steady state condition, the soliton can propagate over an infinite distance. The difference between the laser and this loop is that laser should have a pulse at every time slots but this loop, which is a data transmission line, must preserve data pattern. Furthermore, because of the inherent nature of mode-locking, the jitter problem, called the Gordon-Haus Limit in a soliton transmission, can be removed if the complete locking is accomplished. In addition, this forced shaping technique can remove the interaction forces between adjacent solitons which have thus far limited the maximum speed of soliton communication, resulting in an increase in the bit-rate. This has been also confirmed by computer simulations.

Figure 4.13(a) is a single-pass data signal <110011...> after 510 km, where the reshaping has already been achieved by the modulator. The soliton pulse coupled into the loop was 42 ps, which was reduced to 35~37 ps by the shaping. By closing the 510 km loop, soliton waveforms are transmitted over one million kilometres as shown in Fig. 4.13(b) No pulse broadening appears and very stable transmission has been attained. It is important to note that the accumulation of ASE and non-soliton components at "0" signal are negligible. Because of the low dispersion and 30~45 ps pulse width, the N=1 soliton power was as low as 0.6~2 mW. With such a low signal power, the accumulation of ASE noise causes serious problem for ultra-long distance transmission. The accumulated ASE at "0" signal may be built up to "1" but soliton control prevent the accumulation.

It should be also noted that EDFAs operate in a saturated gain regime, resulting in a self stabilization of the soliton power and width.^[12]

In the system, a sinusoidal electric signal for reshaping fed to a modulator can be extracted from the coded data signal by using a narrowband SAW filter. The synchronization between the transmitting soliton and the reshaping signal can be tuned by a phase controller (Delay unit). Laser diode amplifiers are also advantageous since they combine amplifiers and modulators at high speed.

Figure 4.14 shows spectra corresponding to Fig. 4.13(a) and (b). Spectral widths (-3dB down) at the input, after 510 km transmission, and one million km (loop condition) are 0.08, 0.09, and 0.11 nm, respectively. The slight broadening which occurs after one million km can probably be attributed to the accumulation of ASE and slight spectral broadening due to self-phase modulation in each circulation and its amplification by the EDFAs.

Fixed data patterns after transmissions over one million km at 7.2 Gbit/s and 400 thousand km at 10 Gbit/s are shown in Fig. 4.15. Fig. 4.15(a) and (b) are soliton trains coded with <100101011001> and <001110100011> at 7.2 Gbit/s and Fig. 4.15(c) is <0010110011> at 10 Gbit/s. No pulse broadening occurs even when these data signals are transmitted over such long distances. A small difference in the peak intensity of each soliton is probably caused by the slightly insufficient bandwidth of the electrical power amplifier fed to the LiNbO₃ modulator for the data coding and partly by irregularities in the sensitivity of the S₁ tube of the streak camera. The present technique is not applicable to linear high speed IM/DD systems.

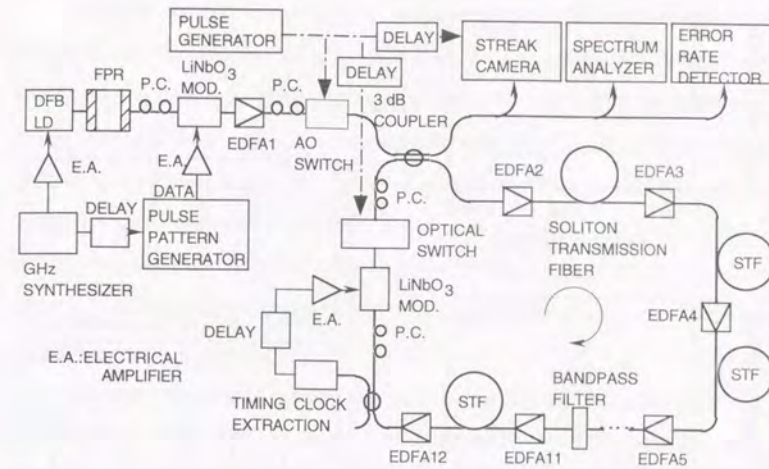


Figure 4.12 Experimental setup for circulating a coded soliton train in a 510 km loop. The LiNbO₃ modulator and the optical delay are for soliton reshaping and retiming. The optical switch is for cleaning and initiating the loop. The ON/OFF ratio of the AO switch was -54 dB.

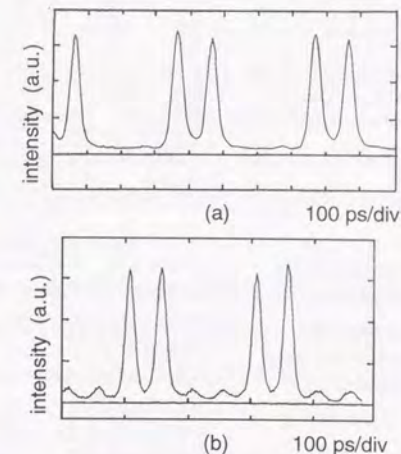


Figure 4.13 10 Gbit/s soliton data transmission over one million km. (a) soliton waveforms at 500 km with reshaping. (b) soliton waveforms over one million km

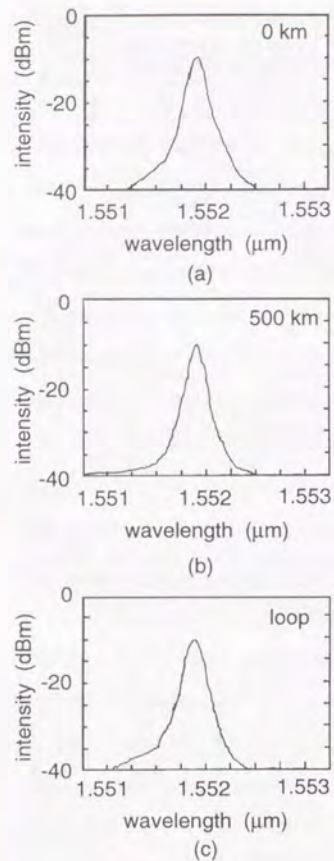


Figure 4.14 Spectra for 10 Gbit/s soliton transmission over one million km. (a) spectrum at input. (b) spectrum at 500 km with reshaping. (c) spectrum after one million km transmission.

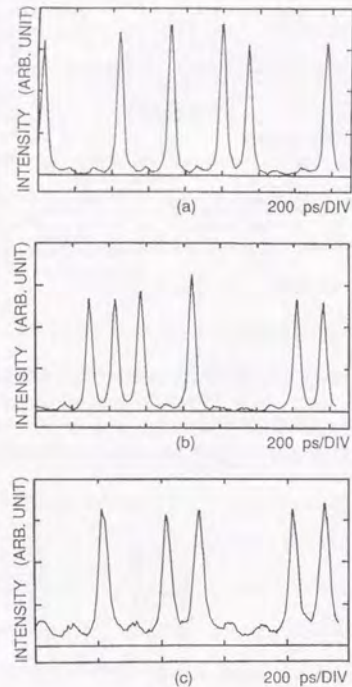


Figure 4.15 Transmitted data patterns over one million km. (a) 7.2 Gbit/s data over 1 million km coded as $\langle 100101011001 \rangle$. (b) 7.2 Gbit/s data over 1 million km coded as $\langle 001110100011 \rangle$. (c) 10 Gbit/s data over 400 thousand km coded as $\langle 0010110011 \rangle$.

IV.3 Soliton transmission with long amplifier spacings by soliton control

Optical soliton transmission technology has shown considerable progress through the use of erbium-doped fiber amplifiers (EDFAs).^[13,14] We have succeeded in transmitting solitons over unlimited distances by using the dynamic soliton transmission technique and incorporating soliton control.^[15] However, theory suggests that the pulse distortion is proportional to the second order of the amplifier spacing (Z_a) normalized by normalizing distance (Z_0) or soliton period (Z_{sp}).^[16] This means that $(Z_a/Z_{sp})^2$ should be much smaller than unity in order to achieve ultra-long distance soliton transmission.

On the other hand, higher bit-rate communication requires a shorter optical pulse which shortens Z_{sp} . As it is common to set Z_a at longer than 100 km in conventional linear systems, the question arises of how long Z_a can be extended in a soliton system.

The amplified spontaneous emission (ASE) noise added by optical amplifiers also limits the amplifier spacing. It is said that the gain (G) of the EDFA should be less than 10 dB because excess noise grows at a rate of $[(G-1)/\ln G]^2/G$.^[17] That is, Z_a should be shorter than about 50 km. However, these difficulties can be removed through the use of soliton control which reshapes the soliton pulse and removes dispersive non-soliton waves as well as ASE noise. In this letter, we show numerically that soliton control is a good solution to the need for soliton transmissions with increased amplifier spacing.

We assume a 10 Gbit/s soliton transmission with an amplifier spacing of 100 km, which is 2 to 3 times greater than the spacing in a conventional soliton system. Soliton control are incorporated in both the time and frequency domains by which synchronous modulation with a modulation depth of 99% is applied every 500 km. In addition an optical

filter with a bandwidth of 0.4 nm, which can be installed in an optical amplifier, is installed every 100 km.

The amplifier gain is equal to the transmission loss of a 100 km fiber plus an excess gain. In this calculation, excess gain of 1.3 dB and 0.25 dB are required to compensate for the insertion loss of the modulator and the optical filter, respectively. The input soliton pulse is 25 ps wide, and the initial soliton amplitude is as high as $A=2.7$, which is 15 % larger than the average soliton. The bandwidth of the optical filter is 4 times broader than that of the input soliton pulse. The group velocity dispersion (GVD) of the fiber is $|D| = 2.0$ ps/(km·nm), which gives a soliton period of 124 km. Therefore Z_a/Z_{sp} is as high as 0.8. The third order dispersion term and the Raman effect term are ignored because the pulse width is broad. The peak power of the $N=1$ soliton, $P_{N=1}$, is calculated at 3.8 mW where the effective core area is $40 \mu\text{m}^2$. A duty ratio of 4 gives an average power at 0.95 mW.

The ASE noise power generated by the EDFA is given by Eq. (4-1). Here, when $\mu=4$ corresponds to a noise figure of 9 dB, $G=251$ (24 dB = 0.24 dB/km x 100 km), and $B = 0.4$ nm, the ASE power becomes $6.4 \mu\text{W}$. Figure 4.16 shows waveforms of a soliton pair with a separation of 100 ps (10 Gbit/s). It should be noted here that Z_a is almost the same as the soliton period so that a significant amount of dispersive wave (non-soliton components) is generated during the propagation. In spite of the accumulation of the dispersive wave and ASE noise, the soliton pulse propagates stably over a long distance with soliton control. Moreover, the noise level remains very low due to the noise reduction effect of the time-domain soliton control. A stable soliton transmission of more than 20,000 km is easily achieved with soliton control, while ideal solitons without soliton control will collide after as little as 2,000 km.

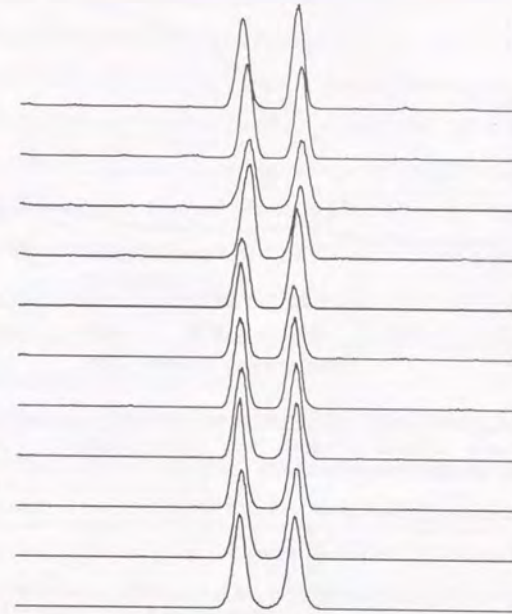


Figure 4.16 Waveform of a 10 Gbit/s pulse pair transmission with 100 km amplifier spacing.

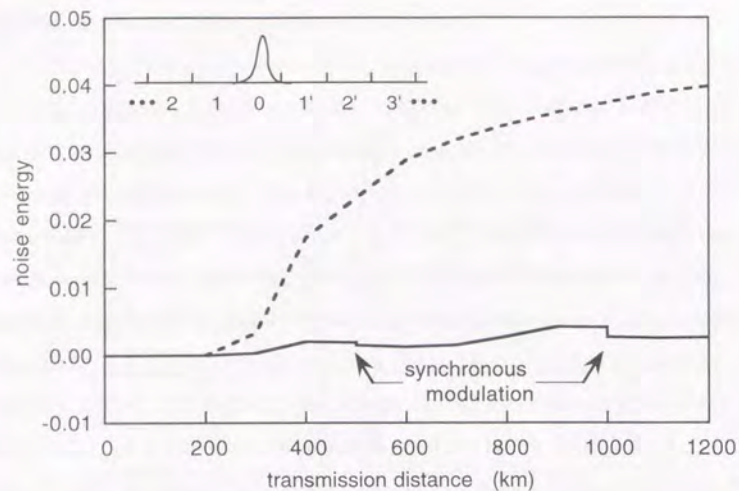


Figure 4.17 Accumulation of dispersive non-soliton components with (solid line) and without (dashed line) soliton control. Synchronous modulation is applied every 500 km.

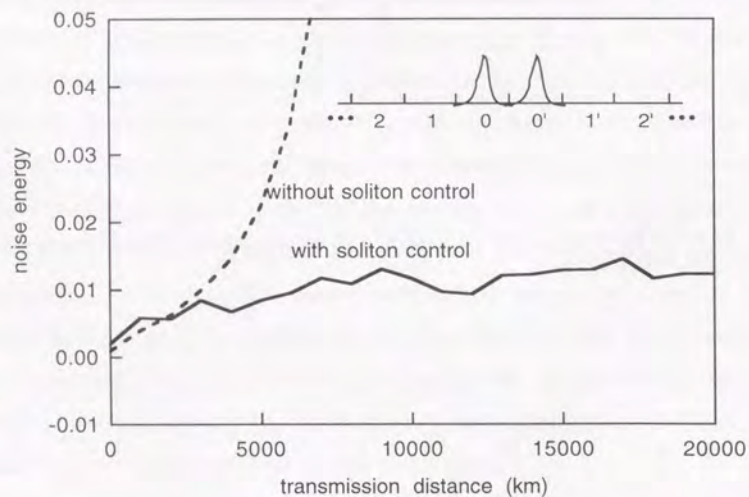


Figure 4.18 Accumulation of noise with (solid line) and without (dashed line) synchronous modulation. Synchronous modulation is applied every 500 km.

A significant amount of dispersive wave are generated from a soliton under the condition of $Z_a/Z_{sp} \sim 1$. In addition, strong soliton control slightly modifies the soliton pulse resulting in dispersive wave. These effects are overcome because the noise reduction effect of soliton control is much stronger than the noise generation effects.

Figure 4.17 shows dispersive wave accumulation during the propagation. A single soliton pulse without ASE noise is propagated under the same conditions as in Fig. 4.16. A dynamic soliton without soliton control is calculated as a reference. Here we define the time segments in a series beginning 0, 1, 1', 2, 2', as shown in the inset in Fig. 4.17. Each segment is 100 ps wide and the segment 0 contains a signal pulse. The energy in each segment is evaluated by a numerical integration and is normalized with the signal energy.

The total energy in segments 2 through 6 and 2' through 6', which represents a dispersive wave which behaves as noise, is also shown in Fig. 4.17. Segments 1 and 1' are not counted because they include tail parts of the signal pulse. The solid line indicates the pulse with soliton control and the dashed line indicates the reference pulse without soliton control. The dashed line shows that a significant amount of noise is generated and accumulated because Z_a is comparable to Z_{sp} . By contrast soliton control can successfully eliminate the dispersive wave accumulation as shown by the solid line, that is, significant noise reduction is achieved.

Figure 4.18 shows the noise accumulation throughout the soliton transmission. The solid line is total noise energy (ASE plus dispersive) with soliton control corresponding to Fig. 4.16. The dashed line is ASE noise without synchronous modulation as a reference. Here we again define the time segments 0, 0', 1, 1', 2, 2', as shown in the inset in Fig. 4.18, where no soliton pulses were added when the reference was calculated.

As shown by the dashed line, without soliton control, the ASE noise accumulates monotonously and eventually destroys the soliton signal. It is estimated from the solid line that the ratio of the average soliton power to the average noise power is about 100 with soliton control. Such a low level of noise will not affect soliton propagation over long distances.

IV.4 Ultrahigh speed soliton transmission using soliton control under soliton self frequency shift

An optical soliton in an optical fiber is regarded as a dispersion-free carrier for optical communications, and it is said that Tbit/s communication will become possible through the use of optical solitons. We have demonstrated picosecond and femtosecond soliton pulse transmissions using a distributed erbium doped fiber amplifier (DEDFA) as a step to Tbit/s communication.^[18-20] There are two main difficulties in propagating such a short soliton pulse over long distances. One is the short soliton period and the other is the effect of the soliton self frequency shift (ssfs)^[21] which is due to self Raman gain (or the non instantaneous response of the nonlinearity). The former property prevents the use of a simple lumped amplifier configuration. A pulse width of 1 ps and a group velocity dispersion (GVD) of 0.15 ps/km-nm give a soliton period (Z_{sp}) of 2.6 km, which decreases further when shorter pulses are used. An amplifier spacing of 10 km is much longer than this Z_{sp} , which means that a large quantity of nonsoliton components will be generated which would prevent a long distance soliton transmission.^[22] It is impracticable to make the amplifier spacing comparable to Z_{sp} because this would require many amplifiers with a low gain. This difficulty can be overcome by using a distributed amplifier. When a distributed amplifier is used, the short soliton period becomes a preferable condition. When the Z_{sp} is short, the

normalized gain or loss becomes small so that the soliton pulse acts adiabatically.

The ssfs problem was overcome by trapping the soliton spectrum in an optical bandpass filter when the ssfs is not strong. The bandwidth of the DEDFA can be used for this purpose but it is not very efficient for femtosecond solitons. With this soliton trapping, the carrier frequency of the soliton signal is slightly different from the transmission maximum of the filter. The net gain at the transmission maximum of the filter is always greater than the gain at the soliton carrier frequency. The result is that the noise tends to grow and the instability grows on the soliton pulse.^[15] Even the use of a distributed amplifier and optical filters can not eliminate soliton-soliton interaction, and therefore this gain trapped instability and interaction force limits the propagation distance.

We have developed a soliton control technique (synchronous modulation with optical filtering) for transmitting solitons over virtually unlimited distances,^[8] which reduces soliton interaction and noise accumulation. The above mentioned instability can also be eliminated with this control technique.

However, it is yet to be proved whether the technique can be applied to picosecond/femtosecond soliton transmissions accompanied by perturbations. In this paper, we show that it is possible to send a 200 Gbit/s soliton signal more than 5000 km by using a distributed amplifier and the soliton control technique.

Femtosecond soliton pulse propagation in optical fibers is modeled by a perturbed nonlinear Schrödinger equation:

$$-i \frac{\partial u}{\partial \xi} = \frac{1}{2} \frac{\partial^2 u}{\partial \tau^2} - \frac{i}{6} \frac{k'''}{|k''| \tau_0} \frac{\partial^3 u}{\partial \tau^3} + |u|^2 u + i \Gamma u - \frac{t_n}{\tau_0} u \frac{\partial |u|^2}{\partial \tau} \quad (4-14)$$

The last term indicates the ssfs effect where t_n is 5.9 fs. For simplicity, we assume that the DEDFA provides a loss-free transmission line ($\Gamma = 0$), and

that the dispersion is constant over wavelength ($k'''=0$). We add amplified spontaneous emission (ASE) noise with a 5.3 nm bandwidth every 25m. This can be seen as a quasi-distributed noise with a Z_{sp} of 2.6 km. A synchronous modulation with a 20 dB extinction was applied every 10 km and an optical filter with a 5.3 nm bandwidth was installed every 5 km. Here, the soliton trapping effect of the DEDFA is not taken into consideration but optical filters play this role. The effects of the filters and modulators are not described in the equation because they are localized every 5 km and 10 km, respectively, but the effects are considered in the calculation.

Figure 4.19 shows soliton waveforms and eye diagrams with synchronous modulation at a bit rate of 200 Gbit/s. The waveform is a 2^5-1 pseudo random bit stream (PRBS) pattern and is shown every 500 km. The phase of the synchronous modulation is adjusted to maximize the transmitted energy. At 500 km, each pulse in the waveform is clearly separated. The rms jitter is 0.1 ps, which corresponds to a bit error rate of less than 10^{-100} by employing Gaussian jitter distribution. As clearly seen in the eye diagram shown in Fig. 4.19(c), there are two stable propagation states at transmission distance longer than 1000 km. The higher peaks on the right correspond to the transmission maximum of the intensity modulation. While the lower peaks on the left correspond to pulses which are "trapped" by the synchronous modulations. That is, a low-intensity (therefore broader) pulse propagates faster than a high-intensity pulse because it suffers from less frequency shift. However, the shoulder of the synchronous modulation pulls the pulse back toward time slot. Therefore there is a point at which walk-off due to ssfs and pulling-back by synchronous modulation balances.

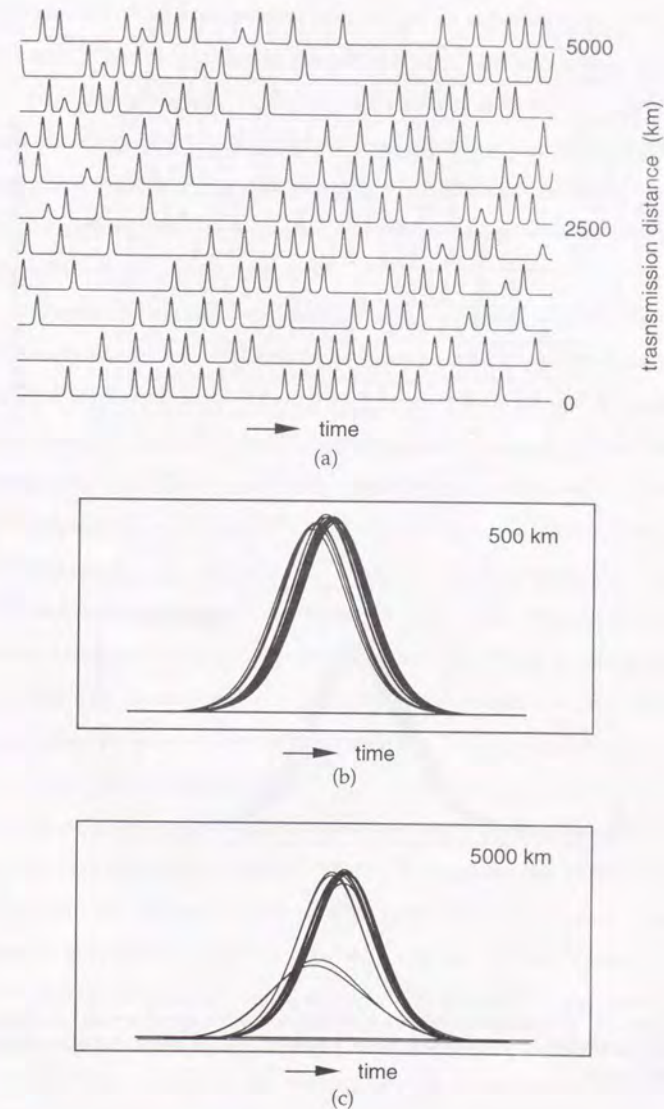


Figure 4.19. Waveforms and eye diagrams with synchronous modulation and optical filters. Modulation is applied to maximize the transmitted energy.

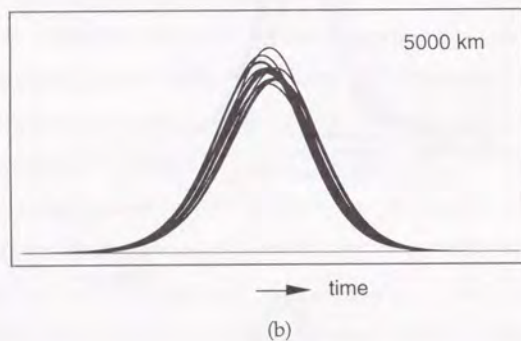
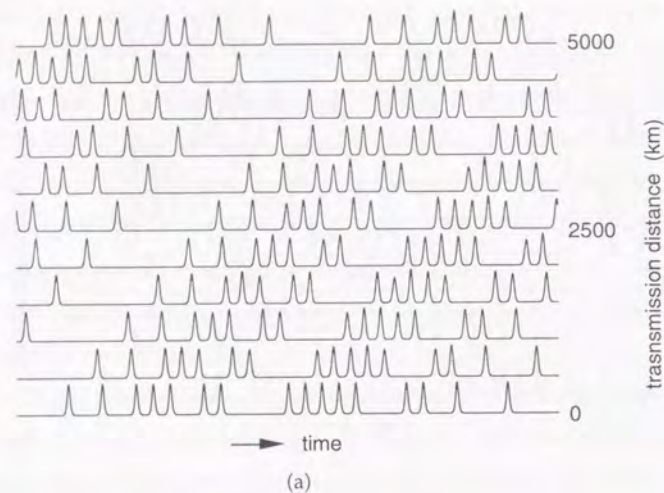


Figure 4.20 Waveforms and an eye diagram with synchronous modulation and optical filters. The modulation phase is moved toward the leading side of the pulse.

It should be noted here that the amplitude (energy) of the lower pulse is also maintained in spite of the modulation. In Fig. 4.19(a), higher pulses are dominant and the modulation maxima tend to exist at around the peaks of higher pulses so low intensity pulses suffer greater loss than high intensity pulses. While a bandpass filter allows more transmission for broad pulse which stabilize the pulse energy. There is at most one steady state for a low amplitude soliton which is determined by the filter bandwidth and the modulation depth.

A small amplitude fluctuation which is generated by the coherent addition of noise by the DEDFA causes a serious jitter under the presence of ssfs. The amplitude fluctuation turns into jitter through GVD, because a soliton with a different amplitude (therefore a different pulse width) suffers a different amount of frequency shift. In addition, synchronous modulation converts jitter to amplitude fluctuation, which increases the jitter and makes the system unstable. To improve stability, the phase of the modulation is shifted toward the low amplitude pulse. Figure 4.20 shows the waveforms and an eye diagram when the modulation phase is moved toward the low intensity pulse by $1/16$ of the modulation period. A single stable transmission state was realized and the jitter was less than 0.05 ps even after a 5000 km transmission.

Figure 4.21(a) and 4.21(b) correspond to the modulation schemes in Figs. 4.19 and 4.20, respectively. When the transmission maxima of the synchronous modulation are set at around the position of high intensity pulses, as shown in Fig. 4.21(a), the high and low intensity pulses each have a steady state as described above. On the other hand, when the maximum transmission of the modulation is shifted to the left, as shown in Fig. 4.21(b), this result in a high transmittance on a low intensity pulse and small transmittance on a high intensity pulse. There is a correlation between amplitude and position in that a high intensity pulse tends to be

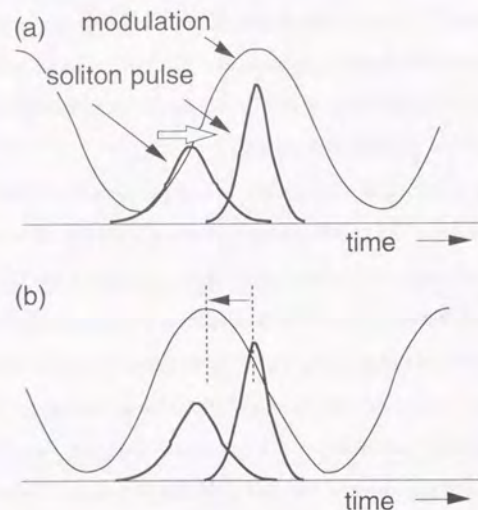


Figure 4.21 Modulation schemes corresponding to Figs. 4.19 and 4.20.

delayed because of ssfs. Eventually, the shifted modulation reduces the amplitude difference between the high and low intensity pulses, thus removing the systematic splitting of the pulse amplitude and position.

We found that the pulse delays shown in the Figs. 4.19(a) and 4.20(a) are almost proportional to the propagation distance. This indicates that the soliton is trapped within the filter bandwidth. The carrier frequency shift is estimated to be as small as 0.1 nm so the dispersion difference due to the frequency shift is negligible.

The k''' causes a serious degradation in the propagation characteristics when the pulse width becomes short or the k'' value becomes small. Such a case requires more intensive control.

IV.5 Conclusion

Soliton control is a promising way for increasing the transmission distance and amplifier spacing because it reshapes the soliton pulse and eliminates dispersive non-soliton waves as well as ASE noise. With this technique, high bit-rate soliton transmission can be achieved with much longer amplifier spacings than with conventional soliton techniques.

Without soliton control, the transmission distance in a sub Tbit/s soliton system is severely limited by jitter due to the ssfs, noise and interaction. However, even in the presence of the ssfs, a transmission of more than 5000 km is possible by employing of soliton control and DEDFAs.

- 1 Y. Kodama and A. Hasegawa: Generation of asymptotically stable optical solitons and suppression of the Gordon-Haus effect, *Opt. Lett.* vol. 17, pp. 31-33 (1992).
- 2 M. Nakazawa, K. Kurokawa, H. Kubota and E. Yamada: Observation of the trapping in an optical soliton by adiabatic gain narrowing and its escape, *Phys. Rev. Lett.* vol. 65, pp. 1881-1884 (1990).
- 3 R. H. Stolen, Chinlon Lin and R. K. Jain: A time-dispersion-tuned fiber Raman oscillator, *Appl. Phys. Lett.* vol. 30, pp. 340-342 (1977).

- 4 K. J. Blow, N. J. Doran and D. Wood: Generation and stabilization of short soliton pulses in the amplified nonlinear Schrödinger equation, *J. Opt. Soc. Am.* vol. B 5, pp. 381-391, (1988).
- 5 M. Nakazawa, H. Kubota, K. Kurokawa and E. Yamada: Femtosecond optical transmission over long distances using adiabatic trapping and soliton standardization, *J. Opt. Soc. Am.* vol. B8, pp. 1811-1817 (1991).
- 6 H. A. Haus and M. Nakazawa: Theory of the fiber Raman soliton laser, *J. Opt. Soc. Am.* vol. B4, pp. 562-660 (1987).
- 7 E. Yamada and M. Nakazawa: Automatic intensity control of an optical transmission line using enhanced gain saturation in cascaded amplifiers, *IEEE J. Quantum Electron.* vol. 27, pp. 146-151 (1991).
- 8 M. Nakazawa, K. Suzuki, E. Yamada, H. Kubota, Y. Kimura, and M. Takaya: Experimental demonstration of soliton data transmission over unlimited distances with soliton control in time and frequency domains, *Electron. Lett.*, vol. 29, pp. 729-730 (1993).
- 9 G. Aubin, T. Montalant, J. Moulou, B. Nortier, F. Pirio and J. B. Thomine: Record amplifier span of 105 km in a soliton transmission experiment at 10 Gbit/s over 1Mkm, *Electron. Lett.* vol. 31, No. 3, pp. 217-219 (1995).
- 10 L. F. Mollenauer, E. Lichtman, M. J. Newbelt, and T. Harvey: Demonstration, using sliding-frequency guiding filters, of error-free soliton transmission over more than 20Mm at 10 Gbit/s, single channel, and over more than 13Mm at 20 Gbit/s in a two channel WDM, *Electron. Lett.* vol. 29 No. 10, pp. 910-911 (1993).
- 11 M. Nakazawa, K. Suzuki, and Y. Kimura: 3.2-5 Gbit/s, 100 km error-free soliton transmission with erbium amplifiers and repeaters, *IEEE, Phot. Tech. Lett.* vol. 2, pp. 216-219 (1990); see also H. Kubota and M. Nakazawa: Long-distance optical soliton transmission with lumped amplifiers, *IEEE, J. Quantum Electron.* vol. 26, pp. 692-700 (1990).
- 12 K. Suzuki and M. Nakazawa: Automatic optical soliton control using cascaded Er³⁺-doped fibre amplifiers, *Electron. Lett.* vol. 26, pp. 1032-1034 (1990).
- 13 M. Nakazawa, K. Suzuki, and E. Yamada: 20 Gbit/s, 1020 km penalty-free soliton data transmission using erbium-doped fibre amplifiers *Electron. Lett.* vol. 28, pp. 1046-1047 (1992)
- 14 H. Taga, M. Suzuki, N. Edagawa, Y. Yoshida, S. Yamamoto, S. Akiba, and H. Wakabayashi: 5 Gbit/s optical soliton transmission experiment over 3000 km employing 91 cascaded Er-doped fibre amplifier repeaters, *Electron. Lett.* vol. 28, pp. 2247-2248 (1992).

- 15 M. Nakazawa, K. Suzuki, E. Yamada, H. Kubota, Y. Kimura, and M. Takaya: Experimental demonstration of soliton data transmission over unlimited distances with soliton control in time and frequency domains, Proc. OFC/IOOC '93, San Jose, PD-7, Feb. (1993)
- 16 A. Hasegawa, and Y. Kodama: Guiding-center soliton, *Phys. Rev. Lett.* vol. 66, pp. 161-164 (1991).
- 17 J. P. Gordon and L. F. Mollenauer: "Effects of fiber nonlinearities and amplifier spacing on ultra-long distance transmission, *IEEE J. Lightwave Technol.* vol. 9, pp. 170-173 (1991).
- 18 M. Nakazawa, H. Kubota, K. Kurokawa and E. Yamada: Femtosecond optical soliton transmission over long distances using adiabatic trapping and soliton standardization, *J. Opt. Soc. Am. B* vol. B 8, pp. 1811-1817 (1991).
- 19 K. Kurokawa and M. Nakazawa: Femtosecond soliton transmission characteristics in an ultralong erbium-doped fiber amplifier with different pumping configurations, *IEEE J. Quantum Electron.* vol. 28, pp. 1922-1929 (1992).
- 20 B. J. Ainslie, K. J. Blow, A. S. Gouveia-Neto, P. G. J. Wigley, A. S. B. Sombra, and J. R. Taylor: Femtosecond soliton amplification in erbium doped silica fibre, *Electron. Lett.*, vol. 26, pp. 186-188 (1990).
- 21 J. P. Gordon: Theory of the soliton self-frequency shift, *Opt. Lett.* vol. 11, pp. 662-664 (1986).
- 22 A. Hasegawa and Y. Kodama: Guiding center solitons in optical fibers', *Opt. Lett.*, vol. 15, pp. 1443-1445 (1990).

V. DISPERSION MANAGEMENT IN SOLITON TRANSMISSION

The advent of erbium-doped fiber amplifiers (EDFAs) has led to numerous interesting reports on high-speed soliton transmission and soliton transmission technology has matured considerably through the use of EDFAs.^[1] Here EDFAs are used as lumped amplifiers, with which the concept of the average soliton, or dynamic soliton has been developed.^[2-5] This technique has a wide range of applicability from L_a (amplifier spacing) $\ll Z_{sp}$ (soliton period) to $L_a \sim Z_{sp}$, depending on the maximum required transmission distance. It is also well known that bright solitons can withstand dispersion fluctuation within the anomalous GVD region when the soliton period Z_{sp} is much longer than the dispersion change-over period.^[6] These conditions are not always possible in practical cases, in particular in a high bit-rate transmission system where the soliton period is short. Below I describe dispersion management techniques to deal with these conditions.

V.1 Partial soliton communication

Many interesting soliton communication experiments have been undertaken based on dynamic soliton method. However the maximum amplifier spacing is limited upto 80 km.

Here, we propose a new technique to extend the amplifier spacing to more than 100 km in optical soliton transmission systems with lumped amplifiers. Here we refer this technique as "partial soliton communication" technique.^[7]

As shown in Chapter III that the "dynamic soliton communication system" is suitable for soliton communication with lumped amplifiers. In this system, the amplifier spacing is almost the same as the distance at

which the pulse width recovers its input width. Under the condition that the amplifier spacing cannot be extended over 100 km. Hasegawa and Kodama showed that a soliton-like pulse can be maintained in optical fiber independent of the amplifier spacing. This is not economically viable for an actual soliton system as many optical amplifiers must be used.

The pulse in a single mode optical fiber is described by a nonlinear Schrödinger equation with loss. The normalized form of the equation is written as eq. (2-3).

A longer soliton period (Z_{sp}) gives a longer L_C , and a longer Z_{sp} is obtained by increasing the pulse width or decreasing the dispersion value, a broader pulse can increase L_C , resulting in a low transmission rate. It is difficult to limit GVD precisely to a small value throughout the fiber length, and when the GVD is small, the transmitting pulse becomes more sensitive to GVD fluctuation. A higher soliton amplitude (A) also makes L_C longer but if A is too high L_C will decrease since excessive spectral broadening produces pulse broadening.

Figure 5.1 shows the pulse width change during propagation. The full width at half maximum of the input pulse intensity is $t_{in} = 10$ ps, the GVD of the fiber is $D = -2$ ps/km/nm, which makes $Z_{sp} = 19.9$ km, loss is $g = 0.22$ dB/km. The soliton pulse restores its width at $L_C = 27.6$ km, 30.4 km, and 30.2 km for $A = 1.5, 1.7,$ and $1.8,$ respectively. Increasing the amplitude from $A = 1.7$ to 1.8 makes L_C shorter. When the pulse propagates longer than L_C , the pulse width broadens monotonously. The broadening rate increases as the input amplitude increases because the high input amplitude (peak power) results in strong SPM so that it generates large frequency broadening than small input amplitude.

Here we investigate the pulse width evolution when the pulse propagates longer than L_C . Figure 5.2 shows the pulse shape and chirp at

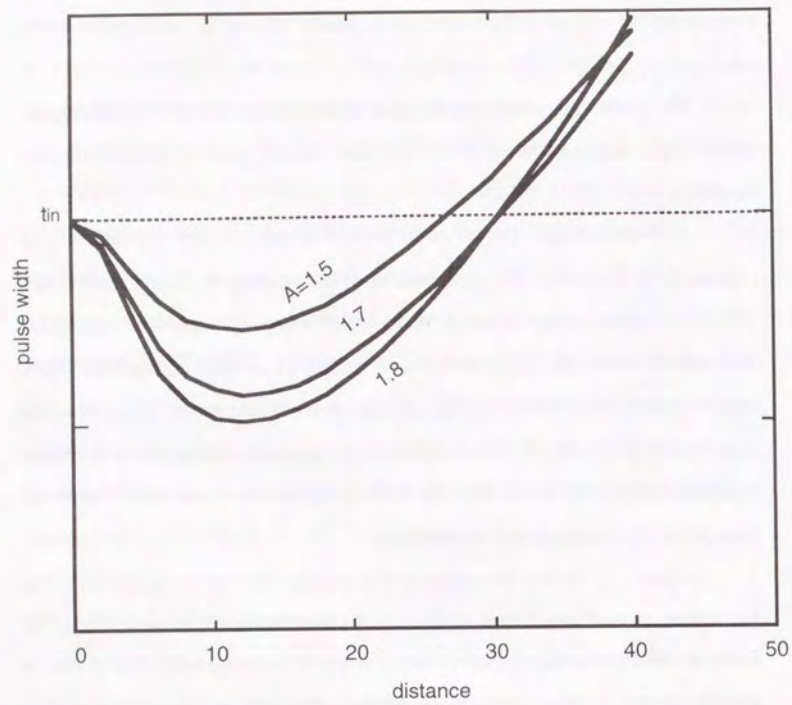


Figure 5.1 Changes in pulse width during propagation for $A = 1.5, 1.7,$ and 1.8 . $t_{in} = 10$ ps, $D = -2$ ps/km/nm, $g = 0.22$ dB/km.

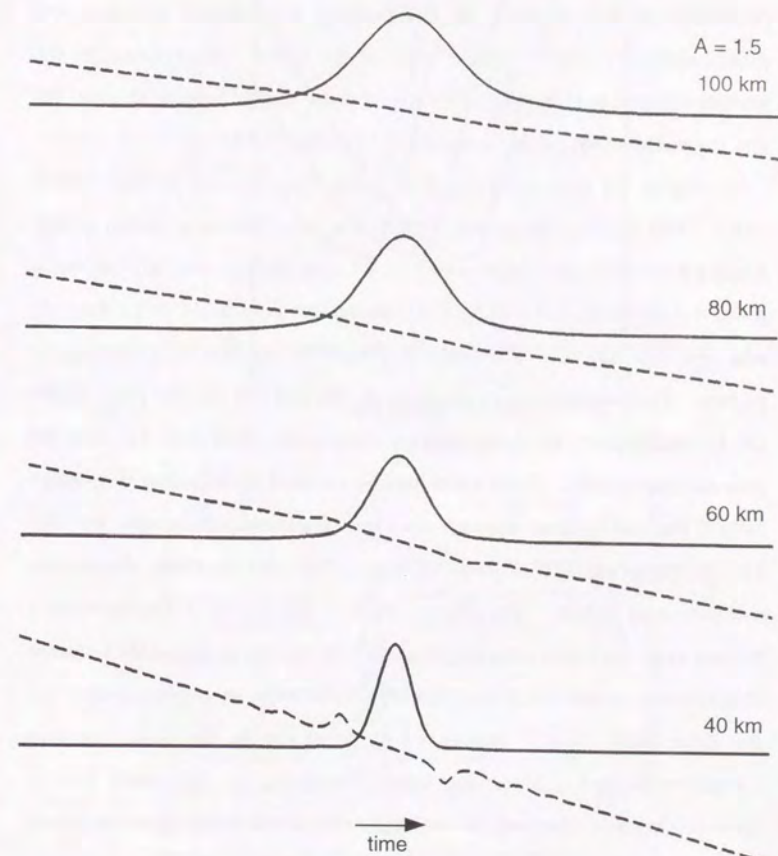
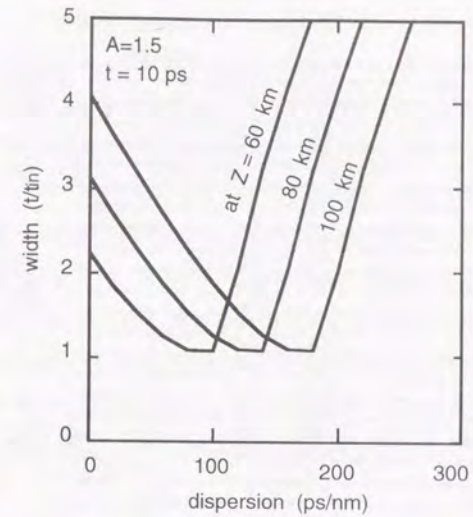


Figure 5.2 Temporal shape (solid line) and chirp (broken line) at 40, 60, 80, and 100 km. $t_{in} = 10$ ps and $A = 1.5$

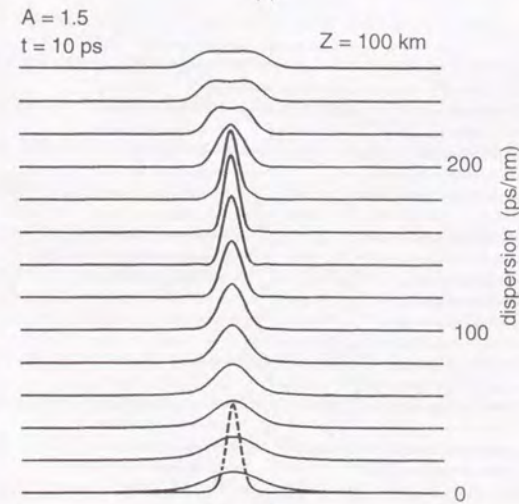
40, 60, 80, and 100 km for $t_{in}=10$ ps and $A=1.5$ input. As expected the pulse width becomes broader than the input pulse. Note here that the center part of the pulse has linear chirp which indicates the dispersion is dominant for that region. As the propagation distance increases, the pulse width broadens. Since most of the pulse energy exists in the linearly chirped part, the linearly chirped pulse should be compensated for and the pulse width can be compressed by normal GVD.

Figure 5.3 shows the result of pulse compression by the normal GVD. The pulse width change during the compression is shown in Fig. 5.3(a) for transmission distances of 60, 80, and 100 km, the original input pulse is $t_{in}=10$ ps, and $A=1.5$. The transmission fiber is $D=-2$ ps/km/nm and $g=0.22$ dB/km. The abscissa shows the amount of dispersion in ps/nm. For transmission distances of 60, 80, and 100 km, the pulse width can be compensated for by appropriate dispersion values of 80, 120, and 160 ps/nm, respectively. Pulse width can be restored by adjusting dispersion even if the transmission distance doubles. Temporal pulse shapes for 100-km propagation are shown in Fig. 5.3(b) for various dispersion compensation values. The original pulse is also shown in the figure by a broken line. At a total dispersion of 160 ps/nm the pulse width becomes shortest and at that point the pulse almost recovers its original shape. At the same time, chirp is minimized, in other words, the pulse becomes transform-limited. Since the pulse amplitude is decreased due to transmission loss, the scale is arbitrarily magnified in the figure to reveal the pulse shape.

Figure 5.4(a) shows the interaction force between two pulses in the present method with multi stage amplification. The condition is $t_{in}=10$ ps, pulse separation (T) is 50 ps (i.e. 20 Gbit/s), and amplifier spacing (L_a) is 100 km. The dispersion used for the compensation is 160 ps/nm, which is obtained from Fig. 5.3(a). The conventional dynamic soliton method with



(a)



(b)

Figure 5.3 Pulse shape change during compression. (a) Pulse width: transmission distances of 60, 80, and 100 km are shown, (b) wave form: ($Z=100$ km) The pulse shape is restored by 160-ps/nm GVD. Original pulse is $t_{in}=10$ ps, $A=1.5$ (broken line).

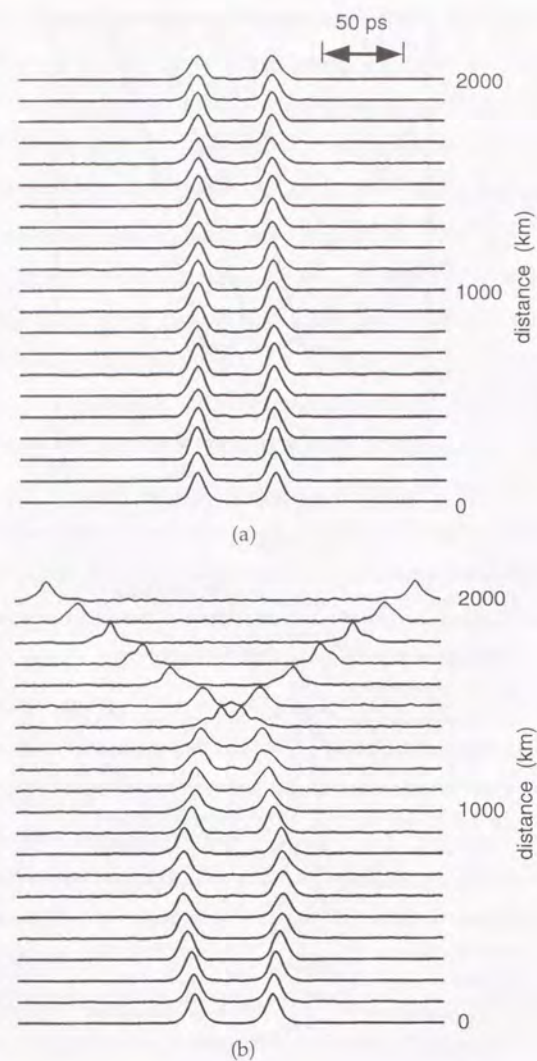


Figure 5.4 Interaction force between 20-Gbit/s, 10-ps pulse pair. (a) Partial soliton method with $L_a=100$ km, dispersion used for compensation is 160 ps/nm. (b) Dynamic soliton method with $L_a= 25$ km.

$L_a= 25$ km is also shown in Fig. 5.4(b) for comparison. In both calculation noise due to amplifiers are not considered. With the partial soliton communication method, the pulse separation is almost constant over 2000 km. A partial soliton can propagate further than dynamic soliton but only requires 1/4 the number of amplifiers. This is not surprising because a partial soliton has less interaction than a dynamic soliton due to the low average pulse energy and has almost no residual chirp at the amplifiers.

In practice, each amplifier generates amplified spontaneous emission (ASE) noise. The ASE causes deterioration of S/N ratio and timing jitter known as Gordon-Haus limit.^[8] In condition for Fig. 5.4 (b), and window of detector acceptance is assumed to be 2/3 of the minimum soliton separation, the Gordon-Haus limit for bit error rate (BER) of 10^{-9} is 1630 km.

Figure 5.5 shows similar calculation as Fig. 5.4 but incorporates ASE noise of amplifiers and the dispersion used for the compensation is 180 ps/nm. Waveform and eye diagram at 2000 km for 2⁵-1 pseudo random pattern are shown in the figure. The complex amplitude of the signal pulse at the fiber output is squared before passing through the baseband filter because a square law detector is assumed in the baseband signal processing. The baseband filter is second order Butterworth type of 13 GHz ($=0.65/T$) in 3-dB bandwidth. The Q value^[9] calculated from the eye diagram is 12.1 at 2000 km propagation.

With this new technique, the amplifier spacing can be greatly changed, and it can be extended to more than 100 km for optical soliton transmission with lumped amplifiers. The optical power loss of a 100-km transmission fiber is about 22 dB, and this amount of gain can easily be obtained using laser diode pumped erbium-doped fiber amplifiers. With this technique, fewer amplifiers are needed for long distance communication and low cost transmission systems can be constructed.

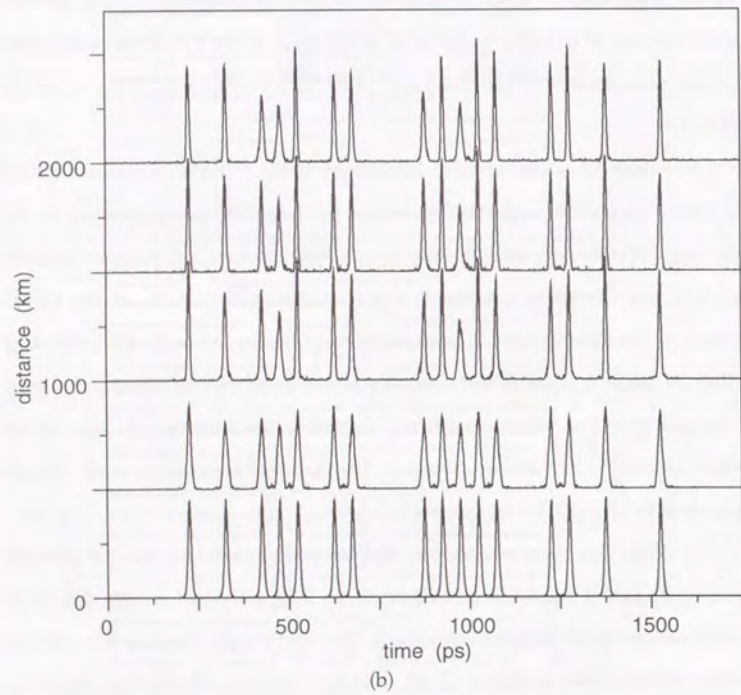
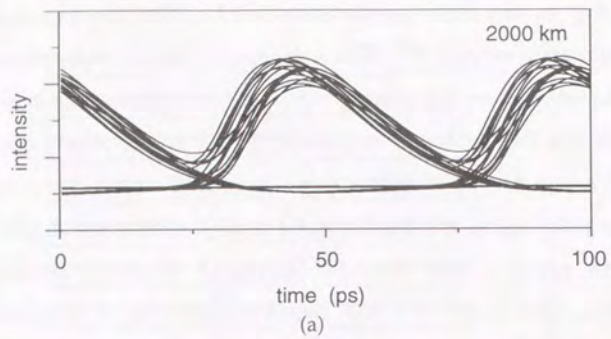


Figure 5.5 Simulation of 20 Gbit/s pulse transmission with 100 km amplifier spacing and ASE. (a) eye pattern with Butterworth type filter of 13GHz bandwidth. (b) waveforms.

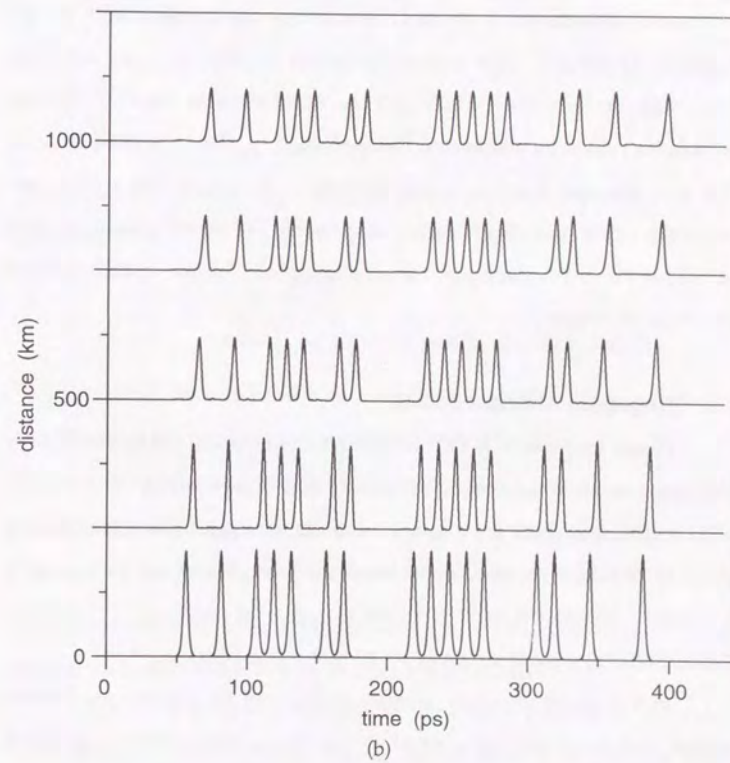
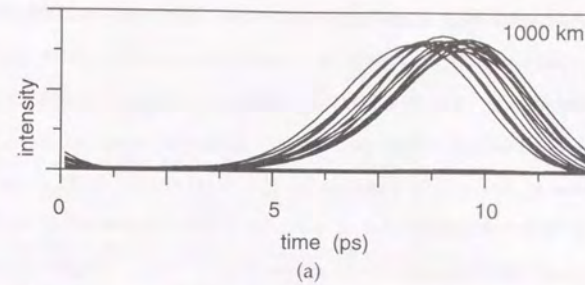


Figure 5.6 Numerical simulation of an 80 Gbit/s soliton transmission with 50 km amplifier spacings.

Here we re-examine the result from another angle, that is, from the viewpoint of ultra-high speed communication. One of the difficulties in realizing ultra-high speed soliton transmission is the need for short amplifier spacings. For 80 Gbit/s the transmission, pulse width should be as short as 3 ps which means that the soliton period becomes about 20 km even if the dispersion is reduced to 0.2 ps/(km.nm). The "dynamic soliton" criterion requires that $L_u < Z_{sp}$ for stable transmission while the partial soliton condition described above is $L_u > 5 \times Z_{sp}$. Figure 5.6 shows a numerical simulation of an 80 Gbit/s soliton transmission with 50 km amplifier spacings. The transmission line consists of a 49 km long dispersion shifted fiber of $D = -0.2$ ps/(km.nm) and 1km of $D = +7.0$ ps/(km.nm) fiber for dispersion compensation. After a transmission of 1000 km, the eye diagram is clearly open. Although, the soliton self frequency shift and high order dispersion are hard problems, this technique is advantageous for realizing ultra-high speed soliton transmission system.

V.2 Dispersion Allocated Soliton

It has long been believed that a bright optical soliton will only propagate in an anomalous GVD region and a dark soliton in a normal GVD region, and there have been no reports to suggest that the reverse is possible. We have reported that a bright soliton can exist and propagate in a normal GVD region as long as the average dispersion D_{ave} throughout the amplifier spacing is properly set so that it is anomalous.^[10,11]

In this paper we show detailed analyses of the dispersion-allocated soliton and point out that a small change in the initial soliton amplitude can control how the soliton stably propagates throughout a fiber over long distances.

Here we consider a sech-type bright soliton. The nonlinear Schrödinger equation with a position dependent dispersion, $\beta(\xi)$, is given by

$$(-i) \frac{\partial u}{\partial \xi} = \frac{1}{2} \beta(\xi) \frac{\partial^2 u}{\partial \tau^2} + |u|^2 u. \quad (5-1)$$

Assuming that u can be described in the form

$$u = U(\xi, \tau) e^{if(\xi, \tau)} \quad (5-2)$$

and that $U(\xi, \tau)$ and f satisfy the following equations.

$$U(\xi, \tau) = 2\eta \operatorname{sech}(2\eta\tau) \quad (5-3)$$

$$\frac{\partial f}{\partial \tau} = 0, \quad (5-4)$$

one obtains

$$U \frac{\partial f}{\partial \xi} = \frac{1}{2} \beta(\xi) \frac{\partial^2 U}{\partial \tau^2} + U^3 \quad (5-5)$$

Thus, the total nonlinear phase change for a propagation distance Z is given by

$$\begin{aligned} f(Z) &= \int_0^Z \left(\frac{\partial f}{\partial \xi} \right) d\xi \\ &= 2\eta^2 \int_0^Z \beta(\xi) d\xi + (2\eta)^2 \operatorname{sech}^2(2\eta\tau) \left[Z - \int_0^Z \beta(\xi) d\xi \right] \end{aligned} \quad (5-6)$$

In order for u to behave as a soliton, f should be time independent and therefore the coefficient of $\operatorname{sech}^2(2\eta\tau)$ should be zero.

$$\frac{1}{Z} \int_0^Z \beta(\xi) d\xi = 1 \quad (5-7)$$

Which means that stable soliton exists by defining D_{ave} , as :

$$D_{ave} = \frac{1}{L} \int_0^L D(z) dz. \quad (5-8)$$

It is permissible to have a random change in the GVD value between normal and anomalous as long as D_{ave} is anomalous.

Each fiber section is allowed to have large normal or anomalous dispersion changes as long as D_{ave} is slightly anomalous over the soliton period. The average soliton period, $Z_{sp(ave)}$, is expressed as

$$Z_{sp(ave)} = 0.322 \frac{\pi^2 c}{\lambda^2} \frac{\tau^2}{D_{ave}}, \quad (5-9)$$

where τ is the input pulse width. $Z_{sp(ave)}$ can be extended much further than L_a , even though we use highly normal or highly anomalous GVD fibers which usually result in short soliton periods in each section. By choosing a small D_{ave} , L_a can be extended to a distance comparable to that in a conventional IM/DD system.

For a pulse width of τ , the soliton peak power in the present system is given by

$$P_{N=1(ave)} = 0.776 \frac{\lambda^3}{\pi^2 c n_2} \frac{D_{ave}}{\tau^2} A_{eff}. \quad (5-10)$$

When the loss is included, the dispersion-allocated soliton amplitude at the input, U_0 , is the same as that of an average soliton.^[3-5] A significant difference between the present soliton and a conventional average soliton is that it can propagate even in a normal GVD region. Here we analyze how much perturbation can be allowed for stable soliton propagation. As D_i is much larger than D_{ave} , the average soliton behaves just like a dispersive wave in each region. Thus, the pulse broadening $\Delta\tau (= \tau_{out} - \tau_0)$ due to D_i is

$$\frac{\Delta\tau}{\tau_0} = \frac{1}{2} \frac{(k_i'' l_i)^2}{\tau_0^4} = \frac{1}{2} \left(\frac{D_i l_i}{D_{ave} Z_0} \right)^2. \quad (5-11)$$

An important requirement for the present soliton is that this broadening should be much less than the original pulse width. Thus, a requirement of

$$\left(\frac{D_i l_i}{D_{ave} Z_0} \right) < 1 \quad (5-12)$$

is obtained. This is quite reasonable because if the broadening is not negligible to the original pulse width, the perturbation to the soliton becomes large and eventually the soliton pulse becomes a mere dispersive wave. A soliton is stable when the product of dispersion and fiber length is smaller than $D_{ave} Z_0(ave)$. Here $Z_0(ave)$ is the normalized distance which has a relationship of $Z_{sp(ave)} = (\pi/2) Z_0(ave)$.

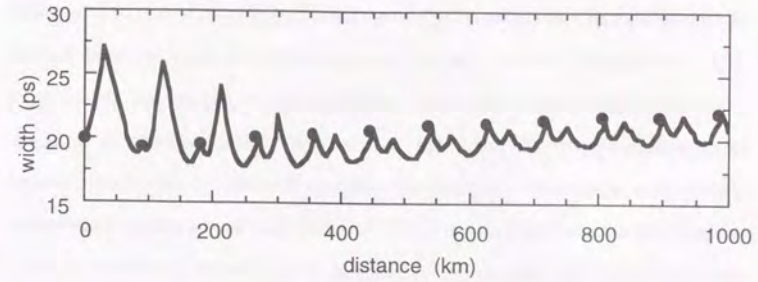


Figure 5.7 Change in the pulse width of a dispersion-allocated soliton as a function of propagation distance. The filled circles show the pulse width at each amplifier position.

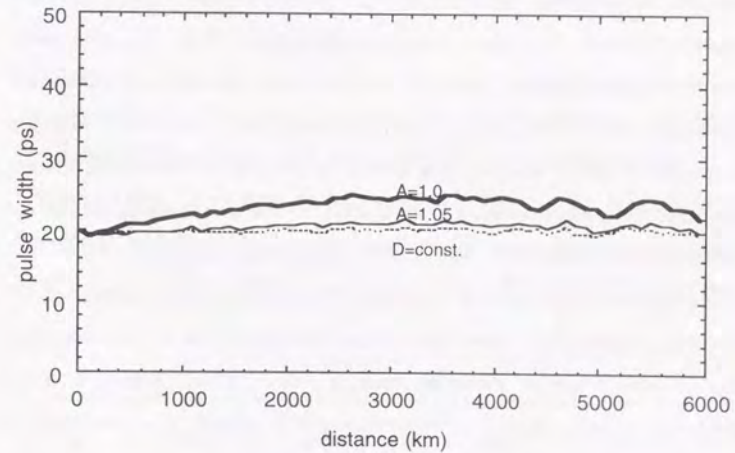


Figure 5.8 Change in the soliton pulse width vs. propagation distance with a different correction factor. The 90 km repeater span consists of a 30 km fiber with + 0.5 ps/km/nm (normal) and a 60 km fiber with -0.4 ps/km/nm (anomalous).

Figure 5.7 shows how the pulse width of this new soliton changes as it propagates down a dispersion allocated fiber. Here L_a is 90 km. The fiber consists of a 30 km fiber with a normal GVD of + 2.0 ps/km/nm and a 60 km fiber with an anomalous GVD of -1.3 ps/km/nm, giving an average anomalous GVD of -0.2 ps/km/nm. The soliton width is 20 ps. The typical feature of the present soliton is that the pulse width changes alternately following the sign of the GVD, but it eventually becomes a steady-state pulse due to the nonlinear phase change over the average soliton period. As the average dispersion is set at $D_{ave} = -0.2$ ps/km/nm, without the nonlinearity, the pulse simply disperses out. However, the pulse width remains near its original value when the input peak intensity is set at that of a conventional average soliton.

We have already shown that a stable soliton exists in the present dispersion-allocated technique.^[9,10] There was no distortion in the waveform when D_{ave} was negative (anomalous). When D_{ave} was made positive (normal) with $D_{ave} = +0.2$ ps/km/nm, nonsoliton transmission occurred where the pulse was distorted and eventually became rectangular. This pulse was the positively chirped nonlinear pulse used for pulse compression with a grating pair.^[12] We also investigated change in the pulse width as a function of propagation distance. When the dispersion perturbation was large, the pulse width of the present soliton deviated slightly from that of a uniform average soliton as it propagated, but it was entirely different from a linear pulse. When a small perturbation was applied to the system, stable soliton pulse propagation was achieved.

As the dispersion-allocated soliton power is small, it does not undergo a large nonlinear phase change, but it behaves like a linear pulse such that the pulse broadening due to normal GVD can be compensated for by anomalous GVD. However, the nonlinear phase change is gradually

accumulated during this process and eventually balances with the average dispersion. Thus, the dispersion-allocated soliton has the nature of a pure soliton over $Z_{sp(ave)}$.

It is important to note that the nonlinear phase rotation in each section is slightly modified because the dispersion-dominant pulse decreases its amplitude during propagation. Therefore, the initial amplitude U_0 is modified to a slightly bigger value U_0A to compensate for the decrease in the nonlinear phase shift of the average soliton. Here A is a correction factor which is close to unity. For simplicity, we use a lossless Gaussian pulse. The loss is compensated for by U_0 . Let the intensity of a Gaussian pulse at $\tau = 0$ be I_G . In the propagation of the pulse $0 < z < l_p$, the average intensity $\overline{I_{Gp}}$ is given by

$$\begin{aligned} \overline{I_{Gp}} &= \frac{1}{l_p} \int_0^{l_p} \left[1 - \frac{1}{2} \left(\frac{4k_p'' z}{\tau_0} \right)^2 \right] dz \\ &= 1 - \frac{8}{3} \left(\frac{k_p'' l_p}{\tau_0^2} \right)^2. \end{aligned} \quad (5-13)$$

As the sign of the dispersion changes in the next fiber section, the slightly broadened soliton in the first stage recovers to its original intensity. It should be noted here that the average dispersion ($k_p'' l_p + k_n'' l_n$) does not have to be zero in order to retain the soliton property, but must be smaller than $k_p'' l_p$. Thus one obtains $\overline{I_{Gn}} \cong \overline{I_{Gp}}$. That is, the correction factor A is

$$A \cong 1 + \frac{4}{3} \left(\frac{D_p l_p}{D_{ave} Z_0} \right)^2 \quad \text{for} \quad \left(\frac{D_p l_p}{D_{ave} Z_0} \right) < 1. \quad (5-14)$$

When the nonlinear phase change due to fiber loss and fiber dispersion are taken into account simultaneously, the correction factor is given as

$$A = 1 + 4 \left(\frac{D_p l_p}{D_{ave} Z_0} \right)^2 \frac{1 - e^{-2\Gamma l_p / Z_0}}{1 - e^{-2\Gamma L_a / Z_0}}. \quad (5-15)$$

where we assume that the decrease in the intensity due to the dispersion is smaller than the that due to the fiber loss. As $(D_p l_p / D_{ave} Z_0)^2 \ll 1$, A is close to unity.

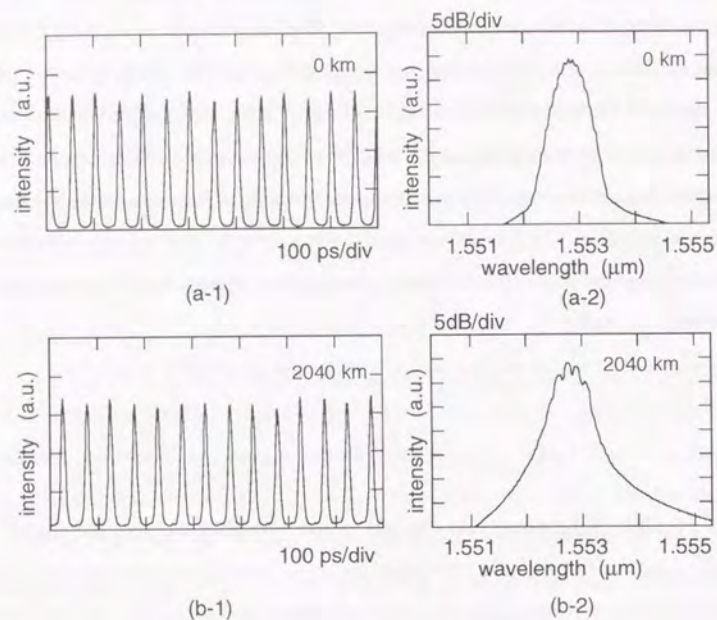


Figure 5.9 20 Gb/s PRBS input and output waveforms and corresponding spectra (a-1) Input pseudo random soliton waveform, (a-2) spectrum, (b-1) Output pseudo random soliton waveform, (b-2) spectrum.

Figure 5.8 shows how the change in the pulse width is modified when the correction factor A changes. L_a is 90 km, and the fiber consists of a 30 km fiber with a GVD of +0.5 ps/km/nm (normal) and a 60 km fiber with a GVD of -0.4 ps/km/nm (anomalous). The correction factor A in this case is calculated to be $A=1.03$ from eq. (5-14). When A is equal to unity, a pulse broadening of 1 ps is observed. However, when A is increased to 1.02-1.05, this broadening is suppressed, and a more uniform propagation is realized. A slight pulse compression occurs in the early stage of the transmission, which is due to the strong accumulation of nonlinear phase change. An over correction using a factor of $A=1.1$ considerably reduces the transmission quality.

These techniques offer us the enormous advantage of being able to construct an actual soliton transmission line using various fiber combinations. Figure 5.9 shows the result of a 20 Gbit/s soliton transmission experiment in the field which uses commercial transmission line. [13]

V.3 Conclusion

These results prove that GVD management will enhance the soliton transmission characteristics. The repeater spacing is extended by using the dispersion compensation technique. It also make it possible to construct a high bitrate transmission system. For practical use, the existence of a soliton in a dispersion-allocated fiber system is proved. This idea makes it possible to undertake soliton transmission experiment in the field.

- 1 M. Nakazawa, Y. Kimura, and K. Suzuki: Soliton amplification and transmission with Er^{3+} -doped fiber repeater pumped by InGaAsP laser diode, *Electron. Lett.* vol. 25, pp. 199-200 (1989).

- 2 H. Kubota, and M. Nakazawa: Long-Distance Optical Soliton Transmission with Lumped Amplifiers, *IEEE, J. Quantum Electron.* vol. **QE-26**, pp. 692 (1990), see also M. Nakazawa, K. Suzuki, and Y. Kimura: 3.2-5 Gbit/s, 100 km error-free soliton transmission with erbium amplifiers and repeaters, *IEEE Photon. Technol. Lett.* vol. **2**, pp. 216 (1990).
- 3 A. Hasegawa, and Y. Kodama: Guiding-center solitons in optical fibers, *Optics Lett.* vol. **15**, pp. 1443-1445 (1990).
- 4 L. F. Mollenauer, S. G. Evangelides and H. A. Haus: Long distance soliton propagation using lumped amplifiers and dispersion-shifted fiber, *IEEE J. Lightwave Technol.* vol. **9**, pp. 194-197 (1991)
- 5 H. A. Haus: Quantum noise in a solitonlike repeater system, *J. Opt. Soc. Am. B* vol. **8**, p. 1122-1126 (1991).
- 6 A. Hasegawa and Y. Kodama: Guiding center soliton in fibers with periodically varying dispersion, *Optics Lett.* vol. **16**, pp. 1385-1387 (1991).
- 7 H. Kubota and M. Nakazawa: Partial soliton communication system, *Optics Communications*, vol. **87**, pp. 15-18 (1992).
- 8 J. P. Gordon and H. A. Haus: Random walk of coherently amplified solitons in optical fiber transmission, *Opt. Lett.* vol. **11**, pp. 665-667 (1986).
- 9 N. S. Bergano, F. W. Kerfoot, and C. R. Davidson: Margin measurement in optical amplifier systems, *IEEE Photon. Technol. Lett.* vol. **5**, pp. 304-306 (1993).
- 10 M. Nakazawa and H. Kubota: Optical soliton communication in a positively and negatively dispersion allocated optical fiber transmission line, *Electron. Lett.* vol. **31** pp. 216-217 (1995).
- 11 M. Nakazawa and H. Kubota: Construction of a dispersion-allocated soliton transmission line using conventional dispersion-shifted nonsoliton fibers, *Jpn. J. Appl. Phys.* vol. **34**, pp. 681-683 (1995).
- 12 W. J. Tomlinson, R. H. Stolen, and C. V. Shank: Compression of optical pulse chirped by self-phase modulation in fibers, *J. Opt. Soc. Am. B* vol. **2**, pp. 139-149 (1984).
- 13 M. Nakazawa, Y. Kimura, K. Suzuki, H. Kubota, T. Komukai, E. Yamada, T. Sugawa, E. Yoshida, T. Yamamoto, T. Imai, A. Sahara, O. Yamauchi, and M. Umezawa, Field demonstration of soliton transmission at 20 Gb/s over 2,000 km in Tokyo metropolitan optical loop network, *Electron. Lett.* vol. **31**, pp. 992-994 (1995).

VI GENERAL CONCLUSION

This paper described the various technologies which will enable a practical soliton communication system to be realized by controlling the characteristics of the transmission line. These characteristics include gain, spectral bandwidth, time domain modulation, and GVD.

The development of a new soliton transmission technique suitable for lumped gain media, which we call the dynamic soliton transmission technique, is a major breakthrough in the field of soliton communication. A key aspect of this technology is to increase the input peak amplitude to above that of an $N=1$ soliton in order to compensate for the decrease in nonlinearity due to optical loss. The remarkable advantage of this technique is its simple configuration which requires no additional elements but which uses only a slightly higher input power than ordinary soliton transmission. Stable soliton transmission can be achieved with lumped EDFAs even when the transmission fiber has an optical loss. With this scheme, a soliton pulse can propagate as if it were an ideal soliton even though the optical fiber has a loss. Numerical analysis proves that a 20 ps pulse can propagate for more than 10,000 km with a 30 km repeater spacing. The repeater spacing can be extended to more than 50 km by reducing the GVD of the transmission fiber. Many experiments have proved that this technique is practical for soliton transmission and it has become indispensable to soliton transmission research.

Soliton transmission control techniques in the time and frequency domains are described for an ultra-long distance transmission. Soliton control is a promising way to increase the transmission distance and amplifier spacing because it reshapes the soliton pulse and eliminates

dispersive non-soliton waves as well as ASE noise. Numerical simulations show that a stable 10 Gbit/s soliton can propagate for more than one million kilometers when the repeater spacing is 50 km, and more than 20,000 km when the spacing is 100 km. Soliton interaction and ASE noise accumulation are successfully eliminated through the use of synchronous modulation and optical filters. This astonishing capability is proved by loop experiments. Solitons have been transmitted over vast distances through the use of synchronous modulation and optical filters. The loop transmission system is analogous to the mode-locked laser, but stable "data" transmission is only possible by soliton transmission as it enables the noise of the vacant time slot to be suppressed.

Soliton control can also be used for ultra-high speed soliton transmission. Without soliton control, the transmission distance in a sub Tbit/s soliton system is severely limited by ssfs, ASE noise and soliton interaction. Even in the presence of ssfs, a transmission of more than 200 Gbit/s- 5000 km is possible by employing frequent soliton control and DEDFAs.

The dispersion management of a transmission line drastically improves the soliton transmission characteristics. A simple dispersion compensation technique makes it easy to extend the repeater spacing to more than 100 km for a 20 Gbit/s - 2000 km soliton transmission. A high GVD of $-2 \text{ ps}/(\text{km}\cdot\text{nm})$ results in a good SN ratio. This technique is also applicable to high bitrate soliton transmission. An 80 Gbit/s soliton can propagate for more than 1000 km with a 50 km amplifier spacing.

For more practical applications of soliton transmission, we analyzed the existence of a soliton pulse under serious GVD fluctuation. The soliton is robust in the face of this fluctuation and the soliton parameters can be described by using the average GVD value. Any discrepancy from a

uniform GVD transmission line can be compensated for by using a slightly higher input amplitude. The use of dispersion management provides soliton transmission with the power it needs for practical applications. A field demonstration was successfully completed using installed commercial cable through the use of the dispersion management technique and its success marks a great step forward for soliton transmission.

As summarized above the combination of EDFAs and optical solitons is a promising way to achieve high bitrate, long distance optical communication. This is not only interesting in terms of practical applications but also for theoretical research. The present work opens the new research field of soliton transmission with strong perturbations. This approach will extend to many areas of nonlinear optical science and technology.

Appendix 1 Numerical procedure

The propagation equation is a nonlinear partial differential equation or called nonlinear Schrödinger equation. An analytic solution to the equation is obtained only in a special case through the use of the inverse scattering method. This means, therefore, that numerical approach is very important for an understanding of the pulse propagation in optical fibers.

The pulse propagation in an optical fiber is classified as an initial value problem of the parabolic equation. One method which has been used extensively to solve this type of problem is the split-step Fourier method (or beam propagation method).

Let us consider a modified nonlinear Schrödinger (NLS) equation of the form

$$\begin{aligned} \frac{\partial u}{\partial z} + \frac{\alpha}{2}u + i\frac{k''}{2}\frac{\partial^2}{\partial t^2}u - \frac{k'''}{6}\frac{\partial^3}{\partial t^3}u \\ = i\gamma(|u|^2u - \tau_r\frac{\partial}{\partial t}(|u|^2)u + \frac{2i}{\omega_0}\frac{\partial}{\partial t}(|u|^2u)). \end{aligned} \quad \text{A.0}$$

This equation is formally written in the form^[1]

$$\frac{\partial u}{\partial z} = (D + N)u, \quad \text{A.1}$$

where D is a differential operator which represents dispersion and absorption (or the linear part), N is a nonlinear operator which represents nonlinear effects (self phase modulation, Raman, optical shock wave) in the optical fiber on pulse propagation. These operators are given by

$$D = -i\frac{k''}{2}\frac{\partial^2}{\partial t^2} + \frac{k'''}{6}\frac{\partial^3}{\partial t^3} - \frac{\alpha}{2} \quad \text{A.2}$$

$$N = i\gamma\left[|u|^2 - \tau_r\frac{\partial}{\partial t}(|u|^2) + \frac{2i}{\omega_0}\frac{\partial}{\partial t}(|u|^2u)\right] \quad \text{A.3}$$

The solution to equation A.1 is formally obtained in the form

$$u(z+h, T) = \exp[h(D+N)]u(z, T), \quad \text{A.4}$$

if N is assumed to be z independent. By introducing the Baker-Hausdorff formula for operators a and b

$$\exp(a)\exp(b) = \exp[a + b + 1/2[a, b] + \dots], \quad \text{A.5}$$

where commutator $[a, b] = ab - ba$. When we ignore the non-commuting nature of D and N , equation A.4 can be written as

$$u(z+h, T) \cong \exp[hD]\exp[hN]u(z, T), \quad \text{A.6}$$

where $a = hD$, and $b = hN$. The dominant error term results from $[hD, hN]/2 = h^2[D, N]/2$, so that the SSFM is accurate to the second order in the step size h .

To improve the accuracy, we often apply nonlinearity at the center point of the small step h . i.e.,

$$u(z+h, T) = \exp[hD/2]\exp[hN]\exp[hD/2]u(z, T), \quad \text{A.7}$$

The error term of the order h^2 is canceled out so that it is accurate to the third order in the step size h . Figure A1 shows the schematics of this method.

Thus far, the nonlinearity operator N is assumed to be z independent. For more precise calculation, the z dependence should be taken into account, i.e., $\exp[hN]$ is replaced by $\exp[\int_z^{z+h} N(z')dz']$.

The integral is calculated by a trapezoidal rule,

$$\int_z^{z+h} N(z')dz' \cong \frac{h}{2}[N(z) + N(z+h)]. \quad \text{A.8}$$

However, it is not simple to use this formula because $N(z+h)$ is unknown at the time of the first calculation. It is necessary to introduce an iterative procedure to obtain a self consistent condition.

The dispersion term of Eq. A.7 is solved using a Fourier transform.

$$\exp[hD/2]u(z, T) = F^{-1}\{\exp[hD(i\omega)/2]F\}u(z, T) \quad \text{A.9}$$

where F denotes a Fourier transformation operation. This numerical procedure is so called the split-step Fourier method.^[2]

It is important to note here that any changes in waveform and pulse position due to walk off or self frequency shift will reduce the accuracy. It may be necessary to repeat the calculation by reducing the step size to ensure the accuracy of numerical simulations.

¹ M. J. Potasek, G. P. Agrawal, and S. C. Pinault: Numerical study of pulse broadening in nonlinear dispersive optical fibers, *J. Opt. Soc. Amer. B* vol. 3, p. 205-211 (1986).

² W. H. Press et al.: *Numerical Recipes*, Cambridge press, Cambridge, 1986.

Appendix 2 Soliton generation methods

Here I list references for soliton generation methods

Bright soliton:

1. Solid laser

Nd:YAG laser (1.3 μm) [1,2]

Color center laser [3]

Soliton laser using color center laser [4,5]

2. Wavelength conversion

Differential frequency generation [6]

Optical parametric oscillation [7]

3. Fiber lasers/ Fiber amplifier

Raman based [8,9,10,11]

Erbium based [12,13]

4. Laser diode with optical amplifier

Gain switching with spectral filtering [14]

Electro absorption modulator [15,16,17]

Dark soliton:

Spacial masking [18]

M-Z interferometer [19,20,21]

LN modulator [22]

¹ A. S. Gouveia-Neto, A. S. L. Gomes and J. R. Taylor: Generation of 33-fsec pulse at 1.32 μm through a high-order soliton effect in a single-mode optical fiber, *Opt. Lett.* vol. 12, pp. 395-197 (1987).

- 2 K. Tai and A. Tomita: 1100x optical fiber pulse compression using grating pair and soliton effect at 1.319 μm , *Appl. Phys. Lett.* vol. 48, pp. 1033-1035 (1986).
- 3 L. F. Mollenauer, R. H. Stolen and J. P. Gordon: Experimental observation of picosecond pulse narrowing and solitons in optical fiber, *Phys. Rev. Lett.* vol. 45, No. 13, pp. 1095-1098 (1980).
- 4 L. F. Mollenauer and R. H. Stolen, *Opt. Lett.* vol. 9, p. 13 (1984).
- 5 F. M. Mitschke and L. F. Mollenauer: Ultrashort pulse from the soliton laser, *Opt. Lett.* vol. 12, No. 6, pp. 407-409 (1987).
- 6 K. Kurokawa and M. Nakazawa: Femtosecond 1.4-1.6 μm infrared pulse generation at a high repetition rate by difference frequency generation, *Appl. Phys. Lett.* vol. 55, pp. 7-9 (1989).
- 7 K. Suzuki, M. Nakazawa and H. A. Haus: Parametric soliton laser, *Opt. Lett.* vol. 14, No. 6, pp. 320-322 (1989).
- 8 H. A. Haus and M. Nakazawa: Theory of fiber Raman soliton laser, *J. Opt. Soc. Am. B* vol. 4, pp. 652-660 (1987).
- 9 J. D. Kafka and T. Baer: Fiber Raman soliton laser pumped by a Nd:YAG laser, *Opt. Lett.* vol. 12, pp. 181-183 (1987).
- 10 A. S. Gouveia-Neto, A. S. L. Gomes and J. R. Taylor: Femtosecond soliton Raman ring laser, *Electron. Lett.* vol. 23 p. 537-538 (1987).
- 11 A. S. Gouveia-Neto, A. S. L. Gomes, J. R. Taylor and K. J. Blow: Soliton reconstruction through synchronous amplification, *J. Opt. Soc. Am. B* vol. 5, pp. 799-803 (1988).
- 12 M. Nakazawa, E. Yoshida, and Y. Kimura: Ultrastable harmonically and regeneratively modelocked polarization-maintaining erbium fibre ring laser, *Electron. Lett.* vol. 30, p. 1603 (1994).
- 13 M. Nakazawa, E. Yoshida, T. Sugawa and Y. Kimura: Continuum suppressed, uniformly repetitive 136 fs pulse generation from an erbium-doped fibre laser with nonlinear polarization rotation, *Electron. Lett.* vol. 29, pp. 1327-1329 (1993).
- 14 M. Nakazawa, K. Suzuki, and Y. Kimura: Transform-limited pulse generation in the gigahertz region from a gain-switched distributed-feedback laser diode using spectral windowing, *Opt. Lett.* vol. 15, p. 715 (1990).
- 15 M. Suzuki, H. Tanaka, H. Taga, Y. Yamamoto, and Y. Matsushima: 3V-10 Gbit/s modulator and 0.5 Tb/s-km transmission using a $\lambda/4$ -shifted DFB laser / E-A modulator integrated light source, Paper PD 7, Optoelectronics Conf. Tokyo, (1991).
- 16 M. Suzuki, H. Tanaka, K. Utaka, N. Edagawa, and Y. Matsushima: Transform-limited 14ps optical pulse generation with 15GHz repetition rate by InGaAsP electroabsorption modulator, *Electron. Lett.* vol. 28, p. 1007 (1992).
- 17 S. Kondo, K. Wakita, Y. Noguchi and N. Yoshino: Fabrication of a polarization insensitive electroabsorption modulator with strained InGaAs/InAlAs MQW by MOVPE, 7th Int. Conf. Indium Phosphite and Related Materials, Sapporo, pp. 61-64, paper WA2.4 (1995).
- 18 A. M. Weiner, J. P. Heritage, R. J. Hawkins, R. N. Thurston, E. M. Kirschner, D. E. Leaird, and W. J. Tomlinson: Experimental observation of the fundamental dark soliton in optical fibers, *Phys. Rev. Lett.* vol. 61, pp. 2445-2448 (1988).
- 19 P. Empl, J. P. Hamaide, R. Reynaud, C. Froehly, and A. Barthelemy: Picosecond steps and dark pulses through nonlinear single mode fibers, *Opt. Commun.* vol. 62, pp. 374-379 (1987).
- 20 W. Zaho and E. Bourkoff: Generation of dark solitons under a cw background using waveguide electro-optic modulators, *Opt. Lett.* vol. 15, pp. 405-407 (1990).
- 21 W. Zaho and E. Bourkoff: Generation, propagation, and amplification of dark solitons, *J. Opt. Soc. Am. B* vol. 9, pp. 1134-1144 (1992).
- 22 M. Nakazawa and K. Suzuki: 10 Gbit/s pseudorandom dark soliton data transmission over 1200 km, *Electron. Lett.*, vol. 31, pp. 1076-1077 (1995).

Publications

Papers concerning to Soliton Transmission

Letters

- [1] H. Kubota and M. Nakazawa; "Maximum transmission capacity of a soliton communication system with lumped amplifiers", *Electron. Lett.*, Vol. 26, No. 18, pp. 1454-1455, 1990.
- [2] H. Kubota and M. Nakazawa; "Partial soliton communication system", *Opt. Commun.*, Vol. 87, No. "1,2", pp. 15-18, 1992.
- [3] H. Kubota and M. Nakazawa; "Soliton transmission with long amplifier spacing under soliton control", *Electron. Lett.*, Vol. 29, No. 20, pp. 1780-1781, 1993.

Papers

- [4] H. Kubota and M. Nakazawa; "Long-distance soliton transmission with lumped amplifiers", *IEEE J. Quantum. Electron.*, Vol. 26, No. 4, pp. 692-700, 1990.
- [5] H. Kubota and M. Nakazawa; "Recent progress on optical soliton communication", *IEICE Trans.*, Vol. E74, No. 6, pp. 1373-1378, 1991.
- [6] H. Kubota and M. Nakazawa; "Soliton transmission controls", *IEICE Trans.*, Vol. J76C1, No. 5, pp. 147-157, 1993.(in Japanese)
- [7] H. Kubota and M. Nakazawa; "Soliton transmission control in time and frequency domains", *IEEE J. Quantum Electron.*, Vol. 29, No. 7, pp. 2189-2197, 1993.
- [8] H. Kubota and M. Nakazawa; "Soliton transmission control for ultra high speed system", *IEICE Trans. Electron.*, Vol. E78C, No. 1, pp. 5-11, 1995.

Papers concerning to Short Pulse Generation

- [1] H. Kubota, K. Kurokawa and M. Nakazawa; "29-fsec pulse generation from a linear-cavity synchronously pumped dye laser", *Opt. Lett.*, Vol. 13, No. 9, pp. 749-751, 1988.
- [2] H. Kubota and M. Nakazawa; "Compensation of nonlinear chirp generated by self-steepening using third order dispersion of a grating pair", *Opt. Commun.*, Vol. 66, No. "2,3", pp. 79-82, 1988.
- [3] H. Kubota and M. Nakazawa; "Study of optical pulse compression with higher order nonlinearity and dispersion", *Jap. J. Appl. Phys.*, Vol. 28, No. 4, pp. 609-614, 1989.

Co-authored papers

- [1] M. Nakazawa, T. Nakashima, H. Kubota and S. Seikai; "65-femtosecond pulse generation from a synchronously pumped dye laser without a colliding-pulse mode-locking technique", *Opt. Lett.*, Vol. 12, No. , pp. 681-683, 1987.
- [2] T. Nakashima, M. Nakazawa, K. Nishi and H. Kubota; "Effect of stimulated Raman scattering on pulse-compression characteristics", *Opt. Lett.*, Vol. 12, No. 6, pp. 404-406, 1987.
- [3] M. Nakazawa, T. Nakashima, H. Kubota and S. Seikai; "55 kW, 240 fs pulse generation from a cavity dumped, synchronously pumped dye laser and its application to pulse compression", *Appl. Phys. Lett.*, Vol. 51, No. 10, pp. 728-730, 1987.
- [4] M. Nakazawa, T. Nakashima and H. Kubota; "Optical pulse compression using a TiO₂ acousto-optical light deflector", *Opt. Lett.*, Vol. 13, No. 2, pp. 120-122, 1988.
- [5] M. Nakazawa, T. Nakashima, H. Kubota and S. Seikai; "Efficient optical pulse compression using a pair of Brewster-angled TeO₂ crystal prisms", *J. Opt. Soc. Am. B*, Vol. 5, No. 2, pp. 215-221, 1988.
- [6] K. Kurokawa, H. Kubota and M. Nakazawa; "48 fs, 190 kW pulse generation from a cavity dumped, synchronously pumped dye laser", *Opt. Commun.*, Vol. 68, No. 4, pp. 287-290, 1988.
- [7] M. Nakazawa, K. Suzuki, H. Kubota and H. A. Haus; "High-order solitons and the modulational instability", *Phys. Rev. A*, Vol. 39, No. 11, pp. 5768-5776, 1989.
- [8] M. Nakazawa, Y. Kimura, K. Suzuki and H. Kubota; "Wavelength multiple soliton amplification and transmission with Er³⁺-doped optical fiber", *J. Appl. Phys.*, Vol. 66, No. 7, pp. 2803-2812, 1989.
- [9] M. Nakazawa, K. Suzuki, H. Kubota and H. A. Haus; "The modulational instability laser - Part II: Theory", *IEEE J. Quantum. Electron.*, Vol. 25, No. 9, pp. 2045-2052, 1989.
- [10] K. Kurokawa, H. Kubota and M. Nakazawa; "Generation of 72-fs pulse from a cavity dumped, synchronously pumped dye laser with a single jet", *Opt. Commun.*, Vol. 73, No. 4, pp. 319-321, 1989.
- [11] M. Nakazawa, K. Kurokawa, H. Kubota and E. Yamada; "Observation of the trapping of an optical soliton by adiabatic narrowing and its escape", *Phys. Rev. Lett.*, Vol. 65, No. 15, pp. 1881-1884, 1990.
- [12] M. Nakazawa, K. Suzuki, H. Kubota, E. Yamada and Y. Kimura; "Dynamic optical soliton communication", *IEEE J. Quantum. Electron.*, Vol. 26, No. 12, pp. 2095-2102, 1990.
- [13] M. Nakazawa, K. Kurokawa, H. Kubota, K. Suzuki and Y. Kimura; "Femtosecond erbium-doped fiber amplifier", *Appl. Phys. Lett.*, Vol. 57, No. 7, pp. 653-655, 1990.
- [14] M. Nakazawa, E. Yamada and H. Kubota; "Coexistence of a self-induced transparency soliton and a nonlinear Schrodinger soliton in an erbium-doped fiber", *Phys. Rev. A*, Vol. 44, No. 9, pp. 5973-5987, 1991.
- [15] M. Nakazawa, E. Yamada and H. Kubota; "Coexistence of a self-induced transparency soliton and a nonlinear Schrodinger soliton", *Phys. Rev. Lett.*, Vol. 66, No. 20, pp. 2625-2628,

- 1991.
- [16] M. Nakazawa, K. Suzuki, E. Yamada and H. Kubota; "Observation of nonlinear interaction in 20 Gbit/s soliton transmission over 500 km using erbium-doped fibre amplifiers", *Electron. Lett.*, Vol. 27, No. 18, pp. 1662-1663, 1991.
- [17] M. Nakazawa, H. Kubota, K. Kurokawa and E. Yamada; "Femtosecond optical soliton transmission over long distances using adiabatic trapping and soliton standardization", *J. Opt. Soc. Am. B*, Vol. 8, No. 9, pp. 1811-1817, 1991.
- [18] M. Nakazawa, E. Yamada, H. Kubota and K. Suzuki; "10 Gbit/s soliton data transmission over one million kilometers", *Electron. Lett.*, Vol. 27, No. 14, pp. 1270-1272, 1991.
- [19] M. Nakazawa, H. Kubota, E. Yamada and K. Suzuki; "Infinite-distance soliton transmission with soliton controls in time and frequency domains", *Electron. Lett.*, Vol. 28, No. 2, pp. 1099-1100, 1992.
- [20] M. Nakazawa and H. Kubota; "Physical interpretation of reduction of soliton interaction force by bandwidth limited amplification", *Electron. Lett.*, Vol. 28, No. 10, pp. 958-960, 1992.
- [21] K. Kurokawa, H. Kubota and M. Nakazawa; "Soliton self-frequency shift accelerated by femtosecond soliton interaction", *Electron. Lett.*, Vol. 28, No. 22, pp. 2052-2053, 1992.
- [22] K. Kurokawa, H. Kubota and M. Nakazawa; "Significant modification of femtosecond soliton interaction in gain medium by small subpulse", *Electron. Lett.*, Vol. 28, No. 25, pp. 2334-2335, 1992.
- [23] M. Nakazawa, K. Suzuki, E. Yamada, H. Kubota and Y. Kimura; "10 Gbit/s, 1200 km error-free soliton data transmission using erbium-doped fibre amplifiers", *Electron. Lett.*, Vol. 28, No. 9, pp. 817-818, 1992.
- [24] M. Nakazawa, K. Suzuki, Y. Kimura and H. Kubota; "Coherent pi-pulse propagation with pulse breakup in an erbium-doped fiber waveguide amplifier", *Phys. Rev. A*, Vol. 45, No. 5, pp. 2682-2685, 1992.
- [25] K. Suzuki, H. Kubota and M. Nakazawa; "Soliton communication using EDFA", *Laser Research*, Vol. 20, No. 8, pp. 666-672, 1992. (in Japanese)
- [26] M. Nakazawa and H. Kubota; "Reply:", *Electron. Lett.*, Vol. 29, No. 2, pp. 226-227, 1993.
- [27] M. Nakazawa, K. Suzuki, E. Yamada, H. Kubota, Y. Kimura and M. Takaya; "Experimental demonstration of soliton data transmission over unlimited distances with soliton control in time and frequency domains", *Electron. Lett.*, Vol. 29, No. 9, pp. 729-730, 1993.
- [28] E. Yamada, K. Suzuki, H. Kubota and M. Nakazawa; "Ultra-high speed optical soliton communication using erbium-doped fiber amplifiers", *IEICE Trans. Commun.*, Vol. E76-B, No. 4, pp. 410-419, 1993.
- [29] M. Nakazawa, K. Suzuki, E. Yamada, H. Kubota and Y. Kimura; "straight-line soliton data transmission over 2000km at 20 Gbit/s and 1000 km at 40 Gbit/s using erbium-doped fibre amplifiers", *Electron. Lett.*, Vol. 29, No. 16, pp. 1474-1475, 1993.
- [30] M. Nakazawa, K. Suzuki, H. Kubota and Y. Kimura; "Active Q switching and mode locking in a 1.53- μ m fiber ring laser with saturable absorption in erbium-doped fiber at 4.2 K", *Opt. Lett.*, Vol. 18, No. 18, pp. 1526-1528, 1993.
- [31] M. Nakazawa, K. Suzuki, H. Kubota and Y. Kimura; "Self-Q-switching and mode locking in a 1.53- μ m fiber ring laser with saturable absorption in erbium-doped fiber at 4.2 K", *Opt. Lett.*, Vol. 18, No. 8, pp. 613-615, 1993.
- [32] K. Suzuki, E. Yamada, H. Kubota and M. Nakazawa; "Optical soliton communication system using erbium-doped fiber amplifiers", *fiber and Integrated optics*, Vol. 13, No. , pp. 45-64, 1994.
- [33] K. Kurokawa, H. Kubota and M. Nakazawa; "Femtosecond soliton interactions in a Distributed Erbium-doped fiber amplifier", *IEEE J. Quantum Electron.*, Vol. 30, No. 9, pp. 2220-2226, 1994.
- [34] M. Nakazawa, K. Suzuki, H. Kubota, E. Yamada and Y. Kimura; "Straight-line soliton data transmission at 20 Gbit/s beyond Gordon-Haus limit", *Electron. Lett.*, Vol. 30, No. 16, pp. 1331-1332, 1994.
- [35] M. Nakazawa, E. Yoshida, H. Kubota and Y. Kimura; "Generation of a 170fs, 10GHz transform limited pulse train at 1.55 μ m using a dispersion-decreasing, erbium-doped active soliton compressor", *Electron. Lett.*, Vol. 30, No. 24, pp. 2038-2040, 1994.
- [36] M. Nakazawa and H. Kubota; "Optical soliton communication in a positively and negatively dispersion allocated optical fiber transmission line", *Electron. Lett.*, Vol. 31, No. 3, pp. 216-217, 1995.
- [37] T. Sugawa, K. Kurokawa, H. Kubota and M. Nakazawa; "Soliton self-frequency shift in orthogonally polarized femtosecond solitons", *Electron. Lett.*, Vol. 30, No. 23, pp. 1963-1964, 1994.
- [38] M. Nakazawa and H. Kubota; "Construction of a dispersion-allocated soliton transmission line using conventional dispersion-shifted nonsoliton fibers", *Jpn. J. Appl. Phys.*, Vol. 34, No. 6A, pp. L681-L683, 1995.
- [39] M. Nakazawa, Y. Kimura, K. Suzuki, H. Kubota, T. Komukai, E. Yamada, T. Sugawa, E. Yoshida, T. Yamamoto, T. Imai, A. Sahara, H. Nakazawa, O. Yamamuchi and M. Umezawa; "Field demonstration of soliton transmission at 10 Gbit/s over 2000 km in Tokyo metropolitan loop network", *Electron. Lett.*, vol. 31, No. 12, pp. 992-994, 1995.
- [40] T. Sugawa, K. Kurokawa, H. Kubota and M. Nakazawa; "Polarization dependence of soliton interactions in Femtosecond soliton transmission"; *IEICE Trans. Electron.*, Vol. E78-C, No. 1, pp. 28-37, 1995.
- [41] M. Nakazawa and H. Kubota; "Analyses of the Dispersion-allocated bright and dark solitons", *Jpn. J. Appl. Phys.*, Vol. 34, No. 7B, pp. L889-891, 1995.
- [42] T. Sugawa, H. Kubota and M. Nakazawa; "Polarization dependence of femtosecond soliton-soliton interaction on dispersion-shifted fiber", *Opt. Lett.* vol. 20, No. 13, pp. 1453-1455, 1995.
- [43] M. Nakazawa and H. Kubota; "Optical soliton communication in a positively and negatively dispersion-allocated optical fiber transmission line", *Electron. Lett.* vol. 31, No. 3, pp. 216-217, 1995.

